UAB

Universitat Autònoma de Barcelona

Mechanistic, Temporal and Spatial insights of the regulatory network controlling plant responses to vegetation proximity

Pedro Pastor Andreu

PhD THESIS

UNIVERSITAT AUTÒNOMA DE BARCELONA

FACULTAT DE BIOCIENCIES

MECHANISTIC, TEMPORAL AND SPATIAL INSIGHTS OF THE REGULATORY NETWORK CONTROLLING PLANT RESPONSES TO VEGETATION PROXIMITY

Pedro Pastor Andreu

2021

UNIVERSITAT AUTÒNOMA DE BARCELONA

FACULTAT DE BIOCIENCIES

Doctoral program of Plant Biology and Biotechnology

PhD thesis

MECHANISTIC, TEMPORAL AND SPATIAL INSIGHTS OF THE REGULATORY NETWORK CONTROLLING PLANT RESPONSES TO VEGETATION PROXIMITY

Dissertation presented by Pedro Pastor Andreu for the degree of Doctor of Plant Biology and Biotechnology at Autonomous University of Barcelona. This work was performed in the Centre for Research in Agricultural Genomics.
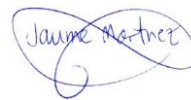

Directors		Tutor	PhD Candidate
Dr. Jaime F. Martínez-García	Dr. Jordi Moreno-Romero	Dr. Jaime F. Martínez-García	Pedro Pastor Andreu

Barcelona, September 2021

AGRADECIMIENTOS

Como todo, esta etapa llega a su fin y es hora de mirar atrás y dar las gracias.

En primer lugar, me gustaría agradecer a Jaume Martínez-García, por la confianza depositada en mí al brindarme la maravillosa oportunidad de formar parte de su laboratorio como estudiante de doctorado. Gracias por abrirme las puertas al mundo de la investigación. En segundo lugar, quiero agradecer a Jordi Moreno-Romero, por su paciencia y transmisión de conocimientos, por su ayuda en el laboratorio y con la redacción de la tesis y por su disponibilidad en todo momento. Esta aventura no solo me ha permitido aprender y formarme, sino que también me ha aportado muchas otras experiencias irrepetibles, como mi estancia en el laboratorio de Antía Rodríguez-Villalón en Zurich, a quien agradezco haberme permitido formar parte de su equipo durante esos dos fríos meses en Suiza. Gracias también a Elizabeth por su ayuda en las interminables horas en el confocal. Deseo dar las gracias también a los integrantes del 205. Gracias Sandi, María José, Wenting, Irma y a todos los que han pasado laboratorio por vuestro apoyo, enseñanzas y otros momentos divertidos como los cafés o desayunos. Gracias a vosotros el laboratorio era como una segunda casa para mí.

Esto no solo se trata de aprender y trabajar. También hay tiempo para divertirse y esta experiencia me ha permitido conocer a muchas personas y crear una nueva familia en Barcelona. No puedo dejar de dar las gracias a los miembros de dicha familia, por su amistad incondicional y por los momentos pasados juntos. Gracias Camila, Violeta, Laia, Ari, Belén, Carlos y Andrea. Tampoco puedo olvidarme de aquellos que, aunque ahora no la tengan, en su momento tuvieron la tarjeta para entrar en el CRAG. Gracias a Lucia y Laura por sus perlas de sabiduría y gracias a Serena por ser única. Además, quiero agradecer a Víctor por estar siempre ahí y saber siempre que hacer o que decir. Por último, quiero agradecer a mi familia, por tanto apoyo y amor y porque de una manera u otra todos ellos han hecho posible que cumpla mis metas.

Gracias a todos por tanto y gracias a ti si estas leyendo estas líneas.

SUMMARY

Light is essential for plants, not only for fueling photosynthesis, but also as environmental information that allows them to adapt their development to thrive in different scenarios. In shade-avoider (sun-loving) plants, such as Arabidopsis thaliana, proximity of potentially competing vegetation triggers a group of responses known as Shade Avoidance Syndrome (SAS), including the well-studied hypocotyl elongation. Phytochromes are the photoreceptors that detect vegetation proximity signals that, by binding to PHYTOCHROME INTERACTING FACTORs (PIFs), integrate light signals into acclimation changes in plant development. The current regulatory model states that the shade-induced inactivation of phytochrome B (phyB) releases the repression imposed over PIFs, which results in the rapid activation of gene expression changes and in hypocotyl elongation promotion.

PIFs contain an active phyB-binding (APB) motif and a basic helix-loop-helix (bHLH) domain, responsible of DNA-binding. Among PIFs, the photostable PIF7 has a major role in promoting hypocotyl elongation in shade. However, it is unknown if PIF7 DNA- and phyB-binding activities can modulate independently different aspects of the light-regulated development, as it occurs in the well-studied and founder member PIF3. To address this question, we carried out a structure-function analysis by generating PIF7 derivatives with the bHLH and the APB domains mutated. In the first chapter of this work we show that both the PIF7 DNA- and phyB-binding activities are linked and fundamental to rapidly induce the expression of PIF7 targets and the hypocotyl growth in shade.

Other components classified as positive and negative regulators participate in the modulation of SAS by building a complex regulatory network. Nevertheless, it is still unclear how these components are organized. To refine the architecture of this signaling network and establish the connections between its components, in the second chapter of this thesis we carried out physiological, cell biology and transcriptomic analyses of the shade-induced hypocotyl elongation using defective mutants of the different regulators. Our results demonstrate that the SAS regulatory components are organized in two main branches that act in slightly different moments and modulate the elongation of different cells along the hypocotyl axis. Nevertheless, we also found a signaling convergence between the two branches, as PIFs and ELONGATED HYPOCOTYL 5 (HY5), components that belong to these separate branches, regulate the expression of common target genes.

RESUMEN

La luz es esencial para las plantas, no solo como fuente de energía para la fotosíntesis, sino también como una señal de información ambiental que les permite adaptar su desarrollo para prosperar en diferentes escenarios. En las plantas que evitan la sombra, como *Arabidopsis thaliana*, la proximidad de vegetación potencialmente competidora desencadena un grupo de respuestas conocido como síndrome de huida de la sombra (SAS, de sus siglas en inglés), que incluye el alargamiento del hipocótilo. Los fitocromos, que son los fotorreceptores que detectan las señales de proximidad vegetal, interaccionan con los factores de transcripción PHYTOCHROME INTERACTING FACTORs (PIFs). Esta interacción resulta en la integración de las señales de luz para ajustar el desarrollo de las plantas a estos cambios ambientales. La hipótesis actual establece que la inactivación inducida por la sombra del fitocromo B (phyB) libera la represión impuesta sobre los PIFs, lo que resulta en cambios rápidos en la expresión génica y la promoción del alargamiento del hipocótilo.

Los PIFs contienen un motivo de unión a phyB activo (APB) y un dominio básico-hélice-bucle-hélice (bHLH), responsable de la unión al ADN. Entre los PIFs existentes, PIF7 es el más importante en la promoción del alargamiento del hipocótilo en sombra. Se desconoce si la unión de PIF7 al ADN y al phyB modula independientemente diferentes aspectos del desarrollo regulado por la luz, como ocurre con PIF3, el miembro fundador y probablemente mejor estudiado de los PIFs. Para abordar esta cuestión, llevamos a cabo análisis de estructura-función generando derivados de PIF7 con los dominios bHLH y APB mutados. En el primer capítulo de este trabajo, mostramos que las actividades de PIF7, tanto de unión al ADN como al phyB están vinculadas y son fundamentales para inducir rápidamente la expresión de genes diana de PIF7 y el crecimiento del hipocótilo en sombra.

Otros componentes clasificados como reguladores positivos y negativos participan en la modulación de SAS mediante la construcción de una compleja red reguladora. Sin embargo, no está claro cómo se organizan estos componentes. Para profundizar en la arquitectura de esta red de señalización y en las conexiones entre sus componentes, en el segundo capítulo de esta tesis realizamos análisis fisiológicos, celulares y transcriptómicos del alargamiento del hipocótilo inducido por la sombra utilizando mutantes deficientes en los diferentes reguladores. Nuestros resultados demuestran que los componentes reguladores del SAS se organizan en dos ramas principales que actúan en momentos ligeramente

diferentes del desarrollo de la plántula y modulan el alargamiento de diferentes células a lo largo del eje del hipocótilo. Además, también encontramos una convergencia de las señales de las dos ramas, ya que los PIFs y ELONGATED HYPOCOTYL 5 (HY5), componentes que pertenecen a estas ramas separadas, regulan la expresión de genes diana comunes.

TABLE OF CONTENTS

TABLE OF CONTENTS

GENERAL INTRODUCTION

GENERAL INTRODUCTION

1. Importance of light in plant life.

Plant life is highly influenced by diverse light conditions in the natural environment. To adapt growth and development to the constantly changing scenario, plants must continuously perceive the surrounding conditions. One of the vital environmental factors that plants need to sense is light, which plays a double function: it is a source of energy to fuel the photosynthesis and gives information about the environment where the plants grow. In the absence of this signal (darkness), plant development is known as **skotomorphogenesis**. By contrast, the light-triggered responses that affect the plant development are known as **photomorphogenesis**. In any case, caption and detection of light as a source of information is carried out by a complex signaling system with photoreceptor molecules as main characters capable to modulate a wide variety of physiological responses such as seed germination, seedling growth, definition of the architecture in the adult plant, regulation of flowering time and facing vegetation proximity (Casal, 2012, 2013; Possart *et al.*, 2014; H. Smith, 2000; Harry Smith, 1982).

2. Plant development in dark conditions.

In darkness (when seeds germinate buried on the soil) seedlings adopt a skotomorphogenic developmental program, in which most of the resources are focalized in the hypocotyl elongation at the expense of cotyledon and root development. As a result, seedlings grown in darkness, known as etiolated seedlings, present a thin and extremely elongated hypocotyl (seeking for the light), with small and yellow cotyledons that remain curled up and unable to carry out photosynthesis that, together with meristematic region, are protected from damage by an apical hook (Josse & Halliday, 2008).

3. Plant development in light conditions.

When seedlings grow under light conditions (de-etiolated or photomorphogenic plants), they present a thick and short hypocotyl, opened and expanded cotyledons (no apical hook) with a green color due to the transformation of etioplasts into photosynthetically active chloroplasts (Arsovski *et al.*, 2012; Han *et al.*, 2007). In this case, plants adopt a photomorphogenic program of development in which a wide variety of photoreceptors,

transcription factors and other molecules such as plant hormones are involved, building a complex regulatory network that has been deeply studied.

4. Plant development in shade conditions.

The fraction of the light spectrum used by plants to perform the photosynthesis is called photosynthetically active radiation (PAR), which corresponds to the visible spectrum of the human eye, from 400 nm or blue light (B) to 700 nm or red light (R). However, in natural conditions PAR radiation does not stay completely constant. Its composition changes during the twilight, when it is enriched in B and far-red light (FR) and also depending on the time of the year, the presence of covering clouds or the proximity of other vegetation (Hughes *et al.*, 1984; Harry Smith, 1982). In dense plant communities, neighboring vegetation can alter light intensity because of a selective reflection and absorption of parts of light spectrum by the photosynthetic pigments at the photosynthetic tissues. Among these pigments, chlorophylls and carotenoids absorb most of the PAR, with peaks of absorbance in B (400-500 nm) and R (600-700 nm). In contrast, some of the green and most of the FR spectrum (700-750 nm) is transmitted through or reflected from the plant tissues what modifies light quality perceived for a subject plant (**Figure 1A**) (Fiorucci & Fankhauser, 2017). These last settings, where plants are affecting PAR levels and light quality, is often referred as shade. When we focus on the effect of the absence or presence of neighboring vegetation on light conditions, we can find three different scenarios:

- Unshaded situation, that happens in low density vegetation communities where plants are growing far enough from each other. In this situation, neighboring plants do not impact the light intensity and quality of sunlight (high B and R) that has a R to FR ratio (R:FR) of about 1.2–1.5 (considered high R:FR) (**Figure 1B**) (Casal, 2013; Martínez-García *et al.*, 2010; Roig-Villanova & Martínez-García, 2016). We mimic these conditions in the lab with continuous white light (W), that provides a R:FR > 1.5.

- In dense plant communities, the transmission through and reflection of FR from plant tissues leads to a local enrichment of FR what lowers the R:FR of horizontally propagated light although the overall light intensity may not be significantly changed (high B and R) (**Figure 1B**) (Casal, 2013; Roig-Villanova & Martínez-García, 2016; Vandenbussche *et al.*, 2005). In many plant species, this scenario induces the activation of a set of responses called Shade Avoidance Syndrome (SAS) that aim to avoid shade (Roig-Villanova and Martínez-García 2016). We name this low R:FR

scenario as **proximity shade** (**Figure 1B**), and we mimic it by applying an extra FR radiation to a fixed intensity of white light (W), that results in a R:FR of about 0.50–0.30 (Martínez-García *et al.*, 2014).

- In very dense plant communities where some plants are growing under a taller plant canopy that produces plant shade, light availability is limited. Below the vegetation canopy, sunlight is depleted in UV-B light and PAR (low B and R) but not so much in FR. This happens because of strong and specific filtration by the leaves in canopy vegetation (**Figure 1A**). Drop in R in this condition results in a R:FR that tends to be lower than in proximity shade, and both, light quality and intensity are affected (**Figure 1B**), e.g., in a forest, the top of the tree crowns is receiving the highest available light irradiation but the amount of irradiation that arrives to the ground is highly reduced. In this example we can observe a vertical light gradient that is reduced when we go down from the top of a tree towards the ground. Understory plants are the ones affected by canopy shade and must survive and efficiently use the available light energy to complete its life cycle under these conditions (Roig-Villanova & Martínez-García, 2016). We name this very low R:FR scenario as **canopy shade** (**Figure 1B**), and in the laboratory, we mimic this scenario by applying higher amounts of FR radiation than in proximity shade conditions to a fixed intensity of white light (W) obtaining a very low R:FR (<0.29) (Martínez-García et al., 2014).

As happens in the unshaded situation, light available for understory plants (growing under canopy shade) is highly heterogeneous and depends on location, the time of the day or season, i.e., light availability can suffer changes during the time of the day or seasonally such as those produced by sun flecks that can appear in a specific moment during the day and increase the irradiation locally in the ground (Sellaro *et al.*, 2011). Moreover, deciduous vegetation loses leaves seasonally or due to a severe dry season what increases light availability for the underneath vegetation. This variability adds complexity to the mechanistic regulation of response to environmental light cues. Overall, plants have adopted two main strategies: shade avoider (sun-loving) plants growing in high vegetation density implement SAS whereas shade tolerant plants have adapted its development to survive in those conditions.
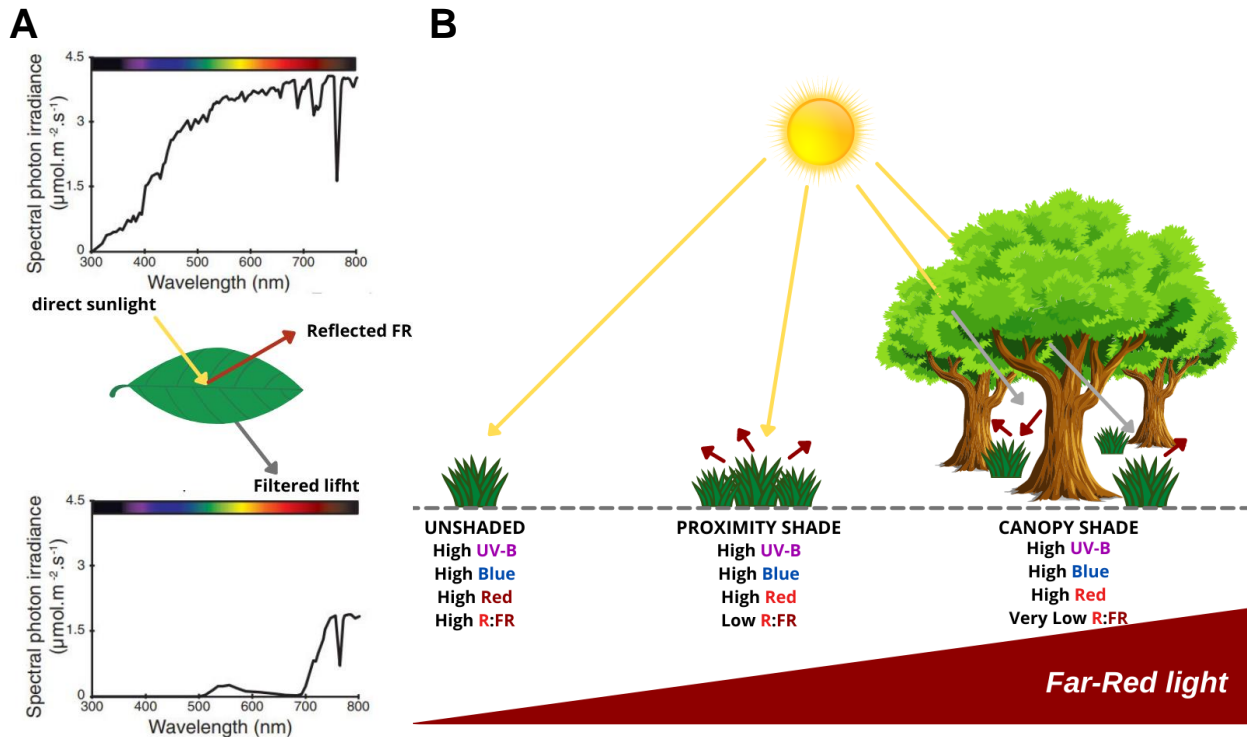
Figure 1. **Vegetation filters and reflects part of the light spectrum producing different shade conditions. (A)** Sunlight (top graph) filtered by green tissues (lower graph) has a much lower amount of PAR. Photosynthetic pigments of green tissues mainly absorb B and R whereas FR is reflected from the leaves. **(B)** Light properties found in unshaded and shaded conditions in nature. When growing in low vegetation density (unshaded) light arriving from the sun contains high amounts of UV-B, B and R and low amounts of FR, what results in a high R:FR. By contrast, when growing in dense vegetation communities, neighbor plants reflect FR. This generates an environment with high amounts of UV-B, B and R but a low R:FR (proximity shade), a cue indicating potential canopy by surrounding plants and competition for light resources. When growing under very dense vegetation, such as below other plants (canopy shade), light perceived by understory vegetation is filtered by green tissues of taller plants and is low in UV-B, B and R and with a very low R:FR. Adapted from Fiorucci & Fankhauser, 2017; Kami *et al.*, 2010.

5. The shade avoidance syndrome in *Arabidopsis thaliana*.

Arabidopsis thaliana is a shade avoider species: when growing isolated sunlight provides light of high R:FR and plants follow its life cycle normally. However, when growing under shade conditions (low or very low R:FR) plants respond by displaying a set of responses known as the Shade Avoidance Syndrome (SAS). As a result of the SAS implementation, a series of phenotypic changes occurs at different organs of the plant and along its entire life cycle (Franklin, 2008; Roig-Villanova & Martínez-García, 2016).

The ability of newly germinated seedlings to thrive in shady areas with low energy resources is reduced. To avoid this detrimental situation, during the seed stage, low R:FR inhibits germination and induces secondary dormancy. The germination is mostly delayed until the light conditions improve, i.e., when light reaches higher R:FR (Shinomura *et al.*, 1996; H. Smith & Whitelam, 1997).

At the seedling stage shade impacts the growth of the hypocotyls, cotyledons and primary leaves. Hypocotyl elongation in response to shade is the best characterized response of Arabidopsis. It is a fast response what makes it a reliable indicator of SAS. Regarding cotyledons and primary leaves, it is known that both expand longitudinally mostly due to a petiole elongation, and also tends to bend upwards, that is, they became hyponastic in response to shade. Finally, blades of cotyledon and primary leaf area decreases in response to shade (Lorrain *et al.*, 2008; Martínez-García *et al.*, 2010, 2014; Tao *et al.*, 2008).

In adult plants, organ elongation responses are also observed. As occurs in the seedling stage, it is observed a petiole elongation and a reduction of the size in leaf blade area. Leaves also became hyponastic. In Arabidopsis, and other rosette plants, shade induces bolting that is characterized by the emergence of cauline stems that elongate more than in unshaded situation. In addition, shade promotes apical dominance resulting in less branching (Franklin, 2008; González-Grandío *et al.*, 2013; Tao *et al.*, 2008). Stem and petiole elongation together with leaf hyponasty help the plant to grow above its neighbors to better capture light to perform the photosynthesis. Nevertheless, the energy employed in elongating to reach light and the early flowering phenotype due to the shade conditions leads to a reduction in the number of seeds produced and a truncated fruit development, a strategy developed by shade avoider plants to produce enough of viable offspring in these unfavorable conditions (Halliday *et al.*, 1994; Martínez-García *et al.*, 2010; H. Smith & Whitelam, 1997).

6. Light perception in plants.

As mentioned, plants do not simply detect the absence or presence of light, they use it as a rich informative signal to detect changes in their environment that impact light intensity, spectral composition, light direction and duration. To be able to obtain this information, Arabidopsis possess at least five types of photoreceptors involved in perceiving different regions of the solar spectrum (Hohm *et al.*, 2013). UV-B RESISTANCE 8 (UVR8) acts as a receptor for the ultraviolet-B light (UV-B: 280-315 nm) (Christie *et al.*, 2012; Galvão & Fankhauser, 2015); cryptochromes (CRY1-3), phototropins (PHOT1 and 2) and zeitlupes

absorb ultraviolet-A light (UV-A: ~315-400 nm) and B (~400-500 nm) (E. Chen *et al.*, 2007; Christie *et al.*, 2012; H. Liu *et al.*, 2011); phytochromes (PHYA-E), the biggest and probably the best-characterized family of photoreceptors, are in charge of mediating responses to R (600-700 nm) and FR (700-750 nm) (Franklin & Quail, 2010; J. Li *et al.*, 2011), such as the reductions in the R:FR associated with proximity and canopy shade. All these receptors control together the photomorphogenic development of seedlings through complex regulatory networks depending on the quantity and quality of the perceived light. Besides UVR8 that uses a triad of tryptophane residues to perceive the light (Jenkins, 2017), all the other known plant photoreceptors are chromoproteins. They are composed of an apoprotein and a covalently or non-covalently bound chromofore (Christie *et al.*, 2015; Rockwell & Lagarias, 2006). Although a brief overview of UVR8, cryptochromes, phototropins and zeiplupes will be given, special attention will be paid to the phytochromes in charge of sensing R:FR and controlling SAS implementation.

6.1. UVR8 and Perception of UV-B light.

UVR8 is the only photoreceptor in Arabidopsis discovered to mediate the UV-B perception. This protein is localized in the cytoplasm and the nucleus, and its abundance is not affected by the UV-B radiation or other kind of light (Heijde & Ulm, 2012). However, after irradiance with UV-B, the receptor acts in the nucleus where it binds to promoters of target genes. UVR8 receptors are naturally found as inactive homodimers; but after perception of UV-B light through specific Tryptophans (Trp), dimers dissociate obtaining active monomers that initiate a signaling cascade (Christie *et al.*, 2012). The active monomers establish interactions with CONSTITUTIVE PHOTOMORPHOGENIC 1 (COP1) to mediate several developmental responses such as inhibition of hypocotyl elongation, accumulation of flavonoids and anthocyanins, downward leaf curling and entrainment of circadian clock (Fierro *et al.*, 2015; Morales *et al.*, 2013; Rizzini *et al.*, 2011; X. Yang *et al.*, 2015). UVR8 has also been involved in SAS responses (Hayes *et al.*, 2014) and it has been suggested that active UVR8 represses auxin biosynthesis and elongation in canopy gaps (Mazza & Ballaré, 2015).

6.2. Cryptochromes, phototropins and zeitlupes perceiving UV-A and blue light.

Cryptochromes (crys) are the first UV-A and B photoreceptors discovered in Arabidopsis, that in this species are encoded by three genes (*CRY1-CRY3*) (Christie *et al.*, 2012). They participate in different processes such as inhibition of hypocotyl elongation, control of

flowering time, circadian rhythms, stomata opening, root development, responses to biotic and abiotic stress, fruit and ovule development, etc. (Q.-H. Li & Yang, 2007). Cry1 and cry2 act mainly in the nucleus and present partially overlapping functions (Shalitin *et al.*, 2002; Wu & Spalding, 2007). In general, cry1 has been implicated in temperature-promoted hypocotyl elongation and cry2 in the regulation of photoperiodic flowering (Y. Liu *et* al., 2013, 2018). In contrast, cry3 may be acting in chloroplasts and mitochondria, although its function is less clear (Kleine *et al.*, 2003). Crys are activated by B that provokes conformational changes and enables interaction with other signaling regulators such as SUPRESSOR OF PHYA-105 1 (SPA1) (Z. Yang *et al.*, 2017; Zuo *et al.*, 2011) and PHYTOCHROME INTERACTING FACTORs (PIFs). Specifically, crys have been shown to interact with PIF4 and PIF5, probably repressing PIFs activity (Pedmale *et al.*, 2016). It has been suggested that a reduction in B, as happens in canopy shade, lower the activity of cry1 signaling pathway leading to a SAS response promotion (Keller *et al.*, 2011).

Phototropins also perceive UV-A and B. They participate in phototropism, stomata opening, inhibition of hypocotyl elongation in response to B, intracellular movements of chloroplasts in response to high amount of light and leaf flattening (Folta *et al.*, 2003; Kinoshita *et al.*, 2001; Łabuz *et al.*, 2012; Sakai *et al.*, 2001). In Arabidopsis there are two genes encoding for phototropins, *PHOTOTROPIN 1 (PHOT1)* and *PHOT2,* with redundant functions. They belong to AGC kinase family and structurally contain two Light Oxygen Voltage (LOV) domains non-covalently bound to flavin chromophores: FMN (FLAVIN MONONUCLEOTIDE) or FAD (FLAVIN ADENINE DINUCLEOTIDE) (Freddolino *et al.*, 2013; Möglich *et al.*, 2010). It has been shown that after perception of B, phototropins are involved in the directional growth of the plants towards the light and bending looking for higher amount of B under shaded conditions (Fiorucci & Fankhauser, 2017).

Another type of UV-A and B photoreceptors are the Zeitlupe family: ZEITLUPE (ZTL), FLAVIN-BINDING KELCH REPEAT F-BOX 1 (FKF1) and LOV KELCH PROTEIN 2 (LKP2). These proteins are structurally similar to phototropins and also contain two LOV domains (Ito *et al.*, 2012). They are involved in processes such as floral transition and entrainment of circadian clock (Christie *et al.*, 2015; Y. H. Song *et al.*, 2014), but they do not seem to participate in SAS regulation.

6.3. Phytochromes.

Phytochromes (phys) are a group of dimeric chromoproteins in charge of detecting R and FR. Each subunit is a holoprotein formed by the apoprotein bound to a chromophore called phytochromobiline (Kreslavski *et al.*, 2018; J. Li *et al.*, 2011). In Arabidopsis, five genes were identified encoding for phytochromes: *PHYA*, *PHYB*, *PHYC*, *PHYD*, *PHYE*. All the phys present the same chromofore but they differ in the apoprotein that is encoded by different genes. Phys exist in two photoconvertible forms: the biologically inactive R-absorbing form (Pr) with a maximum of absorption of R (665 nm), and the biologically active FR-absorbing form (Pfr) with a maximum of absorption of FR (730nm) (Quail *et al.*, 1995). They are synthetized in the cytoplasm in the Pr inactive form, where they remain in this state when the plant is in darkness. After perception of R, Pr form photoconverts into the biologically active form Pfr (Eichenberg *et al.*, 2000). This photoconversion produces a conformational change that includes the exposure of a nuclear localization signal (NLS) that results in the phys translocation into the nucleus (Nagatani, 2004). Both, Pr and Pfr forms present different but overlapped absorption spectrums. Thus, active and inactive phys forms coexist in a dynamic equilibrium that depends on light conditions, specifically on the relative amount of R and FR (R:FR) perceived by the plant (M. Chen *et al.*, 2004; Franklin, 2008). High R:FR produces a higher amount of active Pfr form whereas low R:FR decants the equilibrium towards the inactive Pr form (**Figure 2**). One of the first classifications of the phys was biochemical and showed the existence of two main types: type I, which degrade when they perceive R or white light (W) (photolabile) and predominate in etiolated seedlings; and type II, which do not degrade after exposure to light (photostable) and predominate in de-etiolated seedlings (Clough & Vierstra, 1997).

PhyA is the only one considered a type I because it is photolabile and degraded via the 26S proteasome. It was later determined that phyA was exclusively responsible for de-etiolation under continuous FR, where it accumulates. In fact, *phyA* mutants present a similar phenotype to the wild-type plants when grown under light or R. However, in FR, *phyA* mutants display a skotomorphogenic phenotype (they are blind to that kind of light) what confirms the main role of phyA in perceiving and mediating de-etiolation under monochromatic FR (Dehesh *et al.*, 1993; Nagatani *et al.*, 1993; Parks & Quail, 1993; Reed *et al.*, 1994; Whitelam *et al.*, 1993). Moreover, phyA seedlings show long hypocotyls in B (Neff *et al.*, 2000; Whitelam *et al.*, 1993) what suggests that it also has a role in perception and transduction of B signals. Later it was noticed that phyA also plays a fundamental role in controlling SAS and hypocotyl

elongation, but its activity is only detectable at canopy shade (very low R:FR conditions), conditions in which phyA could accumulate (Martínez-García *et al.*, 2014). PhyB-phyE, are type II photostable phys (Quail, 1997). Among them, phyC is the only one without a role in SAS regulation (Franklin *et al.*, 2003). phyB, D and E have redundant roles (Devlin *et al.*, 1998, 1999), and from them, phyB plays the leading role in controlling photomorphogenesis under monochromatic R (Bae & Choi, 2008) and is the main suppressor of SAS. In fact, *phyB* mutants present a similar phenotype to the wild-type plants when grown under FR whereas under R *phyB* mutants display a very long hypocotyl phenotype (they are almost blind to that kind of light). More importantly, in high R:FR (W) *phyB* mutants present a similar phenotype to that of wild-type seedlings grown in low R:FR (Nagatani *et al.*, 1991; Somers *et al.*, 1991). Active Pfr form of phyB is prevalent in high R:FR and represses SAS and hypocotyl elongation (Martínez-García et al., 2010). Upon perception of shade (low R:FR), most of phyB proteins photoconvert into the inactive Pr form resulting in the promotion of SAS and therefore the shade-triggered hypocotyl elongation (**Figure 2**). The differences in the stability of phyA and phyB are translated in an antagonistic role between them: phyB inhibits SAS under high R:FR and phyA under very low R:FR (Martínez-García *et al.*, 2014).

7. Shade signaling.

7.1. Phytochrome-PIFs light signaling hub.

Phytochromes directly interact with and regulate PHYTOCHROME INTERACTING FACTORS (PIFs). PIFs are a group of transcription factors belonging to the basic helix-loop-helix (bHLH) family of proteins (Leivar *et al.*, 2008; Leivar & Monte, 2014). A total of eight PIFs have been identified in Arabidopsis: PIF1 to PIF8 (Lee & Choi, 2017; Paik *et al.*, 2017). They establish a central signaling hub for light-related developmental processes, including SAS. In unshaded conditions (high R:FR), the phys active form (Pfr) interact with PIFs through the active phyA (APA, only present in PIF1 and PIF3) and active phyB (APB) interacting domains. These interactions leads to the PIFs phosphorylation, ubiquitination and, in the case of PIF1, PIF3, PIF4 and PIF5, also known as PIF Quartet (PIFQ), subsequent fast degradation via proteasome (Al-Sady *et al.*, 2006, 2008; Leivar & Quail, 2011; Lorrain *et al.*, 2008; H. Shen *et al.*, 2008; Y. Shen *et al.*, 2007; Zhang *et al.*, 2013). PIF7 is an exception for these processes. After interaction with phyB, PIF7 is phosphorylated and became unable to interact with the DNA to regulate gene transcription, but contrarily to the other PIFs, this process does not lead to its rapid and dramatic degradation (L. Li *et al.*, 2012).
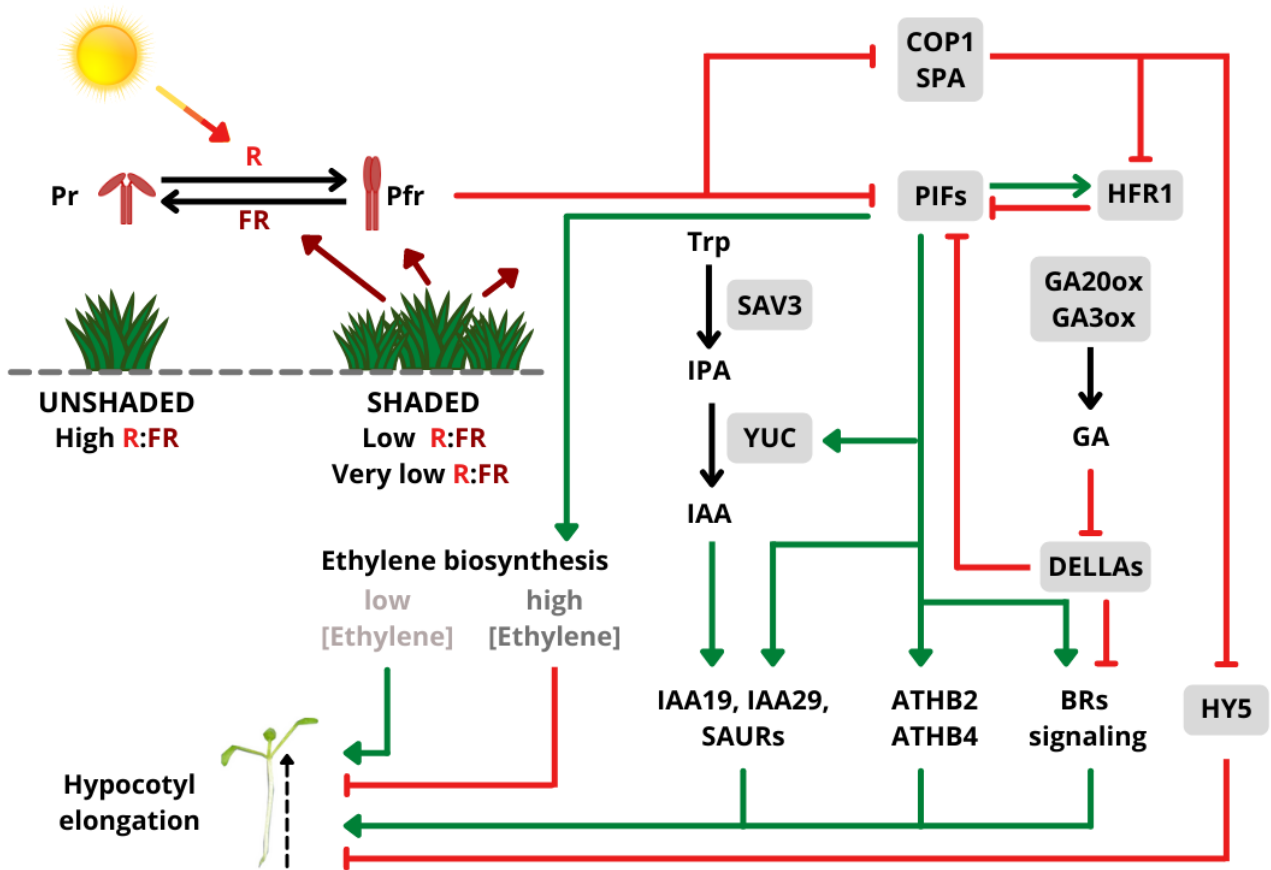
Figure 2. SAS regulation activity is controlled by phytochromes and its photoequilibrium that depends on R:FR ratio. Plants detect vegetation proximity because of changes in the R:FR. When unshaded, phytochrome photoequilibrium is displaced towards the active Pfr form. Under low or very low R:FR phytochrome photoequilibrium decants towards the inactive Pr form. This releases the repression imposed over PIFs that initiate a signaling cascade caused by changes in gene expression of SAS regulators. This cascade results in the shade-induced hypocotyl elongation. Among SAS regulatory players, PIFs, ATHB2, ATHB4, YUCs, IAAs, SAURs, COP1/SPA, and hormones such as auxins, GAs and BRs act as positive regulators. In contrast, HFR1, HY5 and DELLAs act as negative regulators. Ethylene seems to have a dual activity and acts as a SAS repressor or activator depending on its concentration. Adapted from (Pierik & Testerink, 2014; Sheerin & Hiltbrunner, 2017).

Under shade (low R:FR) conditions, phys most abundant inactive form (Pr) is not able to interact with PIFs. Then, PIFs are not phosphorylated and can dimerize and exert its activity as transcription factors modulating gene transcription (**Figure 2**). They bind to E- (CANNGT) and G-boxes (CACGTG) and promote the expression of hundreds of *PHYTOCHOME RAPIDLY REGULATED* (*PAR*) genes, most of them being transcription factors that regulate SAS processes (Roig-Villanova & Martínez-García, 2016) such as the shade-induced hypocotyl elongation. *PAR* genes can be grouped in at least three different families of

transcriptional regulators: (1) bHLH (e.g., BIM1, BEE1, HFR1, PAR1, PAR2, PIL1), (2) homeodomain-leucine zipper (HD-Zip) (e.g., ATHB2, ATHB4, HAT1, HAT2 and HAT3) and (3) B-box Domain Protein (BBX) (e.g., BBX21, BBX22, BBX24, BBX25) (Bou-Torrent *et al.*, 2008; Cifuentes-Esquivel *et al.*, 2013; Gangappa *et al.*, 2013; Roig-Villanova *et al.*, 2006, 2007; Salter *et al.*, 2003; Sessa *et al.*, 2005; Sorin *et al.*, 2009). By performing mutant analysis of these *PAR* genes, their role in SAS regulation was determined, classifying them as positive (BEEs, BIMs, BBX24, BBX25) or negative (HFR1, PAR1, PAR2, PIL1) SAS regulators.

In particular, the negative bHLH regulators LONG HYPOCOTYL IN FAR-RED 1 (HFR1), PHYTOCROME RAPIDLY REGULATED 1 (PAR1) and PAR2 lack the ability to bind the DNA but they are able to form competitive heterodimers with PIFs to prevent the excessive hypocotyl elongation (Galstyan *et al.*, 2011; Hornitschek *et al.*, 2009) in a negative feedback regulation module. Together with phys, this type of negative loops provides another level of PIFs activity regulation to modulate hypocotyl growth in shade.

Another negative regulator, the bZIP transcription factor ELONGATED HYPOCOTYL 5 (HY5) regulates the shade-induced hypocotyl elongation. In this case, *HY5* expression is induced by shade more slowly in a phyA dependent manner (Ciolfi *et al.*, 2013), hence it cannot be considered a *PAR* gene. The mechanism by which it fulfills this negative function in SAS regulation is not well described (Nawkar *et al.*, 2017). However, it is known that phys and crys inhibit the activity of COP1/SPA E3 ubiquitin ligase which mediates the ubiquitin-degradation of some proteins such as HFR1 and HY5. Then, the inhibition of COP1/SPA E3 ubiquitin ligase by active photoreceptors stabilizes HY5 and HFR1 increasing their potential to inhibit hypocotyl elongation (**Figure 2**).

7.2. Hormones involved with Shade Avoidance Syndrome.

Besides phys, PIFs and other transcriptional regulators mentioned above, hormones also play an important role in modulating SAS responses. Among plant hormones, auxins, brassinosteroids (BRs) and gibberellins (GAs) are considered as growth inducers whereas cytokinins (CKs) are considered as inhibitors of growth. Ethylene represents a special case because it has opposite effects in the growth depending on its concentration (Pierik *et al.*, 2004).

In the case of auxins, their implication in hypocotyl elongation in response to shade has been established (Bou-Torrent *et al.*, 2014; de Wit *et al.*, 2015; Roig-Villanova *et al.*, 2007).

GENERAL INTRODUCTION

It is well known that PIFs control auxin biosynthesis and signaling (Hornitschek *et al.*, 2012). The endogenous and bioactive auxin indole-3-acetic acid (IAA), is produced from Tryptophan (Trp) through the SHADE AVOIDANCE 3 enzyme (SAV3, also known as TRYPTOPHAN AMINOTRANSFERASE OF ARABIDOPSIS 1, TAA1) that converts Trp into indole-3-pyruvic acid (IPA). Finally, IPA is transformed into IAA by a group of flavin monooxygenases called YUCCA (YUC) enzymes (**Figure 2**). *YUC* genes play an important role in SAS, i.e. *yuc2589* mutant does not present responses to low R:FR (Kohnen *et al.*, 2016; Müller-Moulé *et al.*, 2016). Moreover, expression of some *YUCs*, including *YUC2*, *YUC5*, *YUC8* and *YUC9*, is induced under low R:FR in a PIF-dependent manner (**Figure 2**) (Hornitschek *et al.*, 2012; Kohnen *et al.*, 2016; L. Li *et al.*, 2012).

Gibberellins (GAs) biosynthesis is also promoted by low R:FR and is involved in the stimulation of hypocotyl growth (Bou-Torrent *et al.*, 2014). Bioactive GAs, synthetized by GA3ox and GA20ox, are able to interact with GIBBERELLIN-INSENSITIVE DWARF 1 (GID1) receptor, leading to polyubiquitination and subsequent degradation of DELLAs (Leone *et al.*, 2014; Schwechheimer & Willige, 2009). DELLAs are able to bind to PIFs (e.g., PIF4) (De Lucas *et al.*, 2008) and inhibits PIF DNA-binding activity. Then, the shade-induced DELLAs degradation releases PIFs allowing the promotion of hypocotyl growth (**Figure 2**).

Brassinosteroids (BRs) act as positive regulators of the shade-induced hypocotyl elongation, i.e., the BR biosynthesis mutant *drarf1* is unable to promote the hypocotyl growth caused by shade (Luccioni *et al.*, 2002). It has been shown that low R:FR increases sensitivity to BRs and full hypocotyl-growth response to shade requires these hormones (Casal, 2012; Keller *et al.*, 2011; Keuskamp *et al.*, 2011). BR signaling is connected to GAs signaling through DELLAs, which negatively regulate BR signaling by binding the positive regulator of the BR signaling BRASSINAZOLE-RESISTANT 1 (BZR1) and reducing the expression of BR-responsive genes (**Figure 2**) (Bai *et al.*, 2012; Gallego-Bartolomé *et al.*, 2012; Qian-Feng *et al.*, 2012). A recent study suggests that phyA inhibits hypocotyl elongation through repressing BRs pathway, by reducing COP1 nuclear speckles leading to changes in downstream genes such as PIF4, PIF5 and HY5, that together regulate BRI1-EMS-SUPPRESSOR 1 (BES1)/BZR1 activity, BRs biosynthesis and BRs target genes *(B. Song et al.*, 2020).

Although ethylene signaling components under shade still needs further investigation, it is known that low R:FR can enhance the production of ethylene in wild-type tobacco (Pierik

et al., 2004). Ethylene signaling seems to present a dual mechanism in regulating the shade response that depends on ethylene concentration: under low concentrations stimulates growth whereas under high concentration inhibits growth (Pierik *et al.*, 2004). (**Figure 2**).

8. An alternative strategy in response to shade: shade tolerance.

As mentioned, *A. thaliana* and many other plants, including most crops, are shade-avoider (or sun-loving) species. However, shade-tolerant plants, such as those that grow in the understory, have adapted to thrive in close proximity or under other plants, where light amount can be limiting for other plant (shade-avoider) species. Shade tolerance often refers to the ability of plants to tolerate low light levels and it is also defined as the minimum amount of light required for plants to survive. Two main hypotheses have been formulated to describe traits responsible to shade tolerance: (1) improvement in the efficiency of light use, including higher photosynthetic capacity and consequently a better carbon gain (Givnish, 1988; Niinemets & Tenhunen, 1997) and (2) maximization of the tolerance to stress (Kitajima, 1994).

To understand shade tolerance, it is fundamental to decipher how these plants are capable to grow with vegetation proximity or direct canopy shade (low R:FR and very low R:FR) without promoting some SAS responses, such as shade-induced hypocotyl elongation. Regarding the hypocotyl response, in contrast to the shade-avoider species Arabidopsis, its close relative *Cardamine hirsuta* is a shade-tolerant species, i.e. its hypocotyls are unresponsive to shade (Hay *et al.*, 2014; Molina-Contreras *et al.*, 2019). This makes *C. hirsuta* a good model species to study divergent physiological traits in *Brassicaceae*, such as insights of evolutionary, genetic and molecular differences that stablish these two divergent strategies: tolerate or avoid shade. Up to now, comparative genetic analyses of *A. thaliana* and *C. hirsuta* have shown that differential activity of related orthologous components can result in the divergent shade responses. For instance, the activities of phyA and HFR1, known to be SAS negative regulators in *A. thaliana*, are enhanced in *C. hirsuta*, which contribute to the lack of shade-induced hypocotyl elongation in the latter species (Molina-Contreras *et al.*, 2019; Paulišić *et al.*, 2021). It seems therefore that these divergent strategies are implemented using the same components that work differently in both species. Therefore, a better understanding of how the shade-induced hypocotyl elongation works in the reference species *A. thaliana* might eventually help to better know how different plants adopt either a shade-avoider or a shade-tolerant strategy to respond to vegetation proximity.

OBJECTIVES

OBJECTIVES

OBJECTIVES

The general objective of the present work is to expand the current knowledge about the regulation of the shade avoidance syndrome (SAS) in *Arabidopsis thaliana*. Specifically, we aim to better understand the mechanisms and molecular connections between the SAS regulatory components that modulate the shade-induced hypocotyl elongation response. To this goal, we defined two specific objectives:

1. Structure-function analysis of PIF7. We aim to establish if the phyB- and DNA- binding activities are both required for the PIF7 role as a positive SAS regulator. We also aim to study the effect of shade on PIF7 activity and binding capacity to its target genes.

2. Refining the architecture of SAS regulatory network. We aim to clarify the relationship between the main components in charge of modulating the shade-triggered hypocotyl elongation by deepening in the temporal and spatial regulation of this response, i.e., to establish when the different regulators act during seedling development and whether the signals provided by the SAS regulators converge in modulating the elongation of the same or different cells along hypocotyl axis.

OBJECTIVES

CHAPTER I

Chapter II is a research article planned for publication:

The shade avoidance syndrome: uncoupling photoreceptor and PIF7 activities in controlling hypocotyl elongation in Arabidopsis

Pedro Pastor-Andreu[1], Sandi Paulisic[1], Jordi Moreno-Romero[1,2], Jaime F. Martínez-García[1,2]*

[1] Centre for Research in Agricultural Genomics (CRAG), CSIC-IRTA-UAB-UB, Cerdanyola del Vallès, 08193-Barcelona, Spain.

[2] Institute for Plant Molecular and Cell Biology (IBMCP), CSIC-UPV, 46022-València, Spain

ABSTRACT

Phytochrome Interacting Factors (PIFs) are transcription factors that form a central signaling hub for light regulated processes such as the *Arabidopsis thaliana* seedlings hypocotyl elongation in response to proximity vegetation or shade. Eight different PIFs have been described: PIF1-8. They contain an Active Phytochrome Binding motif (APB) involved in the interaction with active (Pfr) Phytochrome B (PhyB) and a basic helix-loop-helix (bHLH) domain associated to DNA-binding. When seedlings are grown under shade conditions, PIFs release from interaction with PhyB and initiate a signaling cascade leading to the shade-induced hypocotyl elongation. Among PIFs, the photostable PIF7 has a major role in promoting this response whereas other PIFs play a secondary role in modulating hypocotyl growth in shade. It is unknown if PIF7 DNA- and phyB-binding activities can regulate different aspects of the light-regulated development, as it occurs in PIF3, where these activities are, at least, partially uncoupled. In the present work we demonstrate that (1) punctual mutations in bHLH domain abolish PIF7 ability to promote hypocotyl growth in response to shade and the expression of genes involved in that process; (2) punctual mutations in the APB motif lead to a more photostable and constitutive active PIF7 with ability to bind DNA with the same strength independently of light/shade conditions.

1. INTRODUCTION

When facing vegetation proximity (shade), shade-avoider species such as *Arabidopsis thaliana* initiate a set of responses known as the Shade Avoidance Syndrome (SAS). The best characterized SAS response is arguably the promotion of hypocotyl elongation in seedlings (Casal, 2012; Cole *et al.*, 2011). SAS responses are initiated after perception of changes in the Red (R) to Far-Red light (FR) ratio (R:FR) caused by nearby vegetation. When the plant is growing isolated and unshaded, i.e., without any nearby competitors, light has a high R:FR. By contrast, when the plant is close to and/or shaded by other plants, surrounding vegetation reflects specifically FR and produces a decrease in the R:FR. In the laboratory, vegetation proximity or shade is mimicked by enriching white light (W) with FR (W+FR), a treatment known as simulated shade.

The changes in the R:FR are detected by the phytochromes photoreceptors. Phytochromes exist in a photoequillibrium between an inactive (Pr) and an active (Pfr) form. The displacement of the equilibrium to one or the other isoform depends on the R:FR. Under high R:FR, the equilibrium decants towards the active Pfr form. This active form can bind to a group of proteins known as PHYTOCHROMES INTERACTING FACTORS (PIFs) (Duek & Fankhauser, 2005; Leivar & Quail, 2011) and inhibits their activity. PIFs are transcription factors, so phytochrome-mediated repression prevents PIF-driven regulation of expression of genes involved in the SAS implementation. By contrast, low R:FR displaces the photoequillibium towards the inactive Pr form what relieves repression imposed over PIFs. This allows PIFs to accumulate and/or interact with DNA regulatory elements, that results in the initiation of the shade-triggered changes of expression on genes with a role in promoting hypocotyl elongation (Leivar, Monte, Al-Sady, *et al.*, 2008; Leivar & Monte, 2014).

PIFs, that were first identified in *Arabidopsis thaliana*, are members of the basic helix-loop-helix (bHLH) family of transcriptional regulators. The bHLH domain allows (i) to dimerize via the HLH and (ii) to bind specific DNA sequences via the basic domain as dimers. As most bHLH proteins, PIFs bind preferentially a type of E-box (CANNTG) variants known as PIF binding E-box (PBE-box, CACATG and CATGTG) and G-box (CACGTG) motifs (Hornitschek et al., 2012; Leivar & Monte, 2014; Oh et al., 2012; Toledo-Ortiz et al., 2003; Zhang et al., 2013). In addition to the bHLH domain, all known PIFs contain an Active Phytochrome B-binding (APB) region, which is necessary and sufficient for active phyB-specific binding (Chen & Chory, 2011; Khanna *et al.*, 2004; Leivar & Quail, 2011). Some PIFs (e.g., PIF1 and PIF3)

also contain an Active Phytochrome A-binding (APA) motif which is needed for active phyA-specific binding (Al-Sady *et al.*, 2006; H. Shen *et al.*, 2008).

Although there is a total of eight PIFs characterized (Leivar, Monte, Al-Sady, *et al.*, 2008; Leivar & Monte, 2014; Leivar & Quail, 2011; Paik et al., 2017) the best studied are PIF1, PIF3, PIF4 and PIF5, also called the PIF quartet (PIFQ). These PIFs have an important role in repressing seedling de-etiolation. Based on the current information, in the dark phytochromes are inactive, PIFs accumulate and bind to DNA that represses photomorphogenesis (promote etiolated phenotype). After light exposure, activation of phyA and phyB leads to interaction with PIFs that triggers rapid degradation of these PIFQ and relieves repression of photomorphogenesis, resulting in seedling de-etiolation (Lorrain *et al.*, 2008; Zhang *et al.*, 2013). Consequently, *pifq* mutants (deficient in all PIFQ members) display photomorphogenic phenotype in the dark (Leivar *et al.*, 2009; Leivar, Monte, Oka, *et al.*, 2008; Shin *et al.*, 2009).

The other PIF with a known role is PIF7, that is a major player in promoting the shade-induced hypocotyl elongation while it has a minor role in repressing seedling de-etiolation (Cole *et al.*, 2011; Li *et al.*, 2012; Lorrain *et al.*, 2008). Consistent with having an APB domain but no an APA domain, PIF7 can interact with phyB but not with phyA (Leivar, Monte, Al-Sady, *et al.*, 2008). This interaction does not result in a rapid degradation of this PIF, pointing that, in contrast with PIFQ, PIF7 is quite photostable (Leivar, Monte, Al-Sady, *et al.*, 2008). Nonetheless, the activity of PIF7 is controlled by the rapid changes in its phosphorylation status in response to shade. Indeed, under high R:FR, phyB interaction with PIF7 results in its phosphorylation, and under low R:FR, phyB deactivation results in PIF7 de-phosphorylation. Phosphorylation reduces its binding to E-boxes in the promoters of its targeted genes (Li *et al.*, 2012). The phosphorylation state of PIF7 is also important to determine its cellular localization. The phosphorylated form is accumulated in the cytoplasm, presumably sequestered by 14-3-3 proteins, a group of proteins that can interact with the phosphorylated forms of their target proteins in response to certain signals, and this binding finalizes the signaling event by enabling a change in the subcellular localization *(Huang et al.*, 2018). When exposed to low R:FR, unknown phosphatases dephosphorylate PIF7 provoking the release from 14-3-3 proteins and the migration to the nucleus, where exerts its activity as a transcription factor initiating changes in gene expression that result in the promotion of hypocotyl growth (Huang *et al.*, 2018; Li *et al.*, 2012). Overall, the current view on how PIF7 acts is that under high R:FR (i.e., low-planting density environments), phyB

interaction results in a phosphorylated form that has little DNA-binding and/or transcriptional activity. This suggests that PIF7 phosphorylation is controlled by phyB activity, that may directly transfer the light signal to DNA-bound PIF7 to affect its phosphorylation status and hence PIF7 target gene expression. Previous analyses in PIF3 showed that its DNA-binding is not required to modulate the hypocotyl elongation under R (Al-Sady *et al.*, 2008), suggesting that the DNA-binding activity is not strictly required for full PIF3 activity. It is however unknown if (1) PIF7 DNA- and phyB-binding activities can regulate different aspects of the light-regulated development, as it occurs in PIF3 (Al-Sady *et al.*, 2008).

The present study aims to deepen in the PIF7 mechanism acting as a transcriptional regulator modulating the shade-induced hypocotyl elongation. We performed a detailed structure-function analysis of PIF7 by *pif7* mutant rescue experiments with transgenically expressed PIF7 mutated derivatives in Arabidopsis. After analyzing the biological activity of these mutated variants in the SAS regulation, we used them as tools to understand PIF7 ability to bind the DNA depending on light conditions and to identify new PIF7 target genes.

2. RESULTS

2.1. Transgenic lines expressing different PIF7 derivatives differ in the shade-induced hypocotyl elongation response.

PIF7 primary structure analyses identified the APB motif in the 5-16 amino acids (Leivar, Monte, Al-Sady, *et al.*, 2008) and the bHLH domain between the 165-216 amino acid positions (Roig-Villanova *et al.*, 2007) from the first N-terminal methionine (**Figure X1A**). Based on that information, we cloned three PIF7 derivative constructs, using cDNA as a source of PIF7 coding sequence (therefore without introns): (1) a wild-type form of PIF7 (PIF7wt), (2) a PIF7 derivative with the bHLH domain mutated (PIF7Bm) and (3) a PIF7 variant with the APB motif mutated (PIF7APBm) (**Figures X1B-D**). The mutations in the sequences were selected based on mutations previously demonstrated to abolish PIF1 and PIF3 interaction with the DNA and with active phyB (Al-Sady *et al.*, 2008; H. Shen *et al.*, 2008) and PIF7 interaction with phyB (Leivar, Monte, Al-Sady, *et al.*, 2008). In particular, the mutations introduced in PIF7 produced a change of Glu in the position 175 by an Asp (E175D) in the PIF7Bm derivative (**Figure X1A, C**) and changes of Glu in position 8 and Gly in position 14 by Ala in both places (E8A and G14A) in the case of PIF7APBm derivative (**Figure X1A, D**).

Each of the three derivatives were fused to a triple hemagglutinin tag (3xHA) in the C-terminal end for immunodetection purposes. Finally, these PIF7-derivative coding sequences were expressed under the control of fragment of about 2 Kbp (1961 bp) of the *PIF7* promoter (*pPIF7*) (**Figure X1B-D**). The Arabidopsis *pif7-1* mutant (in Col-0 background) was transformed which the resulting constructs and the obtained lines were named as follows: (1) *pif7*^{PIF7wt}, containing the PIF7wt derivative (*pPIF7:PIF7wt-3xHA*, **Figure X1B**); (2) *pif7*^{PIF7Bm}, containing PIF7Bm (*pPIF7:PIF7Bm-3xHA*, **Figure X1C**); (3) *pif7*^{PIF7APBm} containing PIF7APBm (*pPIF7:PIF7APBm-3xHA*, **FigureX1D**).

After selecting for antibiotic resistance (hygromycin), we obtained 20, 17 and 23 resistant lines (independent T1 lines) of the *PIF7wt*, *PIF7Bm* and *PIF7APBm* derivatives, respectively. In the T2 generation, we identified 11, 5 and 8 lines with only one insertion of the *PIF7wt*, *PIF7Bm* and *PIF7APBm* T-DNAs, respectively. Once in homozygosis (T3 generation), we grew Col-0, *pif7*, *pif7*^{PIF7wt}, *pif7*^{PIF7Bm} and *pif7*^{PIF7APBm} during 7 days in continuous white light (W) to measure relative *PIF7* expression in each line. As expected, *PIF7* transcript was detected in Col-0 but not in *pif7* mutant seedlings. Among all the lines obtained, we selected

two that presented similar *PIF7* relative expression levels with Col-0: *pif7*^{PIF7wt} lines #12 and #13 (**Figure X2A**), *pif7*^{PIF7Bm} lines #01 and #17 (**Figure X2B**) and *pif7*^{PIF7APBm} lines #02 and #21 (**Figure X2C**).

A

Figure X1. Generated PIF7 derivatives with different mutations used to transform *pif7*. (A) Amino acid sequence of the ORF of PIF7 derivatives used in this work. The first methionine is highlighted in grey, the APB motif in blue and the bHLH domain in yellow (the basic domain is underlined). Targeted amino acids for the directed mutagenesis are underlined and highlighted in green in the PIF7wt and mutated amino acids in red background in the PIF7APBm and PIF7Bm. Schematic representation of the transgenic **(B)** *PIF7wt*, **(C)** *PIF7Bm* and **(D)** *PIF7APBm* ORFs fused to the 3xHA tag used to transform *pif7* plants. They were expressed under the control of 1961 bp promoter region (*pPIF7*). Introduced mutations to impair the basic and the APB regions in the PIFBm (E175D) and PIFAPBm (E8AG14A) derivatives are indicated in the corresponding panels.

Next, we examined if the different PIF7 derivatives were able to complement *pif7* mutation by measuring the hypocotyl elongation in response to simulated shade. To do that, we grew

the *pif7*^{PIF7wt}*, pif7*^{PIF7Bm} and *pif7*^{PIF7APBm} lines either 7 days in W or 2 days in W and 5 days in simulated shade (W+FR). As controls, we included Col-0 and *pif7* seedlings, that present similar hypocotyl length in W but clearly differ in W+FR: Col-0 hypocotyls strongly elongate in W+FR in contrast to the mild elongation of those of *pif7* (**Figure X2D-F and Supplementary Figure X1**) consistent with published information (Li *et al.*, 2012; Paulišić *et al.*, 2021). In W, hypocotyls of *pif7*^{PIF7wt} seedlings were significantly longer than those of Col-0 and *pif7*, indicating that the *PIF7wt* transgene was active in promoting elongation even in W. In W+FR, *pif7*^{PIF7wt} seedlings responded by elongating their hypocotyls that, however, did not reach the length of Col-0 seedlings (~5 mm vs. almost 7 mm) (**Figure X2D and Supplementary Figure X1**). Hypocotyls of *pif7*^{PIF7Bm} lines were not significantly different from those of *pif7* seedlings in both W and W+FR (**Figure X2E and Supplementary Figure X1**), indicating that the *PIF7Bm* transgene was inactive in promoting elongation in any of the two conditions analyzed. As *pif7*^{PIF7wt} seedlings, hypocotyls of *pif7*^{PIF7APBm} lines were significantly longer in comparison with Col-0 and *pif7*, indicating a PIF7-driven promotion of hypocotyl elongation in W. However, W-grown *pif7*^{PIF7APBm} seedlings were longer than those of *pif7*^{PIF7WT}, suggesting that *PIF7APBm* was more active than *PIF7wt* in promoting elongation in W. In W+FR, *pif7*^{PIF7APBm} lines hypocotyl length was also induced compared to W (**Figure X2F and Supplementary Figure X1**).

We represented the difference in hypocotyl length of W+FR and W (**Figure X2G-I**) to analyze the elongation increase due to the PIF7 derivatives in response to shade, i.e., whether activity of transgenic *PIF7* derivative was enhanced in response to shade. This representation showed that Col-0 elongated the most in response to W+FR (ca. 6 mm difference) and *pif7* showed a remaining but significant elongation of about 1.5-2.0 mm. Transgenic *pif7*^{PIF7wt} lines elongated more than *pif7* but not as much as Col-0 indicating that *PIF7wt* partially rescue the *pif7* phenotype (**Figure X2G**). Importantly, this result indicated that *PIF7wt* activity was enhanced by W+FR. By contrast, *pif7*^{PIF7Bm} lines elongated as non-transformed *pif7* (**Figure X2H**), reinforcing that *PIF7Bm* had no biological activity. Interestingly, *pif7*^{PIF7APBm} lines elongated as *pif7* seedlings (**Figure X2I**), indicating that *PIF7APBm* was active in promoting growth in W but its activity was not enhanced in response to shade, in clear contrast with *PIF7wt*.
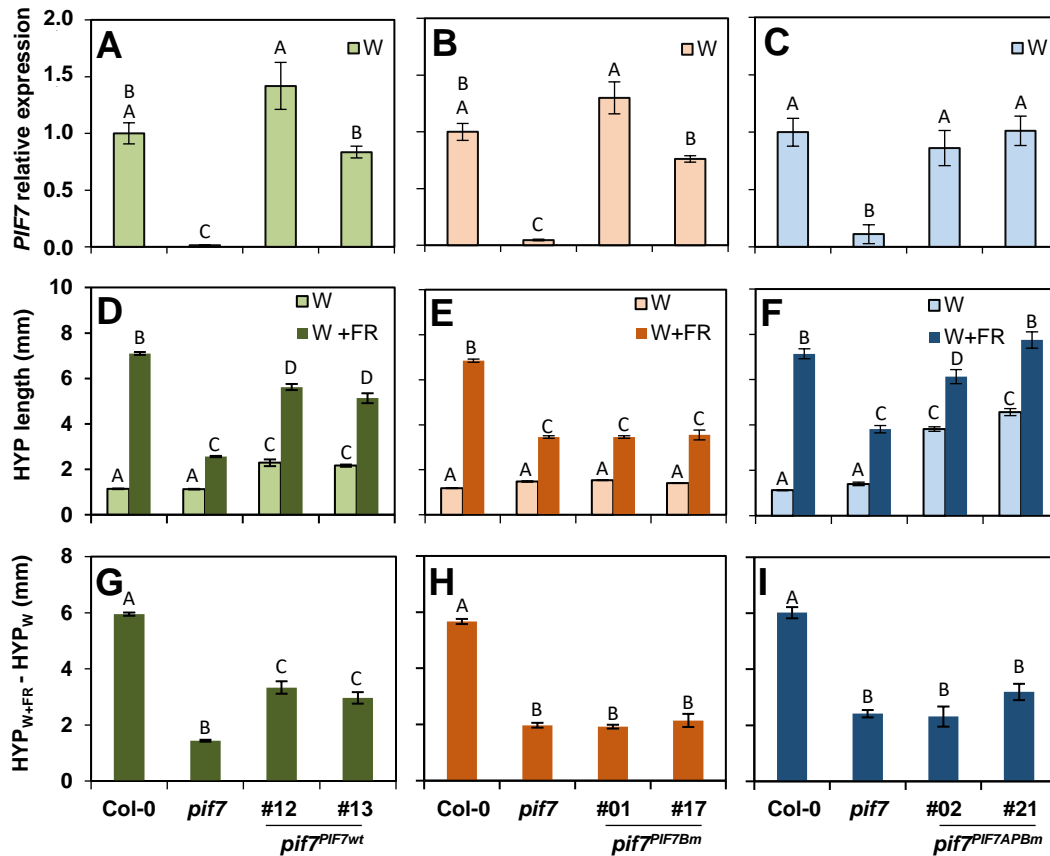
Figure X2. PIF7 derivatives confer different hypocotyl elongation in response to W and W+FR. Relative *PIF7* transcript in Col-0, *pif7-1* and **(A)** *pif7^PIF7wt*, **(B)** *pif7^PIF7Bm* and **(C)** *pif7^PIF7APBm* lines. Seedlings were grown for 7 days in W. *UBIQUITIN 10* (*UBQ10*) was used as endogenous reference gene to normalize the expression of *PIF7*. Hypocotyl elongation in W and W+FR of Col-0 and *pif7-1* compared with **(D)** *pif7^PIF7wt*, **(E)** *pif7^PIF7Bm* and **(F)** *pif7^PIF7APBm* lines. Seedlings were germinated and grown for 2 days in W and then kept in W for 5 days or transferred to W+FR for 5 additional days. Values are means ± SE of three independent biological replicas **(A-F)**. Difference in hypocotyl length in W+FR and W (HYP$_{W+FR}$-HYP$_W$) for Col-0, *pif7-1* and **(G)** *pif7^PIF7wt*, **(H)** *pif7^PIF7Bm* and **(I)** *pif7^PIF7APBm* lines. **(G-I)** HYP$_{W+FR}$-HYP$_W$ was calculated for each of three biological replicas. Values are means ± SE of three independent biological replicas. In all panels, different letters denote significant differences among means (one-way ANOVA with the Tukey test, P-value < 0.05).

2.2. Both APB and basic domains are needed for the shade-induced regulation of *PIF7* target gene expression.

Exposure of Arabidopsis wild-type seedlings to simulated shade rapidly induces the expression of various direct target genes of PIF7, including *PIF3-LIKE 1* (*PIL1*), *YUCCA8* (*YUC8*) and *YUC9* (Ciolfi *et al.*, 2013; Li *et al.*, 2012; Molina-Contreras *et al.*, 2019). As these three genes are direct targets of PIF7 (therefore, their shade-induced expression is PIF7-dependent), in *pif7* seedlings their shade-induction was absent or strongly attenuated (Jiang *et al.*, 2019; Li *et al.*, 2012). We wanted to analyze the activity of our PIF7 derivatives in

rescuing this shade-induced expression. W-grown 7-day-old seedlings were treated for either 1 h of W+FR or W to analyze the induction of *PIL1*, *YUC8* and *YUC9* (**Figure X3**). The expression of these three genes was highly induced by shade in Col-0 but not in *pif7* mutant seedlings, as expected. Nonetheless, the expression of the three marker genes was slightly different. In W, the relative expression of *PIL1* was similar in Col-0, *pif7, pif7^{PIF7wt}* and *pif7^{PIF7Bm}* lines whereas it was strongly induced (10-15 fold) in *pif7^{PIF7APBm}* seedlings (**Figure X3A**). In W+FR, *PIL1* expression was induced 18 fold in Col-0 and about 4 fold in *pif7* seedlings. In *pif7^{PIF7wt}* lines, *PIL1* expression was induced to almost similar levels as Col-0 (line #12 with comparable expression levels to those of Col-0), whereas that in *pif7^{PIF7Bm}* was comparable to *pif7.* In W+FR, *PIL1* expression in *pif7^{PIF7APBm}* was even higher than in W (**Figure X3A**).
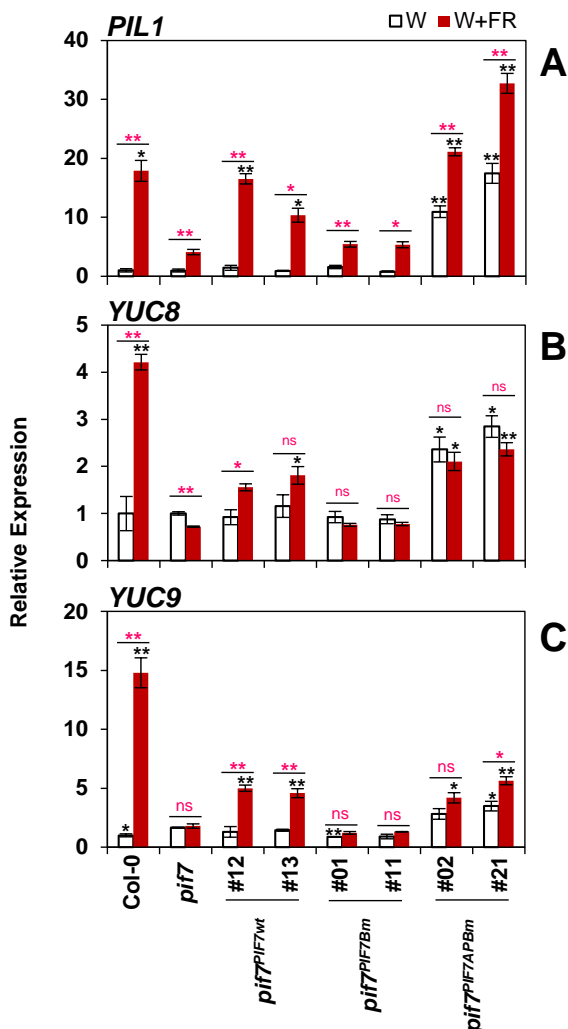
Figure X3. PIF7 derivatives confer different transcriptional response of three shade-regulated genes in W and W+FR. Relative expression of **(A)** *PIL1*, **(B)** *YUC8* and **(C)** *YUC9* in 7-days old Col-0, *pif7-1*, *pif7^{PIF7wt}*, *pif7^{PIF7Bm}* and *pif7^{PIF7APBm}* lines in W and W+FR. Seedlings were grown 7 days in W and then treated with either 1 h of W or W+FR. Expression values are the means ±SE of three independent biological replicates relative to the data of 7 days old wild-type transcript. *ELONGATION FACTOR 1α* (*EF1α*) was used as endogenous reference gene to normalize the expression. Black asterisks mark significant differences between genotypes and *pif7* in the same light conditions and pink asterisk mark significant differences between W and W+FR for each genotype. Student t-test: ** p-value < 0.01; * p-value < 0.05; ns, not significant.

In W, *YUC8* relative expression was not significantly different in Col-0, *pif7*, *pif7^{PIF7wt}* and *pif7^{PIF7Bm}*, but it was higher in *pif7^{PIF7APBm}* (2-3 fold) (**Figure X3B**), as happened in *PIL1*. Similarly, *YUC9* relative expression was not significantly different in *pif7*, *pif7^{PIF7wt}*, *pif7^{PIF7Bm}*

(line #11) and in *pif7^PIF7APBm* (#line 02). However, it was significantly lower in Col-0 and *pif7^PIF7Bm* (line #01) and significantly higher in *pif7^PIF7APBm* (#line 21) compared to *pif7* (**Figure X3C**). Shade treatment produced a significant increase in the relative amount of *YUC8* and *YUC9* in Col-0, less strongly in *pif7^PIF7wt*, and a mild induction in *pif7^PIF7APBm* (line #21). No significant changes in expression were found in *pif7^PIF7Bm* and *pif7^PIF7APBm* (line #02).

In summary, (1) the *pif7^PIF7wt* lines, that presented wild-type levels of expression in W, showed shade-induced expression of *PIL1*, *YUC8* and *YUC9* although attenuated when compared to Col-0; (2) *pif7^PIF7Bm* expression levels of these genes in W and W+FR mimicked those observed in *pif7* in the same conditions, and (3) *pif7^PIF7APBm* lines, that already presented their expression induced in W, showed a shade-induced expression similar to that observed in *pif7* for *YUC8* and more responsive for *YUC9* and *PIL1*.

2.3. PIF7APBm protein is more abundant than PIF7wt and PIF7Bm.

Accumulation of transgenic PIF7 derivatives was studied by immunoblot assay after growing for 7 days in W and then transferred to W+FR for 1 h (**Figure X4A**). Despite the differences in loading detected with an anti-actin antibody, a faint band corresponding to PIF7 proteins was detected using an anti-HA antibody in the *pif7^PIF7wt* and *pif7^PIF7Bm* seedlings. The results indicated that these two PIF7 derivatives accumulated to similarly low but detectable levels (**Figure X4B**). In contrast, PIF7APBm accumulated to much higher levels than PIF7wt protein (**Figure X4C**). Thus, although all PIF7 derivatives were translated into protein, PIF7APBm strongly accumulated compared to the other two PIF7 derivatives. As all transgenic lines had similar *PIF7* RNA expression levels (**Figure X2A-C**), these observations suggest that PIF7APBm is more stable than the other two PIF7 derivatives.
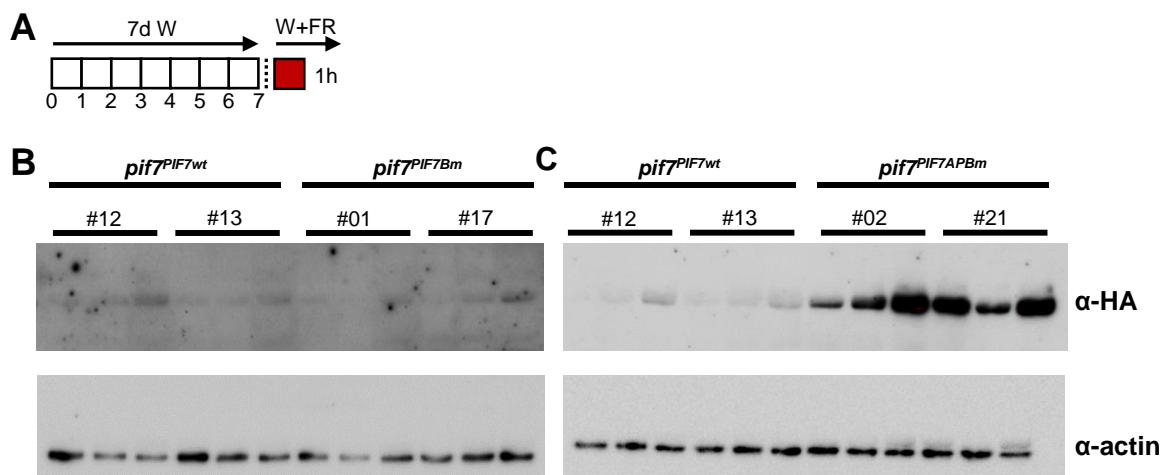
Figure X4. PIF7APBm accumulates to higher levels than PIF7wt and PIF7Bm derivatives. (A) Schematic representation of the light conditions used to carry out the immunoblot assay. Immunoblot analyses to identify PIF7wt, PIF7Bm and PIF7APBm from two *pif7^PIF7wt^*, two *pif7^PIF7Bm^* lines **(B)** and two *pif7^PIF7APBm^* lines **(C)**. For each line, three biological replicas were extracted. PIF7-3xHA derivatives were detected with an α-HA antibody (upper part of the immunoblot images) and an α-actin antibody was used as a loading control.

To study differences in photostability between the three types of transgenic lines, seedlings were grown in W and at day 7 they were differentially treated with W or W+FR for a few hours (**Figure X5**). As PIF7wt and PIF7Bm were accumulated at very low levels, to increase the detection, in this experiment PIF7 derivatives seedlings of all three lines were treated with MG132, a 26S proteasome inhibitor effective in blocking protein degradation and known to be effective in the study of photolabile PIFs (Lee & Goldberg, 1998; Yu Shen *et al.*, 2007). After 3 h of MG132 application, plants were (i) maintained for 3 h more in W, (ii) transferred for 3 h to W+FR, or (iii) transferred for 3 h to W+FR and then back to W for an additional hour (**Figure X5A**). We observed that MG132 allowed to detect more easily PIF7wt and PIF7Bm in these immunoblot assays. More importantly, the relative abundance of these two derivatives increased in response to W+FR compared to those kept in W, and rapidly decreased when transferred back to W. By contrast, PIF7APBm abundance remained virtually unaffected in all three treatments (**Figure X5B**). Moreover, PIF7APBm seemed to be more abundant than PIF7wt and PIF7Bm, not only in W+FR, but also in W. These results suggest that PIF7APBm is more photostable in comparison to PIF7wt and PIF7Bm derivatives.
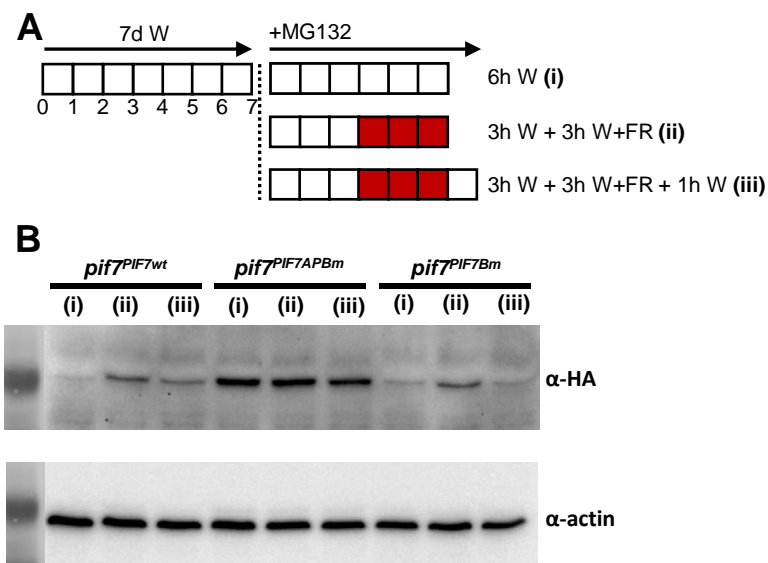
Figure X5. The APB domain controls the shade-modulated of PIF7. (A) Schematic representation of the different treatments used to detect PIF7 derivatives accumulation. After 7 days growing in W, seedlings of *pif7^PIF7wt^* (line #12), *pif7^PIF7Bm^* (line #17) and *pif7^PIF7APBm^* (line #21) were treated with 50 µM MG132 and then exposed to (i) 6 h of W, (ii) 3 h of W and 3 h of W+FR, or (iii) 3 h of W, 3 h of W+FR and transferred again to W for 1 h. **(B)** Immunoblot detection of PIF7 derivatives abundant in each condition

described in **A**. PIF7-3xHA derivatives were detected with an α-HA antibody (upper part) and an α-actin antibody was used as a loading control (bottom part).

2.4. PIF7APBm binds target genes in both W and W+FR.

Genome-wide PIF7 target genes have been recently described in seedlings treated in response to warm temperature and to shade (Chung *et al.*, 2020; Willige *et al.*, 2021). Based on the available information, PIF7 binding preferentially occurs in shade conditions, when the inhibitory effect of phyB is removed (Li *et al.*, 2012; Lorrain *et al.*, 2008; Roig-Villanova & Martínez-García, 2016). For that reason, we expect the PIF7APBm derivative, where phyB is not able to exert its action, will bind DNA also in W. Therefore, taking advantage of the constitutive active *pif7^{PIF7APBm}* line, we wanted to test if the target genes of this shade-independent PIF7APBm derivative, change with the shade conditions. To this goal, we performed a ChIP assay using *pif7^{PIF7APBm}* seedlings treated with and without 50 µM MG132 under W and W+FR. First, we checked on the known target *PIL1* gene the binding capacity of this PIF7 derivative including *pif7^{PIF7wt}* and *pif7* as controls (**Figure X6A**). Due to the low abundance of the PIF7wt protein on the *pif7^{PIF7wt}* line (**Figure X4B**), we used the protease inhibitor MG132 (50 µM) to enhance the accumulation of the PIF7wt protein and increase detection by ChIP. This treatment was also performed in the line *pif7^{PI7APBm}*, although in this case samples without MG132 treatment were also prepared. When analyzing the *R1* region of *PIL1*, where a G-box element (described to be bound by PIFs) is located, it was enriched in the *pif7^{PIF7wt}* and *pif7^{PIF7APBm}* lines in all conditions in samples immunoprecipitated with anti-HA antibody compared to the control samples (immunoprecipitated with IgG antibody). This enrichment did not happen in the *pif7* samples nor when analyzing the negative control region *R2* of *PIL1* (located in the gene body of *PIL1*, where PIF7 does not bind) in any of the samples (**Figure X6A**). This experiment indicated that PIF7APBm was able to bind DNA in seedlings exposed to W or W+FR, in contrast to what has been described for the wild-type endogenous PIF7 (Leivar, Monte, Al-Sady, *et al.,* 2008; Li *et al.*, 2012). Next, we sampled the W-grown seedlings of *pif7^{PIF7APBm}* lines grown differentially for 1 h under W or W+FR with and without MG132 and performed a ChIP-seq experiment. After the corresponding analyses, very few PIF7 binding peaks were identified. From *pif7^{PIF7APBm}* grown in W, we obtained 8 and 14 peaks with and without MG132 respectively. In W+FR, we obtained 25 and 12 peaks with and without MG132 respectively (**Figure X6B**). These results showed that MG132 only had a positive effect in the number of peaks in W+FR-treated samples. With MG132, we identified

more peaks in W+FR than in W (25 versus 8). This effect might be caused by the MG132 stabilization effect over other regulatory components involved in PIF7 binding, such as PIF4 and PIF5, able to heterodimerize with PIF7. Indeed, without MG132 the number of detected peaks decreased from 14 in W to 12 in W+FR. Among these peaks, 6 were differentially found in W and W+FR. Another possible explanation of several of these differences in the number of peaks is that the bioinformatic analyses were stringent and did not uncover peaks that a visual inspection identified in most of the samples, e.g., peak close to AT1G49780 was only found in W+FR without MG132 but a visual inspection showed that the peak was present in other conditions (**Supplementary Figure X2**). In summary, MG132 treatment helped us to increase the number of peaks identified but for further analyses we only used data from non-treated with MG132 samples to avoid effects due to the stabilization of other regulators apart from PIF7.

Merging the amount of peaks in all the ChIP-seq samples, we identified a total of 26 peaks (named as p7_xx, being xx numbers from 01 to 26, see Supplementary **Table SX1**). From these, 23 were single peaks, 2 were double peaks and 1 was a multiple peak (**Figure X6C**). As PIFs are known to bind E-boxes (CANNTG), we searched for the presence of these motifs in the central part of each peak (sequence between green lines in **Figure X6C**). At least one type of E-box was found in every peak. Specifically, G-boxes (CACGTG) were found in 23 of 26 and PBE-boxes (CACATG) in 8 of 26 peaks. This means that although few peaks were detected, they had a high potential for PIF7 binding. Moreover, all peaks had a G-box (23, in white) or a PBE-box (3, in black) in a central position with a deviation of +/- 10% (**Figure X6D**). We also analyzed the distance in nucleotides of the E-box from the middle position of the peak fragment (**Figure X6E**) and most of the central G/PBE-boxes were located between 10 and 23 nucleotides from that part of the fragment, with a median of 15 nucleotides. This supports that the central fragment of each peak corresponds to the PIF7 binding site and these nucleotides appear to have the highest number of sequenced reads (read coverage).

Taking that into consideration, we used the read coverage in the central G/PBE-box in each of the peaks as reflecting the binding efficiency of PIF7, hence as an indication to compare the effect of W and W+FR on the binding strength of the PIF7APBm protein. In the case of double (p7_01 and p7_21) or multiple peaks (p7_17), the read coverage values were added. No major and consistent differences in average read coverage were found for the various peaks in W and W+FR (**Figure X6F**), what points that PIF7APBm binds to these regions with the same strength, independently of light conditions.
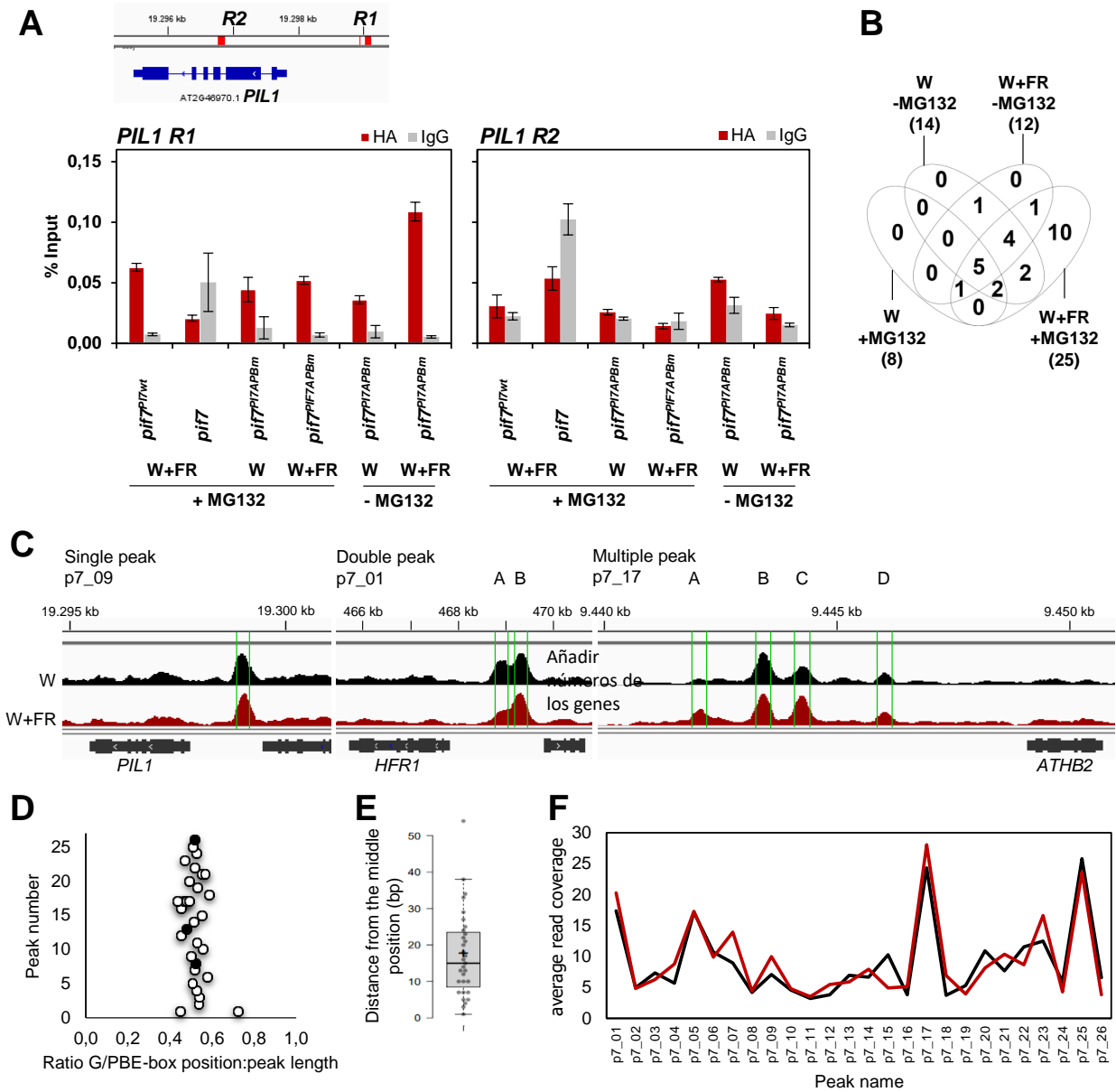
Figure X6. PIF7APBm binds to E-boxes on gene promoters in W- and W+FR-treated seedlings. (A) Chromatin immunoprecipitation (ChIP) assay performed for PIF7 derivatives in seedlings treated with (+MG132) or without (-MG132) MG132 in response to W or W+FR. Seedlings of *pif7PIF7wt* (line #12) and *pif7PIF7APBm* (line #21) were grown for 7 days in W. At day 7 they were treated 2 h with or without 50 µM MG132 applied to the media and then an additional hour in W or W+FR. On top it is shown the schematic location of R1 and R2, two ChIP-qPCR amplified regions in *PIL1* gene. R1 corresponds to the region containing the G-box element in the promoter. R2 corresponds to the *PIL1* gene body. Percentage of input ±SE in R1 and R2 after ChIP with anti-HA and anti-IgG antibodies is shown for each genotype in each condition (W/ -MG132, W+FR/ -MG132, W/ +MG132 and W+FR/ +MG132). Values correspond to one of the biological triplicates that was sent for the ChIP-seq. **(B)** Venn diagram summarizing the peaks found in a ChIP-seq of *pif7PIF7APBm* samples treated with combinations of W/W+FR and +/- MG132. **(C)** Schematic representation of the three peak types found visualized using Integrative Genome Viewer software: single peak (p7_09) at *PIL1*

promoter, double peak (p7_01 A and B) at *HFR1* promoter and multiple peak (p7_17 A, B, C and D) at *ATHB2* promoter. Vertical green lines limit the PIF7-enriched peak region that was used to localize central G/PBE-box and its read coverage. **(D)** Graph showing the relative position of the most central G/PBE-boxes in the defined PIF7-enriched region for each peak (from p7_01 to peak p7_26). Position was calculated as the ratio of the most central G/PBE-box position and the peak fragment length. Black dots represent PBE-boxes and white dots represent G-boxes. **(E)** Distance of the G/PBE-box deviation (number of bp) from the middle point of each peak. **(F)** Representation of the PIF7APBm binding strength for each peak found in both W and W+FR conditions. The binding strength is measured as the average of read coverage normalized to 1 million mapped reads on each of the six nucleotides of the central E-box.

To analyze which genes were associated to the peaks found, we selected the nearest upstream and downstream genes with the right orientation relative to each peak. The farthest located gene we have included was 20 kb from the center of the peak. In some cases (p7_02, p7_15 and p7_26), the closest downstream or upstream gene was in a region that was part of the peak. In these situations, that gene was selected but we also incorporated the next closest gene (**Supplementary Table SX1)**. A special case was the peak p7_21A that was close to *BRI1* although this gene was not in the right orientation. However, we included *BRI1* in our gene list because it has been described as a PIF target (Pfeiffer *et al.*, 2014). Following these criteria, we selected a total of 56 candidate genes whose expression could be regulated by PIF7 binding to their promoter. We compared our 56-candidate gene list with published lists of PIFs-bound genes (**Figure X7 and Supplementary table SX2**). A total of 41 genes had already been described as PIF-bound and target genes: 30 of our 56 genes had been identified previously as PIF7 targets (Chung *et al.*, 2020), and 11 of our 56 genes had been described as other PIFs targets (PIF1, PIF3, PIF4 or PIF5) (Pfeiffer *et al.*, 2014). Only 15 of our found genes have not been identified previously as PIFs targets. This can be in part because although we may find the same peaks, the gene selection criteria could differ between different authors. About 1000 PIF7 binding regions were detected by ChIP-seq in a very recent work (Wilige *et al.*, 2021). However, authors did not associate all the peaks with genes, selecting only those regions where PIF7 binding was strongest to propose a list of 20 PIF7 target genes. From this list, 8 genes were also found in our ChIP-seq analyses (data not shown).

	ChIPseq Pastor-Andreu			ChIP experiments		Genome wide expression																							
	PIF7 APBm 1h of W and 1h of W+FR			Pfeiffer et al., 2014	Chang et al., 2020	Pastor Andreu et al., Chapter II of this thesis				Molina-Contreras et al., 2019		Leivar el at., 2012				Kohnen et al, 2016								Yang et al., 2018	
				Col-0	Col-0	Col-0		hy5-2		Col-0		Col-0				Col-0								Col-0	
						UP	Down	UP	Down	UP	Down	UP		Down		UP				Down				UP	
peak p7	AGI	Gene		PIF1-bound / PIF3-bound / PIF4-bound / PIF5-bound	PIF7-bound	1h	8h	1h	8h	1h	8h	1h	8h	1h	1h	1h	3h	24h	1h	3h	24h	15 min	45 min	90 min	180 min	15 min	45 min	90 min	180 min	1h (0.8) / 1h (0.2)

peak	AGI	Gene
#01	AT1G02340	HFR1 ←
	AT1G02350	→
#02	AT1G19300	GATL1 ←
	AT1G19310	←
	AT1G19320	→
#03	AT1G49780	PUB26 ←
	AT1G49820	MTK →
#04	AT1G75450	CKX5 ←
	AT1G75460	→
#05	AT2G18780	←
	AT2G18790	PHYB →
#06	AT2G23760	BLH4 ←
	AT2G23808	→
#07	AT2G28056	MIR172A ←
	AT2G28070	ABCG3 →
#08	AT2G43040	NPG1 ←
	AT2G43060	IBH1 →
#09	AT2G46970	PIL1 ←
	AT2G46990	IAA20 →
10	AT3G12920	BRG3 ←
	AT3G12930	DG238 →
11	AT3G14410	←
	AT3G14430	←
12	AT3G15200	←
	AT3G15240	→
13	AT3G16750	←
	AT3G16800	EGR3 →
14	AT3G19380	PUB25 ←
	AT3G19390	→
15	AT3G44290	←
	AT3G44310	NIT1 →
	AT3G44320	NIT3 →
16	AT4G01245	→
	AT4G01250	WRKY22 ←
17	AT4G16770	←
	AT4G16780	ATHB2 →
18	AT4G17430	←
	AT4G17460	HAT1 →
19	AT4G19430	←
	AT4G19450	→
20	AT4G36860	DAR1 ←
	AT4G36870	BLH2 →
21	AT4G39400	BRI1 ←
	AT4G39403	PLS ←
	At4G39420	→
22	AT5G02570	HTB10 ←
	AT5G02580	→
23	AT5G12030	HSP17.6A ←
	AT5G12050	BG1 →
24	AT5G54470	BBX29 ←
	AT5G54480	→
25	AT5G57650	←
	AT5G57700	→
26	AT5G57770	FL8 ←
	AT5G57780	P1R1 ←
	AT5G57800	CER3 →

Figure X7. Most of the PIF7 peaks are associated with genes identified are known PIFs targets and are upregulated in response to shade treatment. Table with the peaks found in our ChIP-seq experiment and the closest genes associated to them. The AGI number, the strand (direction) and/or the name of each gene are indicated. Genes identified as PIF targets in other ChIP-seq experiments are marked in yellow. Genes found in published genome-wide expression experiments under different shade time exposures are marked in blue when upregulated and in magenta when downregulated.

We also crossed the 56 genes associated to our ChIP-seq peaks with published lists of genes whose expression was modulated in shade conditions **(Figure X7 and Supplementary Table SX2)**. Thirteen genes did not vary their expression pattern on any of the list of genes. The expression of the remaining 43 genes was affected at least in one condition of the experiments analyzed: 30 of them were only upregulated by shade, 7 were only downregulated and 6 were up and downregulated, depending on the experiment.

Relative to the 15 genes found as PIF7 bound only in our ChIP-seq, 7 of them were not regulated by shade in any of the RNA-seq lists, therefore we will not consider them as PIF7 targets. From the remaining 8 genes that only appear in our list, AT2G23760 (*BLH4*), AT2G46990 (*IAA20*), AT4G19450 and AT5G12030 (*HSP17.6A*) are upregulated or downregulated in 3 or more RNA-seq lists. Importantly, all the peaks but p7_07 have at least one gene associated whose expression was shade-regulated.

3. DISCUSSION

PIFs are known to promote the Shade Avoidance Syndrome (SAS) (Leivar & Quail, 2011). Among the different PIFs, genetic analyses showed a major role of PIF7 in promoting the hypocotyl growth in contrast with the minor role of PIFQ (Cole *et al.*, 2011; Li *et al.*, 2012; Lorrain et al., 2008). For that reason, the study of this specific PIF might help to better understand the SAS. As other PIFs, PIF7 contains an APB and a bHLH domain, which suggested that phyB-PIF7 interaction controls PIF7 DNA-binding and transcriptional activities that, eventually, modulate among other SAS responses, the shade-induced hypocotyl elongation. Structure-function analyses of the photolabile PIF3, the well-studied founder member of the PIF family (Martínez-García *et al.*, 2010; Ni *et al.*, 1998), revealed surprising results about the mechanism employed by PIF3 to promote hypocotyl elongation. These analyses established that the two domain activities (phyB- and DNA-binding) can be separated involving a temporal uncoupling of its two most central molecular functions, i.e., mutated bHLH domain in PIF3, which blocked DNA binding activity, loses its capacity to regulate rapid-response target gene expression in response to constant R (Rc), but fully retains its capacity to regulate phyB levels and hypocotyl growth. In contrast, during long-term Rc PIF3 acts exclusively through its phyB-interacting capacity to modulate hypocotyl growth, independently of its ability to bind DNA (PIF3 with APB motif mutated, unable to bind to phyB active form, failed to rescue *pif3* short hypocotyl phenotype) (Al-Sady *et al.*, 2008). Physical separation of molecular activities was also observed in other transcription factors involved in the modulation of shade-induced hypocotyl elongation, as ATHB4, a transcription factor of the homeodomain-leucine zipper family whose DNA-binding activity is not required for the regulation of the seedling responses to plant proximity (Gallemí *et al.*, 2017). In the case of PIF7, it was not known, however, whether this separation of activities is conserved and if the APB motif is able to modulate hypocotyl growth without DNA-binding activity. Our structure-function analysis of PIF7 aimed to address this point.

After transforming *pif7* mutant with the PIF7wt derivative, we obtained a partial complementation, where the hypocotyl length in shade did not reach the length of Col-0. As observed by some authors (Huang *et al.*, 2018; Li *et al.*, 2012), *pif7^PIF7wt^* seedlings were longer than Col-0 in W. We hypothesize that this could be due to differences in the spatial distribution of PIF7 along the plants and/or differences in their regulation because the chosen promoter region of 1961 bp could be missing some regulatory elements. Moreover, as our PIF7 derivatives do not contain introns, they do not suffer splicing, being defective in this

regulatory mechanism. In contrast to PIF7wt derivative, in lines transformed with PIF7Bm the *pif7* mutant phenotype was not rescued. As the protein was produced to similar levels as the wild type (**Figures X4, X5**), these results support that the mutation in the basic domain (E175), that affects a residue conserved in several bHLH proteins involved in DNA binding, abolishes this activity. More importantly, the lack of DNA-binding of this PIF7 derivative is essential not only for the rapid changes in gene expression driven by PIF7 after shade treatment but also for the shade-induced promotion of hypocotyl length (**Figures X2, X3**). These results contrast to what has been published for PIF3, in which DNA-binding was required for the rapid and direct R-induced changes in gene expression but not for the complementation of the R-induced promotion of hypocotyl (Al-Sady et al., 2008). Despite its lack of activity, abundance of PIF7Bm is affected by the shade treatment, like the active PIF7wt protein, reflecting that the APB domain is functional (**Figure X4. X5**).

The two mutations introduced to abolish phyB-binding (E8AG14A) have been previously shown to inhibit PIF7 binding to active (Pfr) phyB (Leivar, Monte, Al-Sady, et al., 2008), although their impact in PIF7 activity in plants was not studied. The production of the mutant PIF7APBm form resulted in a constitutively active PIF7 in the transformed lines, that displayed much longer hypocotyls in W than Col-0 and the other genotypes (**Figure X2F**). This constitutive phenotype of PIF7APBm contrasts with the null activity in promoting hypocotyl elongation of the equivalent PIF3 molecule unable to bind to any phytochrome (Al-Sady *et al.*, 2008). In W+FR, these lines responded to shade elongating their hypocotyls. However, the increase in hypocotyl elongation in response to shade was similar to that of *pif7PIF7Bm* and *pif7* (**Figure X2I**). Probably, the extra shade-induced elongation detected in these three genotypes is due to other PIFs (PIF3, PIF4, PIF5), whose activity is still present in all phenotypes and were also shown to modulate SAS (Leivar & Quail, 2011; Lorrain *et al.*, 2008; Willige *et al.*, 2021).

Our expression analyses of PIF7 direct targets such as *PIL1* and *YUCCA* genes (Li *et al.*, 2012) agree with hypocotyl elongation. PIF7wt derivative promotes the rapid shade-regulated expression of *PIL1*, *YUC8* and *YUC9*, as it occurs in Col-0. PIF7Bm lacks any biological activity and PIF7APBm enhances the expression of these three *PAR* genes constitutively in W (**Figure X3**). In conclusion, the abrogation of all the biological activities tested in this work caused by mutating the DNA-binding domain of PIF7 (PIF7Bm) and phyB interacting domain (PIF7APBm) indicates that, in contrast to what was observed for PIF3 (Al-Sady *et al.*, 2008),

PIF7 DNA-binding and phyB binding are needed to properly modulate early changes in gene expression of PIF7 targets and hypocotyl growth in a light-dependent manner.

Regarding PIFs photostability, it is known that interaction of phyB active form with PIFs results in their rapid phosphorylation, which is postulated to somehow reduce the activity of the bHLH domain to bind DNA (Al-Sady *et al.*, 2006). In the case of PIFQ (PIF1, PIF3, PIF4 and PIF5), their phosphorylation results in their degradation by the 26S proteasome (Inoue *et al.*, 2016; Lorrain *et al.*, 2008; H. Shen *et al.*, 2008); by contrast, the phosphorylation of PIF7 reduces its capacity to bind the DNA having a poorly impact on its stability but results in its cytoplasmatic localization sequestered by 14-3-3 proteins (Huang *et al.*, 2018; Leivar, Monte, Al-Sady, *et al.*, 2008; Li *et al.*, 2012). These lead to the PIFs classification in two major groups: photolabile (PIF1, PIF3, PIF4 and PIF5) and photostable (PIF7). Our analyses of PIF7 derivatives indicate that PIF7 stability is negatively affected by W when a fully functional APB domain can interact with the active phyB. Consequently, although PIF7 is generally considered a photostable PIF (at least in contrast with the extremely labile PIFQ), its abundance shows a degree of light-dependence, and this stability depends on the interaction with the active phyB. Importantly, abundance of PIF7APBm was virtually unaffected by the shade treatment, supporting that the APB domain provides a level of regulation that is phyB dependent. It must be mentioned that, surprisingly, we could detect the decrease of PIF7wt and PIF7Bm when transferred from W+FR to W, in presence of the 26S proteasome inhibitor MG132 (**Figure X5**). This is consistent with recent results indicating that PIF7 does not appear to be under major regulation by the proteasome, i.e., treatment with MG132 only moderately increases PIF7 abundancy (Chung *et al.*, 2020). Consequently, the degradation of PIF7 might be depending on other degradation pathways and MG132 treatment was useful to improve PIF7wt and PIF7Bm detection but allowed to detect changes in their abundance depending on light conditions.

Electrophoretic mobility shift assays demonstrated *in vitro* binding of PIFs (i.e., PIF1/PIL5, PIF3, PIF4, PIF5/PIL6, and PIF7) to G-box elements (Hornitschek *et al.*, 2009; Huq *et al.*, 2004; Huq & Quail, 2002; Leivar, Monte, Al-Sady, *et al.*, 2008; Oh *et al.*, 2007; Shin *et al.*, 2007; Toledo-Ortiz *et al.*, 2003). Chromatin immunoprecipitation (ChIP) assays have also confirmed *in vivo* binding of PIFs to promoters containing G-boxes (Hornitschek *et al.*, 2012; Oh *et al.*, 2007, 2009, 2012; Shin *et al.*, 2007; Zhang *et al.*, 2013). In addition to G-box elements, PIFs also bind weakly in vitro to a particular E-box element called the PBE-box (Dong *et al.*, 2008; Pfeiffer *et al.*, 2014; Shin *et al.*, 2007; Zhang *et al.*, 2013). As expected,

after performing a ChIP-seq experiment with *pif7* complemented with PIF7APBm derivative, all the peaks found had PBE-boxes or G-boxes in its central part, where PIF7 is supposed to bind. We only could detect 26 peaks that, in comparison to other ChIP-seq works analyzing PIF7 targets (Chung *et al.*, 2020; Pfeiffer *et al.*, 2014; Willige *et al.*, 2021), is a low number of peaks. This could be due to unknown technical limitations of the chromatin immunoprecipitation assay (e.g., antibody chosen to perform the immunoprecipitation). However, our peaks are well defined and similar to those found in published ChIP-seq experiments detecting PIF7 targets, what strengthen the validity of our results (**Supplementary Figure X3**). Surprisingly, among the peaks found, *YUC8* and *YUC9* were not present, although both genes are defined as PIF7 targets (Ciolfi *et al.*, 2013; Li *et al.*, 2012). The absence of these genes in our ChIP-seq analyses could be caused because we only could identify peaks where PIF7 binds with the highest strength. Indeed, *YUC8* and *YUC9* were not found among those genes with the strongest PIF7 binding and activated expression (Willige *et al.*, 2021).

We wondered if shade conditions could be somehow regulating PIF7 activity also in an APB-independent manner, that is, light conditions could also modulate PIF7 strength to bind DNA by affecting other factors that PIF7 such as chromatin openness. However, when analyzing differences in the ability of PIF7APBm to bind to promoter regions depending on light conditions, we observed that this PIF7 derivative binds to DNA regions with the same strength independently of light conditions.

It has been suggested that light regulates chromatin accessibility in a process where PIF7 plays an important role (Peng *et al.*, 2018). In chromatin remodeling, histone acetyltransferases (HATs, catalyzing acetylation) and histone deacetylases (HDACs, catalyzing deacetylation) provoke the transformation of the condensed chromatin into a more relaxed structure to allow gene transcription and the inverse process respectively (Liu *et al.*, 2014; Lusser *et al.*, 2001; Yuan Shen *et al.*, 2015). Other mechanism that affects chromatin condensation is the presence of the histone H2A.Z, a histone variant that represses gene expression in Arabidopsis and is removed from chromatin in response to various environmental stimuli (Coleman-Derr & Zilberman, 2012; Sura *et al.*, 2017; Zander *et al.*, 2019). In shade conditions, dephosphorylated PIF7 is able to interact and recruit MORF RELATED GENE 2 (MRG2) that interacts with HATs, building a multiprotein complex which is essential for histone acetylation and activation of transcription of genes involved with SAS (Peng *et al.*, 2018). Moreover, dephosphorylated PIF7 also interacts with the EEN subunit of

the INO80 chromatin remodeler that reduces the global H2A.Z bind to shade-related genes such as *ATHB2* facilitating transcriptional activation (Alatwi & Downs, 2015; Brahma *et al.*, 2017; Willige *et al.*, 2021). Our results together with these observations lead to conclude that, although shade conditions do not appear to affect the binding strength of PIF7 to DNA within 1 h after shade exposure is initiated, it might affect chromatin accessibility after longer shade exposures or indirectly through the ability of the shade-induced dephosphorylated PIF7 to bind DNA- and recruit chromatin remodeler complex to decondense DNA and allow the gene activation.

In conclusion, we have generated and characterized transgenic lines expressing three *PIF7* derivatives. Two of them had altered molecular functions, what provides powerful tools to investigate PIF7 molecular mechanism in regulating the shade triggered responses. Specifically, *pif7*^{PIF7APBm} is a constitutively active line and an interesting resource to analyze differences in PIF7 activity modulated directly by light/shade conditions without the need to interact with phyB. The transgenic line containing PIF7APBm resulted in the elaboration of a small list of PIF7 direct target genes identifying 8 new direct targets whose investigation could help to decipher, up to now, unknown aspects about the molecular mechanism that control the shade-induced hypocotyl elongation.

4. MATERIAL and METHODS

4.1. Plant material and growth conditions.

Arabidopsis thaliana Col-0 and *pif7-1* (Leivar, Monte, Al-Sady, *et al.*, 2008; Li *et al.*, 2012) were used in this study to generate transgenic lines. To produce seeds, *A. thaliana* plants were grown in the greenhouse under long day photoperiod conditions (16 h light and 8 h dark) as described (Martínez-García *et al.*, 2014). For hypocotyl assays, seeds were sterilized during 10 min in a solution containing 10% bleach (v/v) and 0,1% Tween-20 (v/v). Then seeds were washed five times with sterile water and sown in solid agar plates without sucrose (GM–; 0.215% (w/v) MS salts plus vitamins, 0.025% (w/v) MES pH 5.80). After at least 3 days of stratification at 4 ºC in darkness, plates were incubated in growth chambers at 22 ºC under continuous white light (W) provided by 4 cool-white vertical fluorescence tubes for 2 days (PAR of 20–25 μmol·m^{-2}·s^{-1}, R:FR > 3.3). After that, plates were either maintained in W or transferred to simulated shade conditions (W+FR). Simulated shade was generated by supplementing W with FR provided by 4 horizontal LED lamps (PAR of 20–25 umol·m^{-2}·s^{-1}, R:FR of about 0.07). At day 7, seedlings were lied down on the petri dishes and pictures of them were taken. Each biological replicate corresponded to ~25 seedlings per treatment and genotype. Hypocotyl measurements were carried out by using the National Institutes of Health (NHS) ImageJ software (Bethesda, MD, USA; http://rsb.info.nih.gov/). Hypocotyl measurements from three different biological replicates were averaged.

For plant gene expression analyses or immunoblot assays, seeds were sown over a sterilized nylon membrane located on the top of the solid agar plates previously mentioned. After the germination, *A. thaliana* seedlings were grown for 7 days for all the performed experiments (hypocotyl measurements, expression analyses, immunoblot assays and chromatin immunoprecipitation).

4.2. Generation of PIF7 variants for *pif7-1* complementation.

Wild-type *PIF7* CDS was amplified with the primers JO414 and JO415 using Col-0 cDNA as a template, which generated a DNA fragment that removed the stop codon and introduced a *XhoI* site (*PIF7$^{no\_STOP}$*). This PCR product was subcloned in a selected orientation (ATG close to the *XhoI* site from the multiple cloning site) into PCRII-TOPO (Invitrogen) to generate pRA1. Selected colonies were sequenced to confirm their identity. Plasmid pRA1 was digested with *XhoI* and *PIF7$_{wt}$* was inserted in pSP55 (containing *3xHA* tag) (Paulišić et al.,

2021) previously digested with *Sal*I and dephosphorylated, which gave pRA2. This plasmid contained the wild-type *PIF7* ORF fused in frame with *3xHA* (*PIF7_{WT}-3xHA*). Finally, pRA2 was digested with EcoRI and *PIF7_{WT}-3xHA* was directionally cloned into pENTR3C to obtain pRA3. This plasmid contained *PIF7_{WT}-3xHA*, flanked with attL1 and attL2 sites (attL1<*PIF7_{WT}-3xHA*<attL2).

Derivatives of *A. thaliana PIF7* with the APB (*PIF7_{APBm}*) and basic (*PIF7_{Bm}*) domains mutated were obtained by PCR-based site-directed mutagenesis using pRA3 as a template. To obtain *PIF7_{APBm}*-3xHA, two fragments were amplified using MJO25 plus JO417 and JO416 plus MJO25 primer combinations, respectively. Both PCR fragments were mixed and amplified using the nested JO414 and SPO32 primers. The resulting DNA fragment contained a full-length PIF7 with the mutated APB domain fused to the 3xHA. This PCR product was cloned into PCRII-TOPO generating the plasmid pRA4 (*PIF7_{APBm}-3xHA*). Selected colonies were sequenced to confirm the presence of the two-point mutations that substituted Glu 8 by Ala (E8A) and Gly 14 by an Ala (G14A) in the APB domain.

To obtain *PIF7_{Bm}*, two fragments were amplified using MJO25 plus JO419 and JO418 plus MJO25 primer combinations, respectively. As before, both PCR fragments were mixed and amplified using the nested JO414 and SPO32 primers. The resulting DNA fragment contained a full-length PIF7 with the mutated basic domain fused to the 3xHA. This PCR product was cloned into PCRII-TOPO generating the plasmid pRA5 (*PIF7_{Bm}-3xHA*). Selected colonies were sequenced to confirm the presence a point mutation that substituted Glu 175 by and Asp (E175D) in the basic domain.

pRA4 and pRA5 were digested with *Eco*RI and the inserts containing the *PIF7* derivatives were directionally cloned into pENTR3C to obtain pRA7 (attL1<*PIF7_{APBm}-3xHA*<attL2) and pRA8 (attL1<*PIF7_{Bm}-3xHA*<attL2), respectively. These plasmids contained the *PIF7* derivatives flanked with attL1 and attL2 sites. To express these PIF7 derivatives in plants, pRA3, pRA7 and pRA8 were digested with *Bam*HI and *Xho*I. The resulting *Bam*HI-*Xho*I fragments were subcloned into the *Bam*HI-*Sal*I digested pCAMBIA1300-based pCS14 vector (containing the CaMV 35S promoter, *p35S*) (Sorin *et al.*, 2009) to generate pBA18 *p35S:PIF7_{WT}-3xHA*), pBA6 (*p35S:PIF7_{APBm}-3xHA*) and pBA16 (*p35S:PIF7_{Bm}-3xHA*).

We amplified a ca. 2 kb fragment of *PIF7* promoter (*pPIF7*) starting immediately before the ATG of *PIF7* gene using gDNA of *A. thaliana* wild-type Col-0 as a template and primers JDO14 and SPO20. This fragment was subcloned into pCRII-TOPO to generate pSP94.

Selected colonies were sequenced to confirm their identity. Finally, pBA18, pBA6 and pBA16 were digested with *Eco*RI (that removed the p35S) and dephosphorylated, and the *Eco*RI fragment from pSP94 containing the pPIF7 was subcloned into the same site. The resulting binary vectors were named as pPP8 (*pPIF7:PIF7$_{WT}$-3xHA*), pPP5 (*pPIF7:PIF7$_{APBm}$-3xHA*) and pPP6 (*pPIF7:PIF7$_{APBm}$-3xHA*). These binary vectors confer resistance to kanamycin in bacteria and hygromycin in plants.

A. thaliana pif7-1 plants were transformed with pPP8, pPP5 and pPP6. Transgenic seedlings were selected on 0.5xGM- medium with hygromycin (30 ug/ml) and verified by PCR genotyping using specific primers. Homozygous transgenic plants with 1 T-DNA insertion were finally used for the experiments. The obtained lines were named as *pif7^{PIF7WT}*, *pif7^{PIF7Bm}* and *pif7^{PIF7APBm}*. The primers used for the Cloning are provided in supplementary **Table SX3.**

4.3. RNA extraction and gene expression analyses.

Seven-day-old seedlings grown in the specific conditions for each experiment were used as material to extract total RNA. The seedlings were harvested and frozen in liquid nitrogen. The RNA was extracted using commercial kits (Maxwell® RSC Plant RNA kits; www.promega.com) following manufacturers protocol and quantified using NanoDropTM 8000 spectophotometer (ThermoFischer ScientificTM). Two µg of total RNA were retrotranscribed to cDNA in a final volume of 20 µl by using the Transcriptor First Strand cDNA synthesis KIT (Roche, www.roche.com). Subsequently cDNA was diluted ten-fold with water and stored at -20ºC for further analysis.

Relative mRNA abundance was determined via Real-Time Quantitative Polymerase Chain Reaction (RT-qPCR) in a final volume of 10 µl made up of 0.3 µM of both, forward and reverse primers, 5 µl of the LightCycler 480 SYBR Green I Master Mix (Roche) and 2 µl of ten-fold diluted cDNA (Molina-Contreras et al., 2019). The RT-qPCR was carried out in *LightCycler 480 Real-Time PCR system* (Roche). This analysis was performed with three independent biological replicates for each condition and three technical replicates for each biological replicate. As endogenous reference genes to normalize the expression of the genes of interest, *UBIQUITIN 10* (*UBQ10*) or the *ELONGATION FACTOR 1α* (*EF1α*) were used, as indicated in the corresponding figure legends. The primers used for the RT-qPCR analyses are provided in supplementary **Table SX4.**

4.4. Protein extraction and immunoblot analyses.

About 50 mg of 7-day-old seedlings grown as indicated, were used to extract proteins as follows. In some cases, at day 7 plants were treated with 50 µM MG132 for 6 h applied to the media and exposed to different light conditions specified in each case. Plant material was harvested, weight and frozen in liquid nitrogen. The material was ground to powder, and total proteins were extracted using a buffer containing SDS (1.5 µl per mg of fresh weight). Protein concentration was determined using PierceTM BCA Protein Assay Kit (Thermo Scientific, www.thermoscientific.com). Proteins (45-50 µg) were resolved in a 12% SDS-PAGE gel and transferred to a PVDF membrane (Bio-Rad WET transference system). The membrane was activated with methanol 100% and blocked with 5% powder milk solution in TBST during 1 h. After that, the membrane was immunoblotted with rat monoclonal anti-HA (high affinity, clone3F10, Roche, www.roche.com; 1:2000 dilution), then hybridized with polyclonal peroxidase (HRP) conjugated goat anti-rat (A9037, Sigma, www.sigma Aldrich.com; 1:5000 dilution). Next, the membrane was immunoblotted again with rabbit polyclonal anti-actin (Agrisera, www.agrisera.com; 1:5000 dilution). Then hybridized with HRP-conjugated donkey anti-rabbit (Amersham, www.gelifesciences.com; 1:10000 dilution). Blot pictures were obtaining with ChemiDocTm Touch Imaging system (Bio-Rad, www.bio-rad.com) using ECL Prime Western Blotting Detection Reagent (GE Healthcare, RPN2236).

4.5. Statistical analyses.

The statistical analyses were carried out using the Real Statistics Resource Pack, an Excel add-in that extends Excel's standard statistics capabilities. Type of analyses and compared measurements are indicated in figure legends.

4.6. Chromatin Immunoprecipitation Protocol (ChIP).

Plants were germinated and grown in W. At day 7 treatments were done: seedlings were treated for 3 h without or with 50 µM MG132 applied to the media and transferred to W or W+FR for 1 h more. After that, plant material was harvested and submerged in a crosslinking solution (1xPBS, 0.01% (w/v) Triton, 1% (w/v) formaldehyde). They were vacuum infiltrated for 10 min and the crosslinking was vacuum quenched for 5 min by adding 2 M glycine to a final concentration of 0.125 M. Then, the tissue was rinsed with water, dried on a filter paper and conserved at -80ºC until processing.

For the nuclei extraction samples were grinded into a powder and mixed with MEB buffer [1 M hexylene glycol; 20 mM PIPES-KOH pH 7.6; 10 mM $MgCl_2$; 0.1 mM EGTA, pH 8, 20 mM NaCl; 60 mM KCl; 0.5% (w/v) Triton; 5 mM β-mercaptoethanol; 1x protease inhibitor (PI) cocktail (cOmplete™, Mini, EDTA-free Protease Inhibitor Cocktail, MERK)] for 15 min under rotation at 4ºC. The homogenate was filtered twice through Miracloth and centrifuged 6 min at 4ºC at 1500g to pellet the nuclei. After removing the supernatant, the nuclei were resuspended in Nuclei Lysis Buffer [50 mM Tris-HCl, pH 8.0; 10 mM EDTA; 1% (w/v) SDS; 1x PI cocktail. Then the chromatin was sonicated for 7 to 9 x 20 sec "ON", 45 sec "OFF" (high power) in a Bioruptor (Diagenode). The samples were diluted ten times with ChIP dilution buffer [1.1% (w/v) Triton X-100; 1.2 mM EDTA; 16.7 mM Tris-HCl, ph 8.0; 167 mM NaCl; 1x PI cocktail]. Then, the samples were centrifuged 5 min at 8000g to sonicated chromatin in the supernatant was collected. The chromatin solution was split into the necessary number of tubes (one for each immunoprecipitation, IP) and 10 µl were kept as input. Each chromatin sample was incubated overnight at 4ºC with an α-HA monoclonal antibody (the same used for the western blot).

Dynabeads™ Protein G for Immunoprecipitation (Thermo Fisher Scientific; www.thermoscientific.com) were equilibrated with ChIP dilution buffer and they were added to the chromatin solution. The amount of beads used was 1/10 of the chromatin volume. The samples were rotated gently at 4ºC for 60-90 min. Afterwards, the beads were captured with a magnetic rack and the supernatant was discarded. The beads were washed five times, twice with Low salt buffer [150 mM NaCl; 0.1% (w/v) SDS; 1% (w/v) Triton X-100; 2 mM EDTA; 20 mM Tris-HCl, pH 8.0] and twice with High salt buffer [500 mM NaCl; 0.1% (w/v) SDS; 1% (w/v) Triton X-100; 2 mM EDTA; 20 mM Tris-HCl, pH 8.0] and finally, the immunoprecipitated chromatin was washed with TE buffer. The volume of the buffers utilized for washings was the same volume as chromatin used for the ChIP. Input samples and the immunoprecipitated samples were de-crosslinked by using the IPure kit (diagenode; www.diagenode.com) and following the instructions of the fabricant. Samples were ready to carry out further expression experiments and sequencing.

4.7.   Bioinformatic analyses of the ChIP-seq.

The ChIP-seq analyses was performed using the nf-core/chipseq pipeline (nf-core/chipseq v1.1.0, Nextflow v20.04.1) (10.5281/zenodo.3240506). The internal parameters used were as default, but for the model fold parameter, which was set to -m 4 50. The input

parameters were as follows: – genome TAIR10 – macs_gsize 11.95e7 – single_end – narrow_peak – fragment_size 230. Two different analyses were done to increase the number of peaks detected: with and without pooling the biological replicates.

4.8.   Visualization of ChIP-seq results.

Peaks found in the ChIP-seq, genes associated to the peaks, PBE/G- boxes positions and read coverage in the central G/PBE-box in each of the peaks was analyze using the Integrative Genomics Viewer (Robinson et al., 2011, 2017; Thorvaldsdóttir et al., 2013) and the Integrated Genome Browser (Nicol et al., 2009).

5. SUPPLEMENTARY INFORMATION

5.1. Supplementary Figures
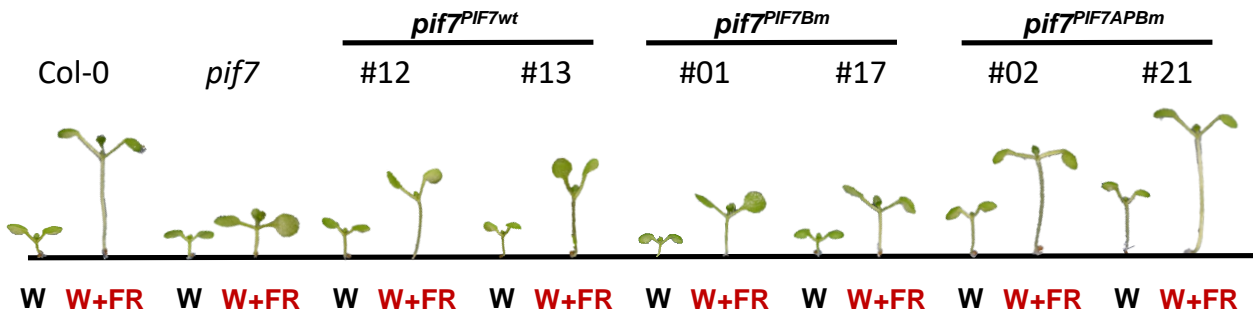
Supplementary Figure SX1. Aspect of seedlings of Col-0, *pif7* and transgenic lines *pif7^{PIF7wt}*, *pif7^{PIF7Bm}* and *pif7^{PIF7APBm}* grown in W and in W+FR. Seedlings were grown as indicated in Figure X2D-F.
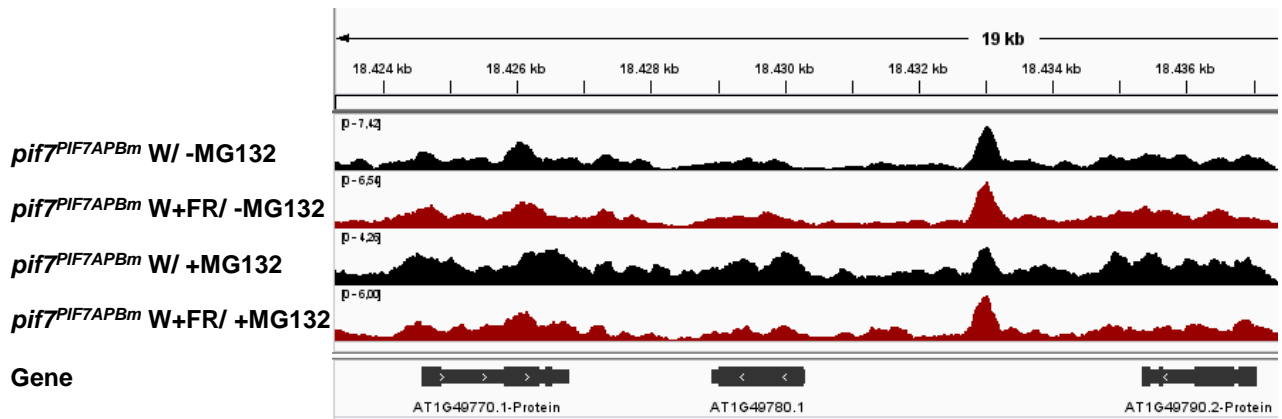
Supplementary Figure SX2. Visualization of peak located close to AT1G49780 using IGV genome browser. Peak p7_03 was only detected bioinformatically in W+FR without MG132 (*pif7^{PIF7APBm}* W+FR/ -MG132). However, it can be visualized in the rest of the samples (W/ -MG132, W/ +MG132 and W+FR/ +MG132). Black color indicates W conditions and red color indicated W+FR.
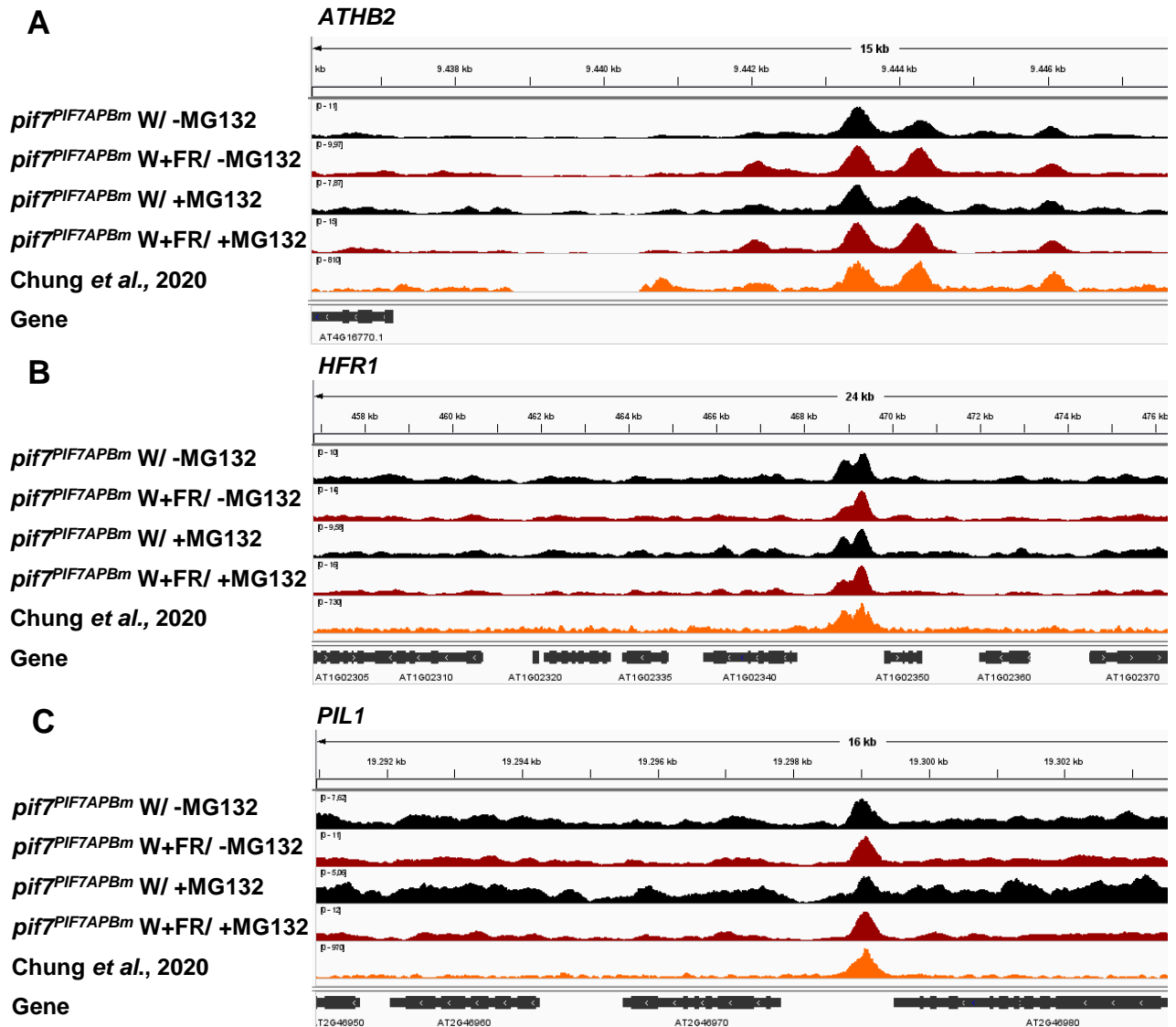
Supplementary Figure SX3. Most of our peaks were already found as PIF7 targets in previous ChIP-seqs. Visualization of peaks corresponding to promoters of **(A)** *ATHB2*, **(B)** *HFR1* and **(C)** *PIL1* compared to those obtained by Chung *et al.*, 2020 (colored in orange). Peaks found in our ChIP-seq are colored in black for samples treated with W and in Red for samples treated with W+FR.

5.2. Supplementary Tables

Table SX1. List of peaks found in the ChIP-seq for PIF7APBm. Each peak is associated to their nearest genes. AGI number, the strand (direction) and the name of each gene are indicated. Information about peak sequences and their coordinates is also provided to localize them in *A. thaliana* chromosomes. Table SX1 is available at https://bit.ly/3hB7ecm.

Table SX2. Lists of PIF-targeted genes found in published ChIP-seq and genes detected in RNA-seqs whose expression is modulated by shade conditions. These lists were obtained from previously obtained data in our and other laboratories (Chung et al., 2020; Kohnen et al., 2016; Leivar et al., 2012; Molina-Contreras et al., 2019; Pastor-Andreu et al. (Chapter 2 of this thesis) Pfeiffer et al., 2014; Yang et al., 2018). When corresponding, genotypes and exposure time to shade for each experiment is indicated. Table SX2 is available at https://bit.ly/3Cer8Sv.

Table SX3. Primers used for cloning.

Gene	Primer name	Sequence (5`- 3`)
AtPIF7	JO414	TAACACATGTCGAATTATGGAG
AtPIF7	JO415	GGCTCGAGATCTCTTTTCTCATGATTC
PIF7 cDNA	JO416	AGCGCTCACATGGGAAAATGCGCAACTAACCGTTCATGGTC
PIF7 cDNA	JO417	GCCCATTTTCCCATGTGAGCGCTTTAACTCCATAATTCGAC
PIF7 cDNA	JO418	CAACGAGTCCGATAGGAGACGGCGTGATAGGAT
PIF7 cDNA	JO419	GCCGTCTCCTATCGGACTCGTTGTGAATCGC
PIF7 cDNA	MJO25	GACTGATAGTGACCTGTTCG
3XHA	SPO32	GGCTCGAGTCAAGCGTAATCTGGA
pPIF7	JDO14	GGTCTAGATAATTGAAAGAGTACATTCAAATATC
pPIF7	SPO20	CCTCTAGAGTGTTACTTAGGCCGC

Table SX4. Primers used for gene expression analyses

Gene	Primer name	Sequence (5`- 3`)
PIF7	BAO06	TGGCCACAGCGTCACTGCAA
	BAO07	TGCTCGTCCCCGTCGTCCAT
UBQ10	BO40	AAATCTCGTCTCTGTTATGCTTAAGAAG
	BO41	TTTTACATGAAACGAAACATTGAACTT
PIL1	BO87	GGAAGCAAAACCCTTAGCATCAT
	BO88	TCCATATAATCTTCATCTTTTAATTTTGGTTTA
EF1α	BO95	TGGTGTCAAGCAGATGATTTGC
	BO96	ATGAAGACACCTCCTTGATGATTTC
YUCCA8	BO134	AATGGACGCGGTTAAGATCG
	BO135	CCCCTTGAGCGTTTCGTG
YUCCA9	BO136	GGCATGGAAGTCTCTCTTGATCTT
	BO137	CGGTAAAACATGAACCGAGCTT
PIL1 R1	JRO62	AATGGGACCCACAATTAGGC
	JRO63	AACACAAAGGGGTGGATGAA
PIL1 R2	JRO64	CGCATGAACTTGTGTCTTCG
	JRO65	GCTGCTTGTCTTAGTTCTTTCACA

6. REFERENCES

Al-Sady, B., Kikis, E. A., Monte, E., & Quail, P. H. (2008). Mechanistic duality of transcription factor function in phytochrome signaling. *Proceedings of the National Academy of Sciences of the United States of America*, *105*(6), 2232–2237. https://doi.org/10.1073/pnas.0711675105

Al-Sady, B., Ni, W., Kircher, S., Schäfer, E., & Quail, P. H. (2006). Photoactivated Phytochrome Induces Rapid PIF3 Phosphorylation Prior to Proteasome-Mediated Degradation. *Molecular Cell*, *23*(3), 439–446. https://doi.org/10.1016/j.molcel.2006.06.011

Alatwi, H. E., & Downs, J. A. (2015). Removal of H2A.Z by INO 80 promotes homologous recombination . *EMBO Reports*, *16*(8), 986–994. https://doi.org/10.15252/embr.201540330

Brahma, S., Udugama, M. I., Kim, J., Hada, A., Bhardwaj, S. K., Hailu, S. G., Lee, T. H., & Bartholomew, B. (2017). INO80 exchanges H2A.Z for H2A by translocating on DNA proximal to histone dimers. *Nature Communications*, *8*. https://doi.org/10.1038/ncomms15616

Casal, J. J. (2012). Shade Avoidance. *The Arabidopsis Book*, *10*, e0157. https://doi.org/10.1199/tab.0157

Chen, M., & Chory, J. (2011). Phytochrome signaling mechanisms and the control of plant development. *Trends in Cell Biology*, *21*(11), 664–671. https://doi.org/10.1016/j.tcb.2011.07.002

Chung, B. Y. W., Balcerowicz, M., Di Antonio, M., Jaeger, K. E., Geng, F., Franaszek, K., Marriott, P., Brierley, I., Firth, A. E., & Wigge, P. A. (2020). An RNA thermoswitch regulates daytime growth in Arabidopsis. *Nature Plants*, *6*(5), 522–532. https://doi.org/10.1038/s41477-020-0633-3

Ciolfi, A., Sessa, G., Sassi, M., Possenti, M., Salvucci, S., Carabelli, M., Morelli, G., & Ruberti, I. (2013). Dynamics of the shade-avoidance response in Arabidopsis. *Plant Physiology*, *163*(1), 331–353. https://doi.org/10.1104/pp.113.221549

Cole, B., Kay, S. A., & Chory, J. (2011). Automated analysis of hypocotyl growth dynamics during shade avoidance in Arabidopsis. *Plant Journal*, *65*(6), 991–1000. https://doi.org/10.1111/j.1365-313X.2010.04476.x

Coleman-Derr, D., & Zilberman, D. (2012). Deposition of Histone Variant H2A.Z within Gene Bodies Regulates Responsive Genes. *PLoS Genetics*, *8*(10).

https://doi.org/10.1371/journal.pgen.1002988

Dong, H. K., Yamaguchi, S., Lim, S., Oh, E., Park, J., Hanada, A., Kamiya, Y., & Choi, G. (2008). SOMNUS, a CCCH-type zinc finger protein in Arabidopsis, negatively regulates light-dependent seed germination downstream of PIL5. *Plant Cell, 20*(5), 1260–1277. https://doi.org/10.1105/tpc.108.058859

Duek, P. D., & Fankhauser, C. (2005). Duek and Fankhauser 2005. *Physiologia Plantarum*, *10*(2), 4. papers://e039176b-8a3a-4ebd-9a1f-447a3ac5092e/Paper/p100

Gallemí, M., Molina-Contreras, M. J., Paulišić, S., Salla-Martret, M., Sorin, Ç., Godoy, M., Franco-Zorrilla, J. M., Solano, R., & Martínez-Garçıa, J. F. (2017). A non-DNA-binding activity for the ATHB4 transcription factor in the control of vegetation proximity. *New Phytologist*, *216*(3), 798–813. https://doi.org/10.1111/nph.14727

Hornitschek, P., Kohnen, M. V., Lorrain, S., Rougemont, J., Ljung, K., López-Vidriero, I., Franco-Zorrilla, J. M., Solano, R., Trevisan, M., Pradervand, S., Xenarios, I., & Fankhauser, C. (2012). Phytochrome interacting factors 4 and 5 control seedling growth in changing light conditions by directly controlling auxin signaling. *Plant Journal*, *71*(5), 699–711. https://doi.org/10.1111/j.1365-313X.2012.05033.x

Hornitschek, P., Lorrain, S., Zoete, V., Michielin, O., & Fankhauser, C. (2009). Inhibition of the shade avoidance response by formation of non-DNA binding bHLH heterodimers. *EMBO Journal*, *28*(24), 3893–3902. https://doi.org/10.1038/emboj.2009.306

Huang, X., Zhang, Q., Jiang, Y., Yang, C., Wang, Q., & Li, L. (2018). Shade-induced nuclear localization of PIF7 is regulated by phosphorylation and 14-3-3 proteins in arabidopsis. *ELife*, *7*, 1–17. https://doi.org/10.7554/eLife.31636

Huq, E., Al-Sady, B., Hudson, M., Kim, C., Apel, K., & Quail, P. H. (2004). Phytochrome-interacting factor 1 is a critical bHLH: Regulator of chlorophyll biosynthesis. *Science*, *305*(5692), 1937–1941. https://doi.org/10.1126/science.1099728

Huq, E., & Quail, P. H. (2002). PIF4, a phytochrome-interacting bHLH factor, functions as a negative regulator of phytochrome B signaling in Arabidopsis. *EMBO Journal*, *21*(10), 2441–2450. https://doi.org/10.1093/emboj/21.10.2441

Inoue, K., Nishihama, R., Kataoka, H., Hosaka, M., Manabe, R., Nomoto, M., Tada, Y., Ishizaki, K., & Kohchi, T. (2016). Phytochrome signaling is mediated by PHYTOCHROME INTERACTING FACTOR in the liverwort Marchantia polymorpha. *Plant Cell*, *28*(6), 1406–1421. https://doi.org/10.1105/tpc.15.01063

Jiang, Y., Yang, C., Huang, S., Xie, F., Xu, Y., Liu, C., & Li, L. (2019). The ELF3-PIF7 Interaction Mediates the Circadian Gating of the Shade Response in Arabidopsis.

IScience, *22*, 288–298. https://doi.org/10.1016/j.isci.2019.11.029

Khanna, R., Huq, E., Kikis, E. A., Al-Sady, B., Lanzatella, C., & Quail, P. H. (2004). A novel molecular recognition motif necessary for targeting photoactivated phytochrome signaling to specific basic helix-loop-helix transcription factors. *Plant Cell*, *16*(11), 3033–3044. https://doi.org/10.1105/tpc.104.025643

Kohnen, M. V., Schmid-Siegert, E., Trevisan, M., Petrolati, L. A., Sénéchal, F., Müller-Moulé, P., Maloof, J., Xenarios, I., & Fankhauser, C. (2016). Neighbor detection induces organ-specific transcriptomes, revealing patterns underlying hypocotyl-specific growth. *Plant Cell*, *28*(12), 2889–2904. https://doi.org/10.1105/tpc.16.00463

Lee, D. H., & Goldberg, A. L. (1998). Proteasome Inhibitors Cause Induction of Heat Shock Proteins and Trehalose, Which Together Confer Thermotolerance in Saccharomyces cerevisiae . *Molecular and Cellular Biology*, *18*(1), 30–38. https://doi.org/10.1128/mcb.18.1.30

Leivar, P., & Monte, E. (2014). PIFs: Systems integrators in plant development. *Plant Cell*, *26*(1), 56–78. https://doi.org/10.1105/tpc.113.120857

Leivar, P., Monte, E., Al-Sady, B., Carle, C., Storer, A., Alonso, J. M., Ecker, J. R., & Quaila, P. H. (2008). The Arabidopsis phytochrome-interacting factor PIF7, together with PIF3 and PIF4, regulates responses to prolonged red light by modulating phyB levels. *Plant Cell*, *20*(2), 337–352. https://doi.org/10.1105/tpc.107.052142

Leivar, P., Monte, E., Oka, Y., Liu, T., Carle, C., Castillon, A., Huq, E., & Quail, P. H. (2008). Multiple Phytochrome-Interacting bHLH Transcription Factors Repress Premature Seedling Photomorphogenesis in Darkness. *Current Biology*, *18*(23), 1815–1823. https://doi.org/10.1016/j.cub.2008.10.058

Leivar, P., & Quail, P. H. (2011). PIFs: Pivotal components in a cellular signaling hub. *Trends in Plant Science*, *16*(1), 19–28. https://doi.org/10.1016/j.tplants.2010.08.003

Leivar, P., Tepperman, J. M., Cohn, M. M., Monte, E., Al-Sady, B., Erickson, E., & Quail, P. H. (2012). Dynamic antagonism between phytochromes and PIF family basic helix-loop-helix factors induces selective reciprocal responses to light and shade in a rapidly responsive transcriptional network in Arabidopsis. *Plant Cell*, *24*(4), 1398–1419. https://doi.org/10.1105/tpc.112.095711

Leivar, P., Tepperman, J. M., Monte, E., Calderon, R. H., Liu, T. L., & Quail, P. H. (2009). Definition of early transcriptional circuitry involved in light-induced reversal of PIF-imposed repression of photomorphogenesis in young Arabidopsis seedlings. *Plant Cell*, *21*(11), 3535–3553. https://doi.org/10.1105/tpc.109.070672

Li, L., Ljung, K., Breton, G., Schmitz, R. J., Pruneda-Paz, J., Cowing-Zitron, C., Cole, B. J., Ivans, L. J., Pedmale, U. V., Jung, H. S., Ecker, J. R., Kay, S. A., & Chory, J. (2012). Linking photoreceptor excitation to changes in plant architecture. *Genes and Development*, *26*(8), 785–790. https://doi.org/10.1101/gad.187849.112

Liu, X., Yang, S., Zhao, M., Luo, M., Yu, C. W., Chen, C. Y., Tai, R., & Wu, K. (2014). Transcriptional repression by histone deacetylases in plants. *Molecular Plant*, *7*(5), 764–772. https://doi.org/10.1093/mp/ssu033

Lorrain, S., Allen, T., Duek, P. D., Whitelam, G. C., & Fankhauser, C. (2008). Phytochrome-mediated inhibition of shade avoidance involves degradation of growth-promoting bHLH transcription factors. *Plant Journal*, *53*(2), 312–323. https://doi.org/10.1111/j.1365-313X.2007.03341.x

Lusser, A., Kölle, D., Loidl, P., & Lusser, A. (2001). *<2001_Trends in plant science_Histone acetylation lessons from the plant kingdom._Lusser, Kölle, Loidl.pdf>*. *6*(2), 59–65.

Martínez-García, J. F., Gallemí, M., Molina-Contreras, M. J., Llorente, B., Bevilaqua, M. R. R., & Quail, P. H. (2014). The shade avoidance syndrome in Arabidopsis: The antagonistic role of phytochrome A and B differentiates vegetation proximity and canopy shade. *PLoS ONE*, *9*(10). https://doi.org/10.1371/journal.pone.0109275

Martínez-García, J. F., Galstyan, A., Salla-Martret, M., Cifuentes-Esquivel, N., Gallemí, M., & Bou-Torrent, J. (2010). Regulatory Components of Shade Avoidance Syndrome. In J.-C. Kader & M. Delseny (Eds.), *Advances in Botanical Research* (Vol. 53, pp. 65–116). Academic Press. https://doi.org/https://doi.org/10.1016/S0065-2296(10)53003-9

Molina-Contreras, M. J., Paulišić, S., Then, C., Moreno-Romero, J., Pastor-Andreu, P., Morelli, L., Roig-Villanova, I., Jenkins, H., Hallab, A., Gan, X., Gomez-Cadenas, A., Tsiantis, M., Rodríguez-Concepción, M., & Martínez-García, J. F. (2019). Photoreceptor Activity Contributes to Contrasting Responses to Shade in Cardamine and Arabidopsis Seedlings. *The Plant Cell*, *31*(11), 2649–2663. https://doi.org/10.1105/tpc.19.00275

Ni, M., Tepperman, J. M., & Quail, P. H. (1998). PIF3, a phytochrome-interacting factor necessary for normal photoinduced signal transduction, is a novel basic helix-loop-helix protein. *Cell*, *95*(5), 657–667. https://doi.org/10.1016/S0092-8674(00)81636-0

Nicol, J. W., Helt, G. A., Blanchard Jr., S. G., Raja, A., & Loraine, A. E. (2009). The Integrated Genome Browser: free software for distribution and exploration of genome-scale datasets. *Bioinformatics*, *25*(20), 2730–2731. https://doi.org/10.1093/bioinformatics/btp472

Oh, E., Kang, H., Yamaguchi, S., Park, J., Lee, D., Kamiya, Y., & Choi, G. (2009). Genome-

wide analysis of genes targeted by PHYTOCHROME INTERACTING FACTOR 3-LIKE5 during seed germination in arabidopsis. *Plant Cell*, *21*(2), 403–419. https://doi.org/10.1105/tpc.108.064691

Oh, E., Yamaguchi, S., Hu, J., Yusuke, J., Jung, B., Paik, I., Lee, H. S., Sun, T. P., Kamiya, Y., & Choi, G. (2007). PIL5, a phytochrome-interacting bHLH protein, regulates gibberellin responsiveness by binding directly to the GAI and RGA promoters in Arabidopsis seeds. *Plant Cell*, *19*(4), 1192–1208. https://doi.org/10.1105/tpc.107.050153

Oh, E., Zhu, J.-Y., & Wang, Z.-Y. (2012). Interaction between BZR1 and PIF4 integrates brassinosteroid and environmental responses. *Nature Cell Biology*, *14*(8), 802–809. https://doi.org/10.1038/ncb2545

Paik, I., Kathare, P. K., Kim, J. II, & Huq, E. (2017). Expanding Roles of PIFs in Signal Integration from Multiple Processes. *Molecular Plant*, *10*(8), 1035–1046. https://doi.org/10.1016/j.molp.2017.07.002

Paulišić, S., Qin, W., Arora Verasztó, H., Then, C., Alary, B., Nogue, F., Tsiantis, M., Hothorn, M., & Martínez-García, J. F. (2021). Adjustment of the PIF7-HFR1 transcriptional module activity controls plant shade adaptation. *The EMBO Journal*, *40*(1), 1–16. https://doi.org/10.15252/embj.2019104273

Peng, M., Li, Z., Zhou, N., Ma, M., Jiang, Y., Dong, A., Shen, W. H., & Li, L. (2018). Linking phytochrome-interacting factor to histone modification in plant shade avoidance. *Plant Physiology*, *176*(2), 1341–1351. https://doi.org/10.1104/pp.17.01189

Pfeiffer, A., Shi, H., Tepperman, J. M., Zhang, Y., & Quail, P. H. (2014). Combinatorial complexity in a transcriptionally centered signaling hub in arabidopsis. *Molecular Plant*, *7*(11), 1598–1618. https://doi.org/10.1093/mp/ssu087

Robinson, J. T., Thorvaldsdóttir, H., Wenger, A. M., Zehir, A., & Mesirov, J. P. (2017). Variant review with the integrative genomics viewer. *Cancer Research*, *77*(21), e31–e34. https://doi.org/10.1158/0008-5472.CAN-17-0337

Robinson, J. T., Thorvaldsdóttir, H., Winckler, W., Guttman, M., Lander, E. S., Getz, G., & Mesirov, J. P. (2011). Integrative Genome Viewer. *Nature Biotechnology*, *29*(1), 24–26. https://doi.org/10.1038/nbt.1754.Integrative

Roig-Villanova, I., Bou-Torrent, J., Galstyan, A., Carretero-Paulet, L., Portolés, S., Rodríguez-Concepción, M., & Martínez-García, J. F. (2007). Interaction of shade avoidance and auxin responses: A role for two novel atypical bHLH proteins. *EMBO Journal*, *26*(22), 4756–4767. https://doi.org/10.1038/sj.emboj.7601890

Chapter I – References

Roig-Villanova, I., & Martínez-García, J. F. (2016). Plant responses to vegetation proximity: A whole life avoiding shade. *Frontiers in Plant Science*, *7*(FEB2016), 1–10. https://doi.org/10.3389/fpls.2016.00236

Shen, H., Zhu, L., Castillon, A., Majee, M., Downie, B., & Huq, E. (2008). Light-induced phosphorylation and degradation of the negative regulator phytochrome-interacting factor1 from Arabidopsis depend upon its direct physical interactions with photoactivated phytochromes. *Plant Cell*, *20*(6), 1586–1602. https://doi.org/10.1105/tpc.108.060020

Shen, Yu, Khanna, R., Carle, C. M., & Quail, P. H. (2007). Phytochrome induces rapid PIF5 phosphorylation and degradation in response to red-light activation. *Plant Physiology*, *145*(3), 1043–1051. https://doi.org/10.1104/pp.107.105601

Shen, Yuan, Wei, W., & Zhou, D. X. (2015). Histone Acetylation Enzymes Coordinate Metabolism and Gene Expression. *Trends in Plant Science*, *20*(10), 614–621. https://doi.org/10.1016/j.tplants.2015.07.005

Shin, J., Kim, K., Kang, H., Zulfugarov, I. S., Bae, G., Lee, C. H., Lee, D., & Choi, G. (2009). Phytochromes promote seedling light responses by inhibiting four negatively-acting phytochrome-interacting factors. *Proceedings of the National Academy of Sciences of the United States of America*, *106*(18), 7660–7665. https://doi.org/10.1073/pnas.0812219106

Shin, J., Park, E., & Choi, G. (2007). PIF3 regulates anthocyanin biosynthesis in an HY5-dependent manner with both factors directly binding anthocyanin biosynthetic gene promoters in Arabidopsis. *Plant Journal*, *49*(6), 981–994. https://doi.org/10.1111/j.1365-313X.2006.03021.x

Sorin, C., Salla-Martret, M., Bou-Torrent, J., Roig-Villanova, I., & Martínez-García, J. F. (2009). ATHB4, a regulator of shade avoidance, modulates hormone response in Arabidopsis seedlings. *Plant Journal*, *59*(2), 266–277. https://doi.org/10.1111/j.1365-313X.2009.03866.x

Sura, W., Kabza, M., Karlowski, W. M., Bieluszewski, T., Kus-Slowinska, M., Pawełoszek, Ł., Sadowski, J., & Ziolkowski, P. A. (2017). Dual role of the histone variant H2A.Z in transcriptional regulation of stress-response genes. *Plant Cell*, *29*(4), 791–807. https://doi.org/10.1105/tpc.16.00573

Thorvaldsdóttir, H., Robinson, J. T., & Mesirov, J. P. (2013). Integrative Genomics Viewer (IGV): High-performance genomics data visualization and exploration. *Briefings in Bioinformatics*, *14*(2), 178–192. https://doi.org/10.1093/bib/bbs017

Toledo-Ortiz, G., Huq, E., & Quail, P. H. (2003). The Arabidopsis basic/helix-loop-helix

transcription factor family. *Plant Cell*, *15*(8), 1749–1770. https://doi.org/10.1105/tpc.013839

Willige, B. C., Zander, M., Yoo, C. Y., Phan, A., Garza, R. M., Trigg, S. A., He, Y., Nery, J. R., Chen, H., Chen, M., Ecker, J. R., & Chory, J. (2021). PHYTOCHROME-INTERACTING FACTORs trigger environmentally responsive chromatin dynamics in plants. *Nature Genetics*, *53*(7), 955–961. https://doi.org/10.1038/s41588-021-00882-3

Yang, C., Xie, F., Jiang, Y., Li, Z., Huang, X., & Li, L. (2018). Phytochrome A Negatively Regulates the Shade Avoidance Response by Increasing Auxin/Indole Acidic Acid Protein Stability. *Developmental Cell*, *44*(1), 29-41.e4. https://doi.org/10.1016/j.devcel.2017.11.017

Zander, M., Willige, B. C., He, Y., Nguyen, T. A., Langford, A. E., Nehring, R., Howell, E., McGrath, R., Bartlett, A., Castanon, R., Nery, J. R., Chen, U., Zhang, Z., Jupe, F., Stepanova, A., Schmitz, R. J., Lewsey, M. G., Chory, J., & Ecker, J. R. (2019). Epigenetic silencing of a multifunctional plant stress regulator. *ELife*, *8*, 1–24. https://doi.org/10.7554/eLife.47835

Zhang, Y., Mayba, O., Pfeiffer, A., Shi, H., Tepperman, J. M., Speed, T. P., & Quail, P. H. (2013). A Quartet of PIF bHLH Factors Provides a Transcriptionally Centered Signaling Hub That Regulates Seedling Morphogenesis through Differential Expression-Patterning of Shared Target Genes in Arabidopsis. *PLoS Genetics*, *9*(1), 11–13. https://doi.org/10.1371/journal.pgen.1003244

CHAPTER I – REFERENCES

CHAPTER II

Chapter II is a research article planned for publication:

Temporal and spatial regulation of the Shade Avoidance Syndrome in Arabidopsis seedlings.

Pedro Pastor-Andreu[1], Jordi Moreno-Romero[1,3], Sandi Paulisic[1], Antía Rodríguez-Villalón[2], Jaime F. Martínez-García[1,3]*

[1] Centre for Research in Agricultural Genomics (CRAG), CSIC-IRTA-UAB-UB, Cerdanyola del Vallès, 08193-Barcelona, Spain;

[2] ETH, Zurich, Switzerland;

[3] Institute for Plant Molecular and Cell Biology (IBMCP), CSIC-UPV, 46022-València, Spain

ABSTRACT

After vegetation proximity perception or shade (low red to far-red ratio) by the phytochrome photoreceptors, shade avoider plant species, such as *Arabidopsis thaliana*, initiate a set of responses known as the Shade Avoidance Syndrome (SAS), including the well-studied hypocotyl elongation. The current SAS regulatory model states that the shade-induced inactivation of the phytochrome B releases the repression imposed over the PHYTOCHROME INTERACTING FACTORs (PIFs), which results in the rapid activation of gene expression changes. But PIFs are not only regulated by phytochrome B; in fact shade signaling consist in a network that contains several positively- and negatively-acting components that work together to implement the shade-induced transcriptional response and the promotion of hypocotyl elongation. However, it is still unclear how these components are organized. To answer this question, we carried out genetic, temporal, cell biology and transcriptomic analyses of the shade-induced hypocotyl elongation using mutants of the different regulators. Our results demonstrate that these regulatory components are organized in two main branches that act separated in time one from another and modulate the

elongation of different cells along the hypocotyl axis. Moreover, RNA-seq analyses indicate that the two branches are not completely disconnected one from another and that PIFs and ELONGATED HYPOCOTYL 5 (HY5), belonging to separate branches, target common genes whose expression is modulated by shade, indicating the existence of a convergence point to modulate the hypocotyl elongation.

1. INTRODUCTION

Light may become a limiting resource for plants when growing under high vegetation density. When shade-avoider (sun-loving) plants, such as *Arabidopsis thaliana*, face this scenario they display a set of responses known as the shade avoidance syndrome (SAS). Some of the SAS responses aim to acclimate photosynthesis in a situation of light shortage caused by the presence of neighboring plants (Morelli *et al.*, 2021), while others focus on redirecting growth to escape from shade, e.g., to promote the elongation and the apical dominance (reduced branching). At the seedling stage, hypocotyl elongation is likely the best characterized and most conspicuous SAS response, and the focus of this work.

In nature, plants detect the proximity of neighbor vegetation because of changes in the red (R) to far-red light (FR) ratio (R:FR). Under low vegetation density (i.e., when plants grow away from surrounding vegetation), the sunlight that impacts the plant changes progressively the intensity with the time of the day but the R:FR remains relatively constant (>1.2) (Roig-Villanova & Martínez-García, 2016; Smith, 1982). By contrast, under higher vegetation density, two different scenarios can be found, both affecting the R:FR: (1) when surrounding plants are close but do not shade, they reflect mainly FR from sunlight compared with other wavelengths; in that case, plant proximity results in a moderate decrease in the R:FR without reducing light quantity; (2) by contrast, when surrounding plants are much closer and their leaves shade each other (canopy shade), photosynthetic tissues not only reflect FR but also absorb preferentially blue and R from sunlight. This determines a reduction of blue and R filtered by the leaves and an increase of the FR reflected, which results in light with a very low R:FR impacting the shaded plant.

In the lab we use white light (W) for high R:FR conditions, and W supplemented with different amounts of FR (W+FR, simulated shade) for low R:FR conditions reproducing two types of simulated shade: proximity (low R:FR) and canopy (very low R:FR).

These changes in the R:FR are perceived by phytochrome photoreceptors. The genome of *A. thaliana* contains five genes that encode for phytochromes (*PHYA* to *PHYE*). Phytochromes exist in two photoconvertible isoforms: (1) an inactive R-absorbing Pr form and (2) an active FR-absorbing Pfr form, which co-exist in an equilibrium that depends on the prevailing R:FR. Under high R:FR, that typically is found in low vegetation density, the photoequillibrium is displaced toward the active Pfr form and SAS is suppressed. Oppositely, under the low R:FR that is found in high vegetation density, the photoequilibrium moves

towards the inactive Pr form and SAS is induced. Genetic and physiological analyses point that phyB is the major phytochrome controlling the SAS (Nagatani *et al.*, 1991; Somers *et al.*, 1991) and other phytochromes act redundantly with phyB in the control of some SAS responses, such as flowering time (phyD, phyE), petiole elongation (phyD, phyE) and internode elongation between rosette leaves (phyE) (Paul F. Devlin *et al.*, 1998, 1999; Franklin, 2008; Martínez-García *et al.*, 2010). PhyA is a particular case, as it is the only photolabile phytochrome (it is usually absent in high R:FR) that under very low R:FR conditions it tends to accumulate (Martínez-García *et al.*, 2014; Yang *et al.*, 2018). As a consequence, genetic analyses indicated that phyA has an antagonistic role over phyB in the SAS control; indeed, under low R:FR wild-type seedlings present a similar elongation as *phyA* whereas *phyB* displays a higher elongation. In contrast, under very low R:FR, wild-type and *phyB* seedlings elongate less than when grown in low R:FR while *phyA* seedlings present a dramatic hypocotyl elongation. This indicates that phyB repression activity is deactivated by both, proximity (low R:FR) and canopy shade (very low R:FR) whereas phyA repressive role is only induced by very low R:FR (Martínez-García *et al.*, 2014).

SAS implementation is regulated by the interaction of phyB with the PHYTOCHROME INTERACTING FACTORS (PIFs). PIFs are a family of basic-helix-loop-helix (bHLH) transcription factors that, in Arabidopsis, have eight members (PIF1 to PIF8) (Paik *et al.*, 2017). Under high R:FR, when PIFs interact with the active form of phyB, are phosphorylated and degradation via 26S proteasome is promoted (Nozue *et al.*, 2007; Lorrain *et al.*, 2008; Leivar *and* Quail, 2011; Zhang *et al.*, 2013). On the other hand, when plants grow under low R:FR, phyB gets inactivated and does not interact with PIFs, which allows their accumulation. As a consequence, PIFs hetero and homodimerize to bind the DNA and positively regulate the response to shade promoting the expression of PHYTOCHOME RAPIDLY REGULATED (*PAR*) genes instrumental to implement the SAS hypocotyl response (Roig-Villanova & Martínez-García, 2016). Compared to other PIFs, PIF7 has a major role in implementing the shade-induced hypocotyl elongation i.e., *pif7* seedling elongation under low R:FR is attenuated compared to wild-type seedlings whereas *pifq* seedlings (quadruple mutant deficient on *PIF1, PIF3, PIF4,* and *PIF5*) are able to reach a similar hypocotyl length that Col-0 in our shade conditions (de Wit *et al.*, 2015; Leivar *et al.*, 2012; Li *et al.*, 2012; Morelli *et al.*, 2021). Within the *PAR* genes, most of them encode for transcription factors that modulate the implementation of the SAS such as *ATHB2, ATHB4, HAT2, HAT3, LONG HYPOCOTYL IN FR 1* (*HFR1*), *PAR1, PAR2, PIL1, BEEs* and *BIMs* (Cifuentes-Esquivel *et al.*, 2013; Ciolfi

et al., 2013; Gangappa *et al*., 2013; Roig-Villanova *et al*., 2007; Sessa *et al*., 2005; Sorin *et al*., 2009).

Among the various *PAR* genes, we will focus on *HFR1* because it has a dramatic phenotype when grown under W+FR and does not present redundancy with other components as happens in the case, for instance, of *PAR1* and *PAR2*. *HFR1*, whose expression is promoted under W+FR, (Ciolfi *et al*., 2013; de Wit *et al*., 2016) plays a key role as a negative regulator of the SAS, inhibiting shade-induced hypocotyl elongation **(Figure Y1A)**. Consistently, *hfr1* mutants have longer hypocotyls than wild-type seedlings under simulated shade (Ciolfi *et al*., 2013; de Wit *et al*., 2016; Galstyan *et al*., 2011; Roig-Villanova *et al*., 2007). HFR1 is a transcription cofactor that interacts with PIF7 and other PIFs (Galstyan *et al*., 2011; Hornitschek *et al*., 2009; Shi *et al*., 2013) and prevents PIFs DNA-binding activity, hence inhibiting PIFs transcriptional activity. Therefore, HFR1 is part of a negative feedback regulation that avoids an excessive shade-induced growth (Paulišić *et al*., 2021) **(Figure Y1B)**.
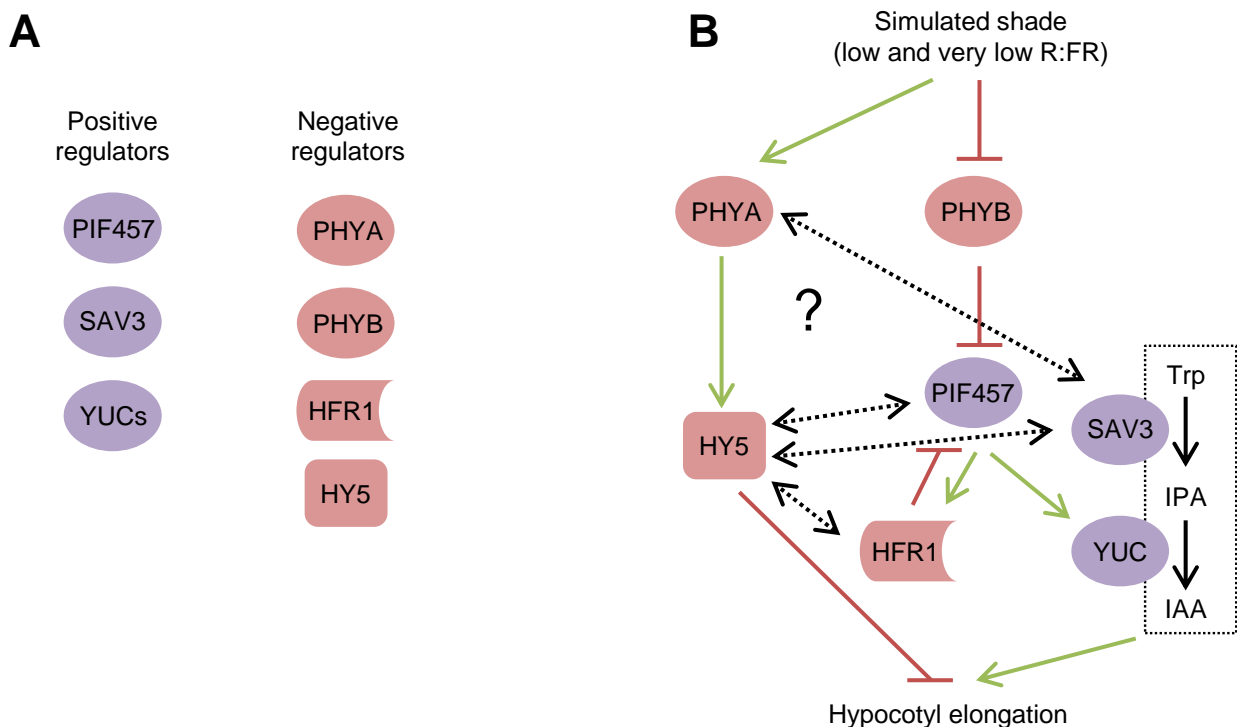

Figure Y1. Shade-induced hypocotyl elongation is modulated by positive and negative regulators that built a complex regulatory network. (A). Main SAS regulators: promoters of hypocotyl elongation are represented in purple and repressors in soft red. **(B).** Current SAS working model integrating the activity of the regulators represented in **A.**

Another component that plays an important role repressing the SAS responses is the transcription factor HYPOCOTYL ELONGATION 5 (HY5) (Gangappa & Botto, 2016). Although *hy5* mutants are already longer than wild-type seedlings under high R:FR, its hypocotyls strongly elongate under low R:FR. There is molecular evidence that HY5 physically interacts with PIF1 and PIF3 during the seedling greening process (Chen *et al.*, 2013) and its negative effect over the shade-induced hypocotyl elongation depends on phyA (Ciolfi *et al.*, 2013). However, how the repressor role of HY5 is integrated in the SAS regulatory network is still unclear **(Figure Y1)** (Bou-Torrent *et al.*, 2015; Roig-Villanova *et al.*, 2006).

Plant hormones also play an important role in the shade-triggered hypocotyl elongation. This is the case of indole-3-acetic acid (IAA), the endogenous bioactive auxin, whose content in Arabidopsis shoots increased by over 50% after 1 h of low R:FR treatment (Kohnen *et al.*, 2016; Li *et al.*, 2012; Tao *et al.*, 2008). The low R:FR-induced *de novo* synthesis of auxin in seedlings initiates a set of complex regulatory processes ultimately leading to cell growth and hypocotyl elongation (Dünser & Kleine-Vehn, 2015). Tryptophan (Trp) is the precursor of the shade-induced IAA biosynthesis that occurs through the SHADE AVOIDANCE 3 (SAV3) pathway (Tao *et al.* 2008) and involves PIF-mediated transcription of *YUCCA* genes that encode rate-limiting enzymes in auxin biosynthesis **(Figure Y1)** (Hornitschek *et al.*, 2012; Li *et al.*, 2012). SAV3 is a SAS positive regulator required in the shade-induced biosynthesis of auxins (needed for the hypocotyl growth) by converting Trp into indole-3-pyruvic acid (IPA) (Zhao, 2012). Consistently, *sav3* mutant seedlings do not produce auxins and fail to elongate their hypocotyls in response to shade (Stepanova *et al.*, 2008) **(Figure Y1)**.

In summary, this study is focused on the regulators that play a major role in the shade-triggered hypocotyl elongation (**Figure Y1A**) because their mutants show a clear alteration in the length of their shade-grown hypocotyls compared to the wild type. As mentioned, seedlings deficient in negative regulators (phyA, phyB, HFR1 and HY5) elongate more than wild-type seedlings whereas those deficient in positive regulators (PIF4, PIF5, PIF7 and SAV3) elongate less than Col-0 seedings under simulated shade.

How the different components are connected and work together to perceive and respond to shade has been partially established (**Figure Y1B**). However, the connections between some of the described SAS regulators are still unclear: for instance, although PIFs are considered to play a central role in the shade-induced hypocotyl elongation when phyB is

inactivated after low R:FR treatment, it is unknown if other transcriptional regulators (e.g., HY5) might be required to induce this response. Moreover, although in Arabidopsis dark-grown seedlings it is known that hypocotyl elongation is the result of a non-regular pattern of elongation of the pre-existing files of 20 cells in the hypocotyl (Gendreau *et al.*, 1997), it is unknown how simulated shade affects this pattern of elongation. In addition, despite all the advances on the molecular genetics of the SAS response, there is still little information on the growth behavior of this organ at the temporal and spatial levels, as well as the impact of several of the SAS regulators at these organization levels.

In this work we deepen in the architecture of the network of regulators implementing the shade-induced hypocotyl elongation in *Arabidopsis thaliana,* with special interest on how the different regulators are working together to modulate this response. We have taken three different approaches to redefine the genetic relationship between the SAS regulators: (1) **genetic analyses**, to establish if different SAS components work in the same of different pathways or regulatory modules of the network; (2) **temporal analyses**, to know when the different components analyzed act in controlling shade-induced hypocotyl elongation; and (3) **spatial analyses**, to identify which cells along the hypocotyl axis are targeted by each of the main SAS regulators.

2. RESULTS

2.1. SAS regulatory network is organized in two main differentiated modules or branches.

To address how the different SAS signaling components are connected in the regulatory network that controls the shade-induced hypocotyl elongation response, we initially performed a series of genetic analyses focusing just on mutants in negative (*phyA, phyB*, *hy5*, *hfr1*) or positive (*sav3*, *pif7* and the triple *pif4 pif5 pif7*, from now on *pif457*) SAS components. As mentioned, these components were selected because their participation in SAS regulation is well known and described; in addition, except PIF mutants, they are not redundant with other SAS regulators which simplifies the process of generation of multiple mutants. For simplicity, the used allele will not be indicated in the text, although this information is provided in the figures and in the material and methods section.

To better visualize the phyA activity all the shade experiments presented were performed under very low R:FR. We first analyzed the response of double mutants between negative regulators, starting with phyA and phyB (**Figure Y2**). In W, length of wild-type (Col-0) and *phyA* hypocotyls was similar, whereas *phyB* hypocotyls were longer and those of *phyA phyB* double mutant seedlings were the longest, as expected (Devlin *et al.*, 2003). In W+FR, *phyA* hypocotyls were longer and *phyB* hypocotyls shorter than the wild type (**Figure Y2A**). Importantly, the *phyA phyB* hypocotyl length was even longer than in W, indicating that other phytochromes can regulate the shade-induced hypocotyl elongation. Together, these data are consistent with phyB repressing hypocotyl elongation in W and phyA in W+FR (Martínez-García *et al.*, 2014). When none of the two phytochromes are present, the absence of repression in both W and W+FR strongly unleashes the hypocotyl elongation (**Figure Y2A**). To visualize better the effect of shade in controlling elongation, particularly useful when comparing genotypes with different hypocotyl length under W (e.g., Col-0 vs. *phyB*), the difference in hypocotyl length in W+FR and W ($HYP_{W+FR} - HYP_W$) was calculated (**Figure Y2B**). This representation showed that the *phyA phyB* double mutant had an intermediate elongation response compared to *phyA* and *phyB* single mutants, suggesting that the effect of the two phytochromes is additive (**Figure Y2B**). This result supports that both photoreceptors act likely independently of one another in controlling the shade-induced hypocotyl length. As the $HYP_{W+FR} - HYP_W$ value helps to visualize better the genetic

relationships between the different mutants, this representation is shown for the following set of experiments. Hypocotyl length data will be shown as supplementary information.
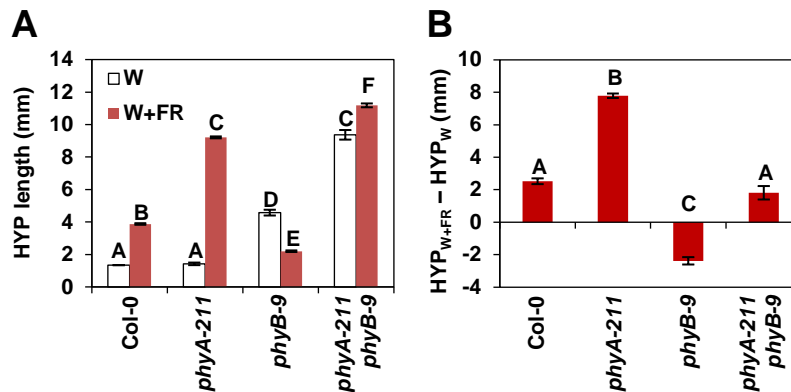
Figure Y2. Effect of phyA and/or phyB on the hypocotyl elongation in response to simulated shade. All the genotypes were germinated in W for 2 days and then they were either maintained in W or transferred to W+FR for 5 more days. **(A)** Hypocotyl length of Col-0, *phyA-211*, *phyB-9* and *phyA-211 phyB-9* double mutant seedings after growing in W or W+FR. **(B)** Difference of hypocotyl length in W+FR (HYP$_{W+FR}$) minus W (HYP$_W$) of the genotypes shown in **A**. Values are means ± SE of three independent biological replicas. Tukey test was performed and different character above the data indicate significant differences between genotypes (p-value <0.05).

We next analyzed the shade-induced elongation response of double mutants deficient in other negative regulators: *phyA hfr1*, *hy5 hfr1* and *phyA hy5* (**Figure Y3, Supplementary Fig SY1**). Whereas *phyA hfr1* and *hy5 hfr1* double mutant elongated more than the single mutants (**Figures Y3A-B**), seedlings of the double *phyA hy5* elongated as much as the single mutant *phyA* (**Figures Y3C**). These results pointed that the pairs phyA-HFR1 and HY5-HFR1 were additive in regulating the shade-induced hypocotyl elongation, whereas phyA was epistatic over HY5. Additivity indicates that HFR1 acts independently of phyA and HY5 in controlling this response. In contrast, phyA and HY5 epistasis points that both regulators act in the same branch of the SAS regulatory network.

Next, we generated multiple mutants between positive and negative SAS regulators (**Figure Y4, Supplementary Fig S2**). Firstly, mutant *hfr1* plants were crossed with *pif7*, and phenotypic analyses showed that *hfr1 pif7* elongated less than *hfr1* and more than *pif7*, presenting an intermediate elongation between the single mutants (**Figures Y4A**) consistent with HFR1 interacting with and inhibiting PIF7 activity (Fiorucci *et al.*, 2020; Paulišić *et al.*, 2021). Because HFR1 is known to heterodimerize with and inhibit transcriptional activity of several PIFs, forming the PIFs-HFR1 transcriptional regulatory module (Galstyan *et al.*, 2011; Paulišić *et al.*, 2021), we reasoned that the intermediate elongation activity observed in *hfr1*

pif7 seedlings was likely caused by the presence of PIF4 and PIF5, also known to promote the shade-induced elongation of hypocotyls (Hornitschek *et al.*, 2009; Li *et al.*, 2012; Lorrain *et al.*, 2008). Therefore, we analyzed *hfr1 pif457* phenotype. As expected, the elongation response to shade was reduced in *hfr1 pif457* (**Figures Y4B**). These results agree with the view that HFR1 activity depends on PIF4, PIF5 and PIF7 (from now on PIF457) to repress the elongation of hypocotyls. Mutant *hfr1* plants were also crossed with auxin biosynthetic mutant *sav3*. Phenotypic analyses showed that *hfr1 sav3* (**Figures Y4C**) was almost as short as *hfr1 pif457*, according with the fact that the PIFs-HFR1 module depends on the SAV3 auxin biosynthetic pathway to control the shade-induced hypocotyl elongation (Ciolfi *et al.*, 2013; Fiorucci *et al.*, 2020; Li *et al.*, 2012; Paulišić *et al.*, 2021).
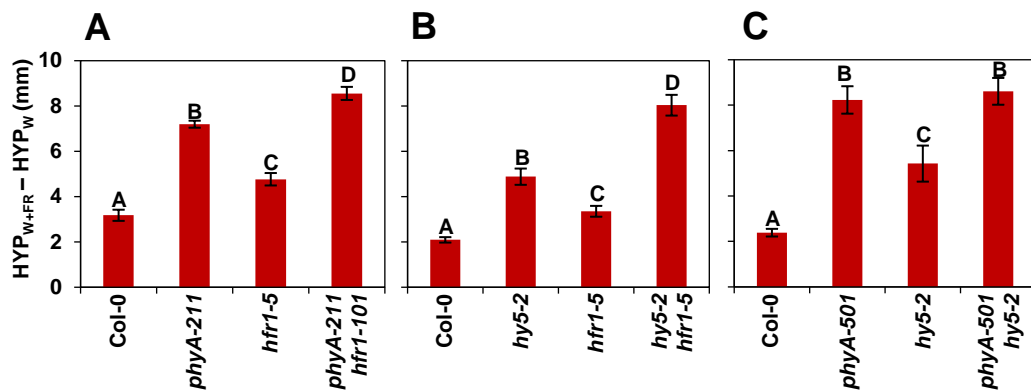
Figure Y3. Combinatory effect of pairs of negative regulators on the shade-induced hypocotyl elongation. Difference of hypocotyl length in W+FR (HYP_{W+FR}) and W (HYP_W) of **(A)** Col-0, *phyA-211, hfr1-5, phyA-211 hfr1-101*, **(B)** Col-0, *hy5-2, hfr1-5, hy5-2 hfr1-1*, **(C)** Col-0, *phyA-501, hy5-2* and *phyA-501 hy5-2*. Seedlings were germinated and grown as indicated in **Figure Y2**. Representation of data and statistical analysis was performed as in **Figure Y2B**.

Secondly, *phyA* plants were crossed with *pif7* and *pif457*. In contrast with the HFR1-related crosses, *phyA pif7* and *phyA pif457* elongation response was similar between them. Moreover, shade-induced elongation in these multiple mutants was closer to *phyA* than to *pif7* (**Figures Y4D-E**), being greater than wild type. These results indicated that the elongation repression imposed by phyA does not depend on PIF4, PIF5 or PIF7 (**Figures Y4D-E**). A similar elongation pattern was observed in the *phyA sav3* seedlings (**Figures Y4F**), showing that phyA repression is (at least partially) auxin independent.

We also crossed *hy5* plants with *pif7* and *pif457*. As before, *hy5 pif7* and *hy5 pif457* showed a similar elongation, i.e., their hypocotyls were longer than *pif7* but shorter than *hy5* (**Figures Y4G-H**). The intermediate elongation of *hy5 pif7* and *hy5 pif457* compared to the

hy5 and *pif7*/*pif457* mutants suggest that HY5 activity is additive to PIF457 in regulating the shade-induced hypocotyl elongation. A similar pattern of elongation was observed for the *hy5 sav3* seedlings, i.e., they were longer than *sav3* but shorter than *hy5* (**Figure Y4I**), further supporting that *hy5* and *sav3* were additive in regulating this response. Together, these results are consistent with PHYA and HY5 acting independently of PIF457, HFR1 and SAV3 to promote the shade-induced hypocotyl elongation.
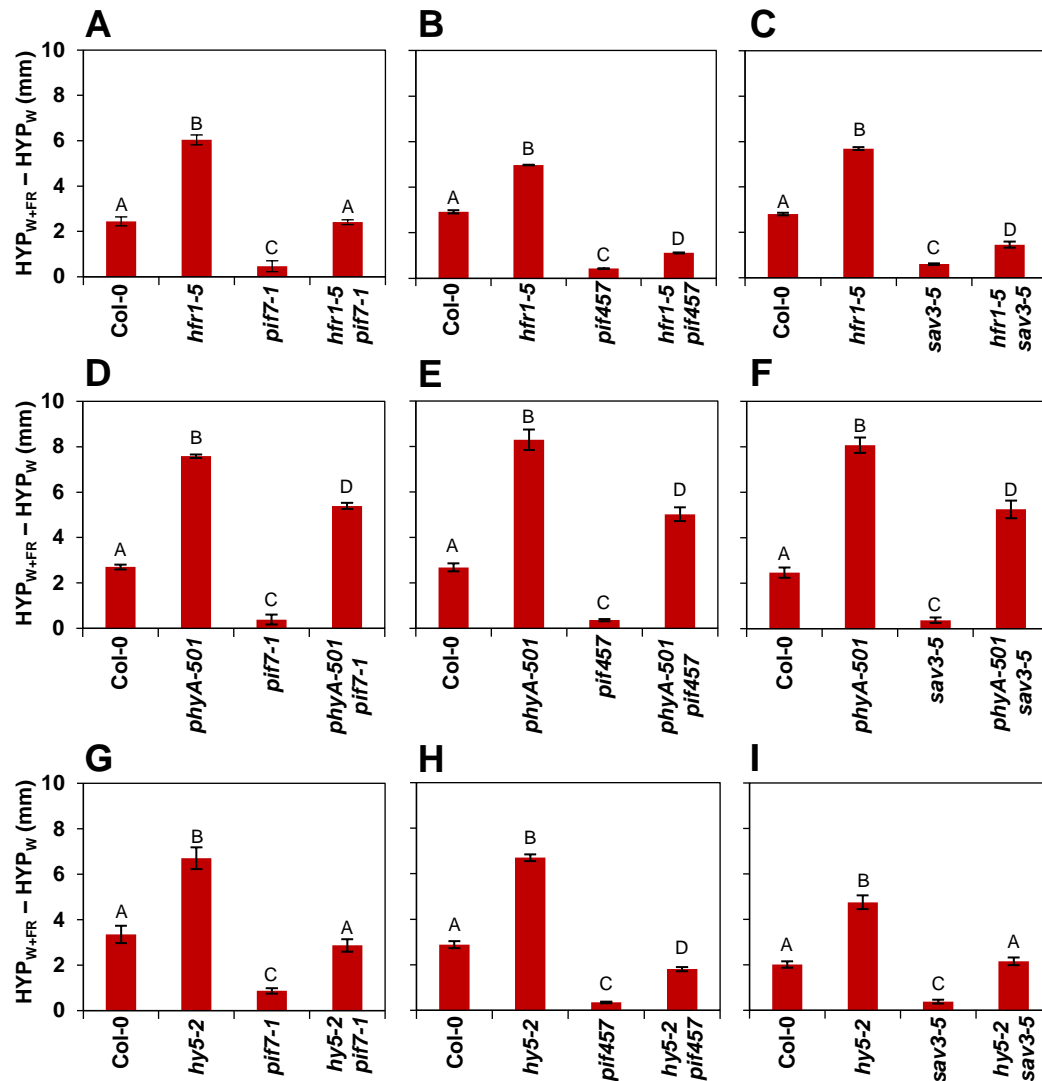
Figure Y4. Combinatory effect of pairs of negative and positive regulators on the shade-induced hypocotyl elongation. The graphs show the difference hypocotyl length in W+FR (HYP$_{W+FR}$) minus W (HYP$_W$) of **(A)** Col-0, *hfr1-5*, *pif7-1*, *hfr1-5 pif7-1*; **(B)** Col-0, *hfr1-5*, *pif457*, *hfr1-5 pif457*; **(C)** Col-0, *hfr1-5*, *sav3-5*, *hfr1-5 sav3-5*; **(D)** Col-0, *phyA-501*, *pif7-1*, *phyA-501 pif7-1*; **(E)** Col-0, *phyA-501*, *pif457*, *phyA-501 pif457*; **(F)** Col-0, *phyA-501*, *sav3-5*, *phyA-501 sav3-5*; **(G)** Col-0, *hy5-2*, *pif7-1*, *hy5-2 pif7-1*; **(H)** Col-0, *hy5-2*, *pif457*, *hy5-2 pif457* and **(I)** Col-0, *hy5-2*, *sav3-5*, *hy5-2 sav3-5*. Seedlings were germinated and grown as indicated in **Figure Y2**. Representation of data and statistical analysis was performed as in **Figure Y2B**.

2.2. *phyA* and *hy5* are more resistant to NPA application than *hfr1* mutant seedlings.

In seedlings of *A. thaliana* and the crop species *Brassica rapa*, shade perception by the cotyledons drives synthesis of IAA, which is then transported to the hypocotyl to induce growth (Procko *et al.*, 2014; Tao *et al.*, 2008). Consistently, treatment of wild-type seedlings with the auxin transport inhibitor naphthylphthalamic acid (NPA) abolishes this response (Sorin *et al.*, 2009). As showed before, the dependency of PIFs-HFR1 on auxin biosynthesis (and consequently on SAV3) and transport to promote the shade-induced hypocotyl elongation, is well established. Less is known about phyA and HY5 dependency on this hormone synthesis and transport to modulate hypocotyl elongation in response to shade. To explore this relationship, we tested how NPA application affected the shade-induced hypocotyl elongation in *hy5* and *phyA* seedlings (**Figure Y5**). Under W, increasing concentrations of NPA resulted in a mild or null reduction of the already short hypocotyls in all the genotypes tested. However, the slightly longer *hy5* hypocotyls showed some resistance to NPA as even the highest NPA concentrations tested did not abolish completely their elongation displaying hypocotyls that were still longer than the rest of genotypes (**Figure Y5C**). Under W+FR, hypocotyl length of genotypes was strongly inhibited by NPA. However, whereas for the case of Col-0, a hypocotyl length very close to the minimum measured was reached with 1 µM NPA, for the case of *phyA* and *hy5* the maximum concentration of 3 µM was required to obtain the minimum hypocotyl length (**Figure Y5B, D**). As *phyA* and *hy5* were much longer than Col-0 under W+FR, we wondered if this was mainly causing the difference in NPA response between genotypes. Therefore, we included *sav3* in the analyses and used the double *phyA sav3* and *hy5 sav3*, which were as long as Col-0 in response to W+FR (**Figure Y4, Supplementary Figure SY2**). The short *sav3* hypocotyls virtually did not vary with the NPA treatment under either W or W+FR, as the double *phyA sav3* under W (**Figure Y5A-D**). Under W+FR, *phyA sav3* mock-treated seedling hypocotyls reached ~6 mm. Hypocotyl length dropped with NPA treatment to similar levels as *phyA*, which was significantly longer than Col-0 or *sav3* (**Figure Y5B**). In W, *hy5 sav3* hypocotyls elongated as the single *hy5* in response to NPA (**Figure Y5C**). In W+FR, *hy5 sav3* were as long as *hy5* and still longer than Col-0 and *sav3* when grown with 3 µM NPA (**Figure Y5D**). Together, these data indicate that shade-induced elongation of *phyA* and *hy5* is less affected by NPA than that of Col-0 (i.e., *phyA* and *hy5* are more resistant to NPA than Col-0), which suggested that these mutants are not exclusively depending on auxin transport to elongate.
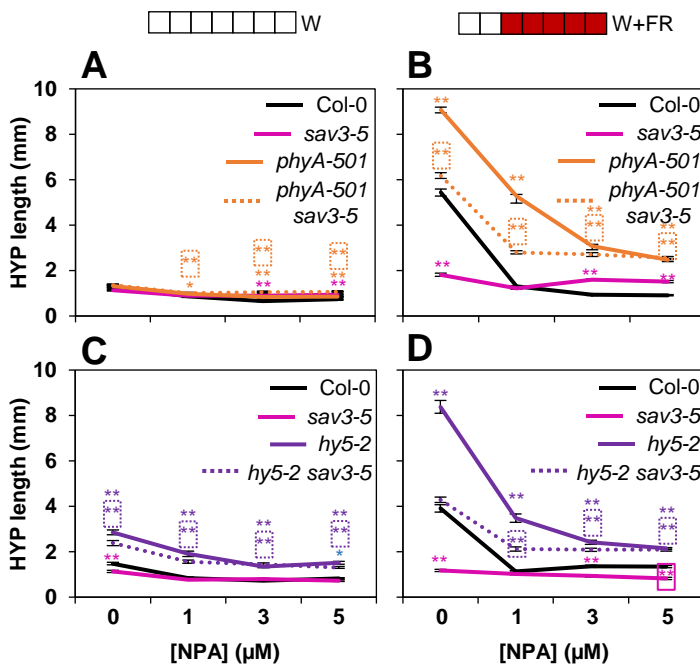
Figure Y5. *phyA-501*, *phyA-501 sav3-5*, *hy5-2* and *hy5-2 sav3-5* reach higher hypocotyl length than other genotypes when grown with increasing concentrations of naphthylphthalamic acid (NPA). The graphs represent the effect of increasing concentrations of NPA over the hypocotyl length of **(A)** Col-0, *phyA-501*, *sav3-5* and *phyA-501 sav3-5* grown in W; **(B)** Col-0, *phyA-501*, *sav3-5* and *phyA-501 sav3-5* grown in W+FR; **(C)** Col-0, *hy5-2*, *sav3-5* and *hy5-2 sav3-5* grown in W and **(D)** Col-0, *hy5-2*, *sav3-5* and *hy5-2 sav3-5* grown in W+FR. All the genotypes were grown with 0, 1, 3 and 5 µM of NPA. They germinated in W for 2 days and then they were either maintained in W or transferred to W+FR for 5 more days. Values are means ± SE of ~25 seedlings. Asterisks mark significant differences between genotypes and Col-0 grown under the same NPA concentration (Student t-test: ** p-value < 0.01; * p-value < 0.05). Magenta, orange and purple asterisks are used for *sav3*, *phyA* and *hy5* respectively. Orange asterisks inside discontinuous-lined orange square correspond to *phyA sav3* and purple asterisks inside discontinuous-lined purple square correspond to *hy5 sav3*.

2.3. SAS regulatory components act in different moments during the shade-induced hypocotyl elongation.

We aimed to provide a temporal framework for the elongation response to shade, i.e., the elongation speed of hypocotyls during the whole exposure of young seedlings to W+FR. This would allow us to address if the different genetic components investigated in here act at the same or different moments during the early development of the seedlings. To address this question, growth rates were first determined in wild-type (Col-0) seedlings grown under W and simulated shade. To do so, hypocotyl length was measured daily from day 2 to day 7, and growth rate was calculated for each condition (**Figure Y6**). As a result, Col-0 growth rate remained constant along time when grown under W (**Figure Y6A and D**), whereas it elongated more from day 4 onwards under W+FR (**Figure Y6B, E**). As a control, we also estimated the growth rate of the hypocotyl *phyB* mutant seedlings that, as expected, was always higher than that of Col-0 in W. Importantly, under W, *phyB* growth rate increased with the age of the seedlings, elongating more at the end of the period analyzed (from day 5 onwards) (**Figure Y6A**). Under W+FR, *phyB* growth rate resembles that of Col-0 but it was

attenuated (**Figure Y6B**), consistent with the reduced shade-induced elongation reported for this *phyB* mutant allele under very low R:FR conditions compared to Col-0 **(Figure Y2A)** (Martínez-García *et al.*, 2014).

Next, we analyzed this phenotype for the SAS negative regulators. Under W, growth rate of *phyA*, *hy5* and *hfr1* did not vary significantly during the seedling development (**Figure Y6D**). Under W+FR, *phyA* growth rate was strongly higher in comparison to Col-0 (or *phyB* under W) at the beginning of the development (on days 2 and 3) but progressively dropped until day 6 to values comparable to those of Col-0. Similarly, *hy5* grew faster at the beginning of the development, although it had a peak on day 4. Seedlings of *hfr1* also had a peak of growth on day 4 but elongated faster in the second half of the period analyzed (**Figures Y6B, E**).
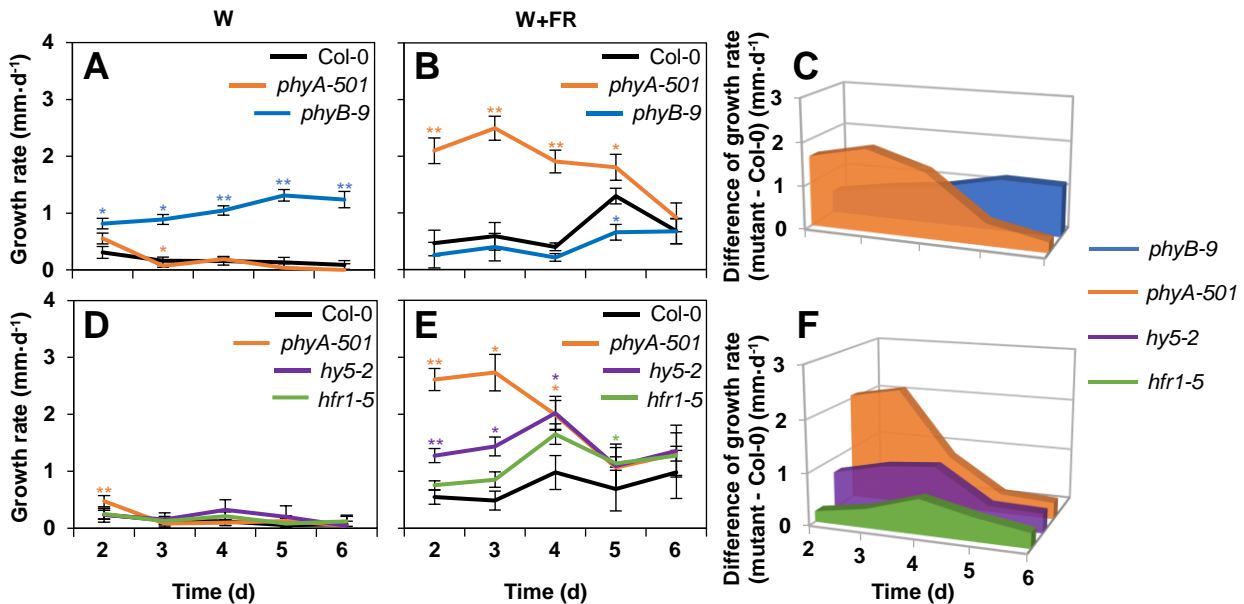
Figure Y6. Growth rate pattern differs between the mutants defective in negative regulators. The graphs show the growth rate of **(A)** Col-0, *phyA-501* and *phyB-9* grown in W; **(B)** Col-0, *phyA-501* and *phyB-9* grown in W+FR; **(C)** difference of the mean growth rate in *phyA-501* and *phyB-9* respect to Col-0; **(D)** Col-0, *phyA-501, hfr1-5* and *hy5-2* grown in W; **(E)** Col-0, *phyA-501, hfr1-5* and *hy5-2* grown in W+FR and **(F)** difference of the mean growth rate in *phyA-501*, *phyB-9*, *hfr1-5* and *hy5-2* respect to Col-0. All the genotypes were germinated in W for 2 days and then they were either maintained in W or transferred to W+FR for 5 more days. Hypocotyl length was measured daily from day 2 until day 7 to calculate the growth rate. Mean values ± SE of biological triplicates are shown. Asterisks mark significant differences between genotypes and Col-0 grown compared the same day (Student t-test: ** p-value < 0.01; * p-value < 0.05). Blue, orange, purple and green asterisks are used for *phyB, phyA hy5* and *hfr1* respectively. The values in **C** were calculated by subtracting the *phyB-9* growth rate in W minus the Col-0 growth rate in W and in **F** as the growth rate of the other mutants in W+FR minus the Col-0 growth rate in W+FR.

To better visualize when the repressor activity of the SAS regulators was more important during hypocotyl elongation, the growth rate of the Col-0 was subtracted to the mutants' growth. The growth conditions represented were those where the phenotype is more obvious: W for *phyB*, and W+FR for *hfr1*, *hy5* and *phyA*. This representation showed when elongation peaked along the early seedling development for these mutants: whereas *phyA* and *hy5* grew faster in the first half of the period analyzed (from days 2 to 4), *hfr1* peaked on day 4 and *phyB* after day 5 (**Figure Y6C, F**). Although the temporal activity of the regulators overlapped, this approach showed that phyA and HY5 repressive activities were stronger at the beginning of seedling development (from day 2 to day 4) and differed from those of HFR1 and phyB, that were more obvious at the second half of the period analyzed, especially for phyB (from day 5 to day 7).

2.4. SAS regulatory components target overlapping but different cells along the hypocotyl axis.

Independently on where the primary site of action of the different regulators is (e.g., cotyledons or hypocotyls), their activity converges on the hypocotyl elongation, which in *A. thaliana* is caused only by cell elongation (i.e., no cell division is involved). Previously, the pattern of cell length in W-grown hypocotyls was shown to take place essentially in all epidermal cells over the entire growth period (from 1 until 9 days after germination), although the area of fastest growth moves up acropetally (from the base on day 2 to the middle of the hypocotyl on days 7-9). Similarly, in dark-grown seedlings growth is initiated in the basal cells but in this case, elongation zone moves up the hypocotyl with time, to become restricted to a small area below the apical hook at day 7 (Gendreau *et al.*, 1997). As growth regulators in shade are different than those in W and during etiolation, we aimed to learn first the pattern of cell length of wild-type (Col-0) hypocotyls when grown under W+FR. Because of the variability observed between experiments and within a population, we grew about 100 seedlings of Col-0 seedlings in W and W+FR for 7 days, and hypocotyls were measured. 15-16 individuals whose hypocotyl length was close to the average were selected to be fixed, stained and the length of the 20 cells that make up a cell file were measured, from bottom to top. Cell elongation of several files of epidermal cells of the hypocotyl longitudinal axis per treatment were measured (**Figure Y7**). These values were averaged for each of the 20 cells that make up a cell file, from bottom to top (**Figure Y7A**). The differences in cell length means in W+FR and W were represented for each of the 20 cells that make up a cell file along the hypocotyl longitudinal axis. This representation showed that the enhanced elongation of wild-

type (Col-0) hypocotyls grown under simulated shade compared to those grown under W was due to an enhanced elongation of cells along the lower-middle part of the hypocotyl, with cells 7-8 showing the elongation peak (**Figure Y7B, C, D, E and F**). These results indicate that shade-induced hypocotyl elongation was the result of a pattern of asymmetric elongation of epidermal cells.
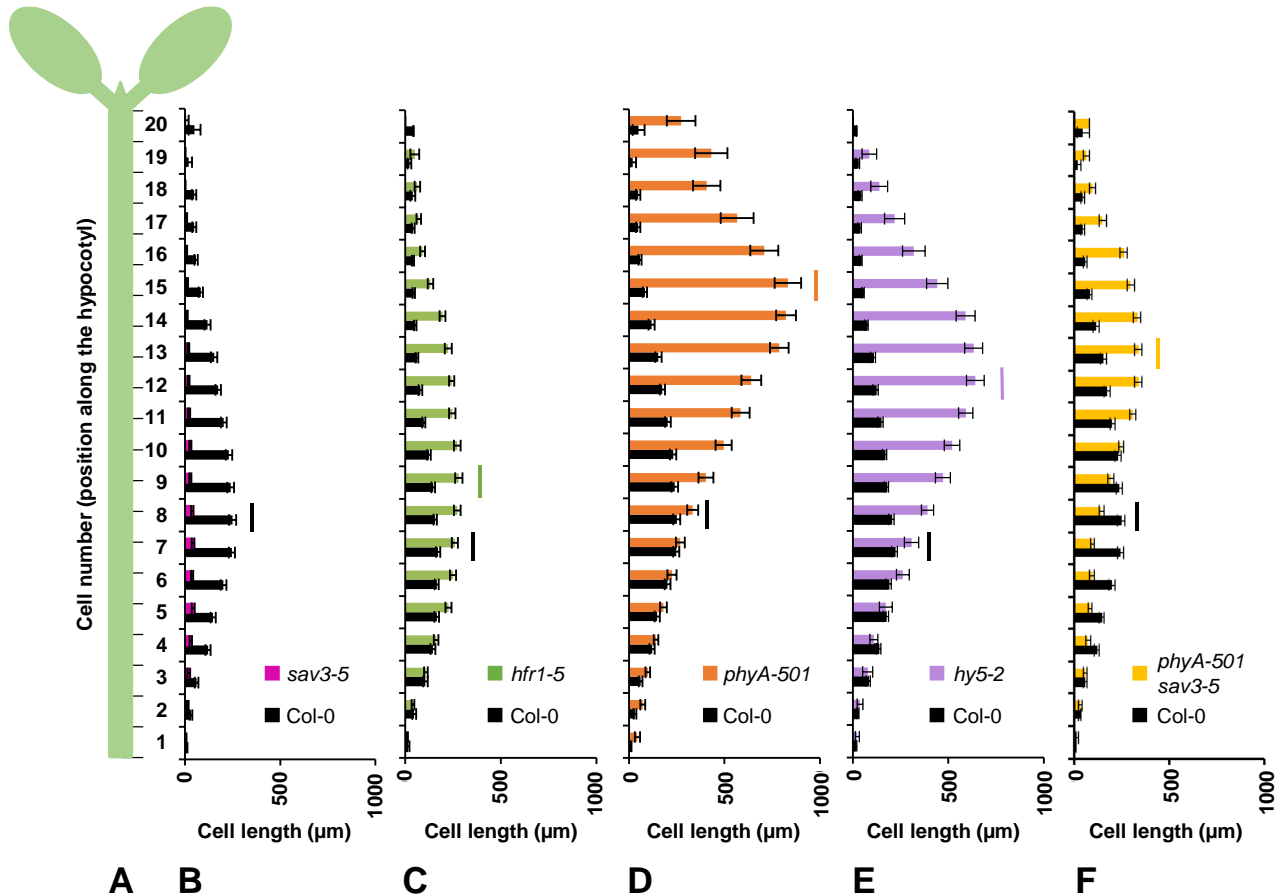
Figure Y7. The shade-induced cell elongation depends on the position of the cell along the hypocotyl and is different for each SAS regulatory mutant. (A) Schematic representation of a cell file composed by 20 cells along the hypocotyl axis of Arabidopsis seedling. The graphs illustrate the cell-specific shade-induced elongation of Col-0 (wild-type control) and **(B)** *sav3-5* mutant; **(C)** *hfr1-5* mutant; **(D)** *phyA-501* mutant; **(E)** *hy5-2* mutant and **(F)** *phyA-501 sav3-5* double mutant. All the genotypes were germinated in W for 2 days and then were either maintained in W or transferred to W+FR for 5 more days. In all the graphs, we represented the cell elongation in W+FR minus the cell elongation in W. The colored lines on the right side of each graph indicate the cell that presents a higher length in (W+FR)-W compared to the corresponding wild-type cell length in (W+FR)-W. For *phyA* and *phyA sav3* the Col-0 used as a control is shared.

Next, we aimed to establish if the pattern of cell length observed in the hypocotyls of seedlings deficient in specific SAS regulators differed from the observed in wild-type hypocotyls, i.e., if the various SAS regulators target the same or different cells along the

hypocotyl axis when this organ elongates in response to simulated shade. To answer this question, we analyzed cell length distribution (or pattern of cell length) of *sav3*, *phyA*, *hy5*, *hfr1* and *phyA sav3*. As expected, the poorly shade-responsive *sav3* hypocotyls did show a similar pattern of cell length as the wild-type hypocotyls but strongly attenuated (**Figure Y7B**). In the *hfr1* hypocotyls, the pattern of cell length extended towards the cotyledons, with cell 9 showing the maximum of elongation compared with the corresponding wild type cells (peak around cells 6-7) (**Figure Y7C**). In the case of *phyA* and *hy5*, the upper part of hypocotyl elongated the most, centered around cells 15 and 12 respectively, in clear contrast with cells 8 and 7 showing the most elongation in wild-type hypocotyls (**Figures Y7D, E**). In the latter two genotypes (*phyA* and *hy5*), the redistribution of the pattern of cell length to the upper hypocotyl was distinct to that observed in the wild-type and *hfr1* seedlings. To check if the redistribution of growth was merely caused by the enhanced hypocotyl shade-induced elongation shown by the *phyA* and *hy5* genotypes, we also analyzed the pattern of cell length in *phyA sav3* hypocotyls, whose shade-induced hypocotyl elongation was similar to that on *hfr1* and shorter than *hy5* hypocotyls (**Figure Y4**). In these seedlings, the hypocotyl region that elongated most was centered around cell 13 (cell 8 in wild-type hypocotyls), indicating that phyA represses the elongation of a group of cells located in the upper half of the hypocotyl (**Figure Y7F**). In summary, these analyses indicate that (1) the hypocotyl cells more responsive to simulated shade are placed in the lower half of the wild-type hypocotyls (centered in cells 7-8), (2) removal of SAS negative regulators changes the pattern of cell length, and (3) although the target cells of the various SAS negative regulators overlap, the pattern of cell length due to loss of *HY5* and *PHYA* function is strongly displaced towards the upper part of the hypocotyl. These results are consistent with phyA and HY5 activities repressing the cells of the upper part of the hypocotyl whereas HFR1 tends to repress the elongation of cells placed in the lower half of the hypocotyl.

2.5. PIF457 and HY5 share target genes and both modulate its expression.

Despite the temporal and spatial preferences shown for each of the SAS regulators analyzed, their activities partially overlap. This agrees with the observation of the hypocotyl elongation data from genetic analyses in the case of *hy5 pif7* and *hy5 pif457* (intermediate elongation between *pif7/pif457* and *hy5*) (**Figures Y4G-H, SY4G-H**), that made us to further investigate a possible convergence between the two groups of regulators described previously. In addition, there is evidence about a relationship between HY5 and PIFs, e.g.,

HY5 directly interacts with PIF1/PIF3 proteins in other photomorphogenic responses (Chen *et al.*, 2013) and HY5 and PIF1/PIF3/PIF4/PIF5 activities converge at shared *cis* regulatory elements (Toledo-Ortiz *et al.*, 2014; Zhang *et al.*, 2017). Then, we decided to perform expression analysis checking the gene expression of shared targets between PIF4/PIF5/PIF7 and HY5.
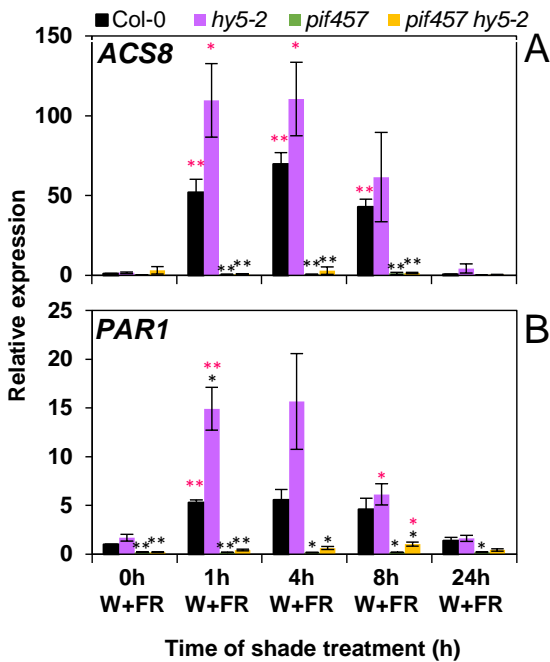
Figure Y8. HY5 and PIFs activity could converge in the regulation of the expression of some common targeted genes. **(A)** Relative expression of *ACS8* in Col-0, *hy5-2*, *pif457* and *hy5-2 pif457* at different times of simulated shade treatment (0, 1, 4, 8 and 24 h). **(B)** Relative expression of *PAR1* in Col-0, *hy5-2*, *pif457* and *hy5-2 pif457* at different time of simulated shade treatment (0, 1, 4, 8 and 24 h). Values are means ± SE of four independent biological replicas. Black asterisks mark significant differences between genotypes and Col-0 in the same light conditions (Student t-test: ** p-value < 0.01; * p-value < 0.05). Pink asterisk mark significant differences between a genotype at a specific time point and itself at 0 h (Student t-test: ** p-value < 0.01; * p-value < 0.05).

First, we focused in the HY5 target genes identified in a ChIP-chip experiment (Lee *et al.*, 2007). Among this group of more than 3800 genes, we focused on *ACS8* and *PAR1* because they were also described as PIFs targets (by ChIP-q-PCR and ChIP-seq, respectively) (Gallego-Bartolomé *et al.*, 2011; Khanna *et al.*, 2007; Yang *et al.*, 2021), hence being possible candidates to have a genetic expression directly modulated by both transcription factors, HY5 and PIFs. Next, we analyzed the relative expression of these two genes in 7-days-old seedlings of Col-0, *hy5*, *pif457* and *hy5 pif457* after different times exposed to W+FR (0, 1, 4, 8 and 24 h). The expression of *ACS8* was similar before the exposure to W+FR (time 0 h) in the four genotypes analyzed, whereas *PAR1* expression was slightly reduced in *pif457* and *hy5 pif457* compared to Col-0 and *hy5* (**Figure Y8**). In Col-0, the expression of both genes was promoted after 1 h of shade treatment. After 4 and 8 h, their expression did not change drastically compared to 1 h and after 24 h *ACS8* and *PAR1* relative amount of transcript decreased reaching comparable levels to those found at 0 h. In *hy5*, expression of both genes was induced after 1 h but reaching higher levels than in Col-0. After 4 h the expression was not different than at 1 h, but at 8 and 24 h the expression decreased being similar to that of

Col-0 at these time points. In contrast, in *pif457* and *hy5 pif457* the levels of *ACS8* and *PAR1* expression remained almost unchanged throughout the entire experiment. These results suggested that (1) HY5 repress *ACS8* and *PAR1* shade-induced expression, whereas (2) PIF457 activate the expression of these two genes. In addition, (3) HY5 repressive activity needs the positive transcriptional activity of PIFs over the expression of these two genes.

With this information we decided to carry out RNA sequencing (RNA-seq) to expand the possible connection between HY5 and PIFs in regulating the shade-triggered changes in gene expression. We sequenced the time points 0, 1 and 8 h after shade exposure of all four genotypes (Col-0, *hy5*, *pif457* and *hy5 pif457*) to learn about the transcriptomic dynamics early (0 h vs. 1 h) and late (0 h vs. 8 h) times after shade treatment (**Figure Y9A**). We discarded the time points 4 and 24 h due to its results similarity with the time points 1 and 0 h respectively (**Figure Y8**). We identified differentially expressed genes (DEGs) up- (fold change $\geq$ 1.5, P < 0.05) and down-regulated (fold change $\leq$ 1.5, P < 0.05) after 1 and 8 h of shade treatment compared with 0 h for each genotype analyzed.

In Col-0 seedlings, 386 and 826 genes were induced after 1 and 8 h of W+FR, respectively, indicating that the number of DEGs activated in response to simulated shade grew with the time of exposure. In *hy5* seedlings, 791 genes were induced after 1 h, that dropped to 542 after 8 h of W+FR (**Figure Y9B**). By contrast, in *pif457* and *hy5 pif457* seedlings only 1 and 3 genes were induced after 1 h of W+FR, respectively. Longer (8 h) exposure to W+FR leads to the activation of 323 and 279 genes in *pif457* and *hy5 pif457* seedlings, respectively (**Figure Y9B**).

Regarding the repressed genes, in Col-0 seedlings, 177 and 654 DEGs were repressed after 1 and 8 h of W+FR, respectively. In *hy5* seedlings, 351 and 568 genes were repressed after 1 and 8 h of W+FR, respectively (**Figure Y9C**). As in the upregulated DEGs, in *pif457* and *pif457hy5* seedlings only 31 and 17 genes were repressed after 1 h of W+FR, respectively, and these numbers grew up to 435 for *pif457* and 690 for *hy5 pif457* after 8 h of W+FR (**Figure Y9C**). The reduced number of induced and repressed genes at 1 h indicates that PIF457 are strongly required for the rapid changes in gene expression that takes place after simulated shade exposure. However, after 8 h, although the impact of PIF457 is still clear, particularly in the up-regulated genes, its influence seems less prominent.
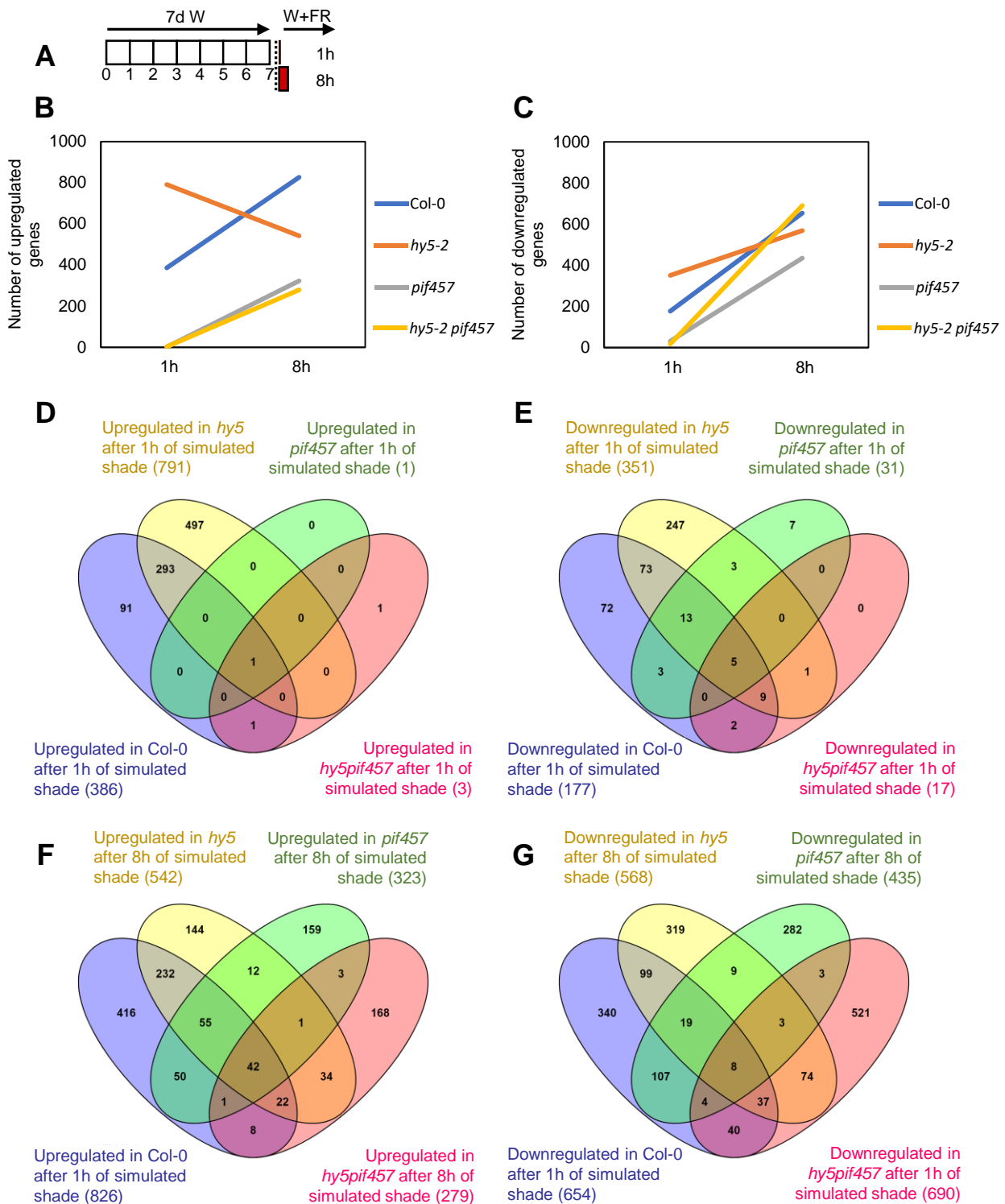
Figure Y9. RNA sequencing results show the possible connection between HY5 and PIF457 regulating the shade-induced changes in gene expression. (A) Conditions utilized to grow plant material for the RNA-seq. **(B)** Number of upregulated genes at 1 h and at 8 h for each genotype. **(C)** Number of downregulated genes at 1 h and at 8 h for each genotype. **(D)** Venn diagram showing the number of upregulated genes at 1 h in each genotype. **(E)** Venn diagram showing the number of downregulated genes at 1 h in each genotype. **(F)** Venn

diagram showing the number of upregulated genes at 8 h in each genotype. **(G)** Venn diagram showing the number of downregulated genes at 8 h in each genotype.

Next, we analyzed the overlapping of the DEGs in the different genotypes. After 1 h of W+FR, 294 upregulated genes were shared between *hy5* (out of 791 genes, 37.2 %) and Col-0 (out of 386 genes, 76.2 %) (**Figure Y9D**) and 100 downregulated genes were shared between *hy5* (out of 351, 28.5 %) and Col-0 (out of 177, 56.49 %) (**Figure Y9E**). Most of these genes did not appear as DEGs after 1 h of W+FR in *pif457* (1 upregulated and 31 downregulated) and *hy5 pif457* (3 upregulated and 17 downregulated) (**Figure Y9D and E**). In fact, specific genes only found in Col-0 or *hy5* are also PIF457 dependent as they were not detected neither in *pif457* nor *hy5 pif457*. After 8 h of W+FR, 460 genes appeared as upregulated in at least two genotypes, but 416, 144, 159 and 168 genes only appear in Col-0, *hy5*, *pif457* and *hy5 pif457,* respectively (**Figure Y9F**). A total of 403 genes were downregulated in at least two genotypes, but 340, 319, 282 and 521 genes only appear in Col-0, *hy5*, *pif457* and *hy5 pif457*, respectively (**Figure Y9G**). These data suggest that although PIF457 and HY5 have a very strong impact in the early shade-regulated changes in gene expression, after 8 h of W+FR treatment, the transcriptional responses diverge and the influence of PIF457 dependence results less apparent and HY5, gains a more prominent role. A clear example of the increasing role of HY5 at 8h are the genes that are upregulated in the *hy5 pif457* but not in the *pif457.*

Regarding the functional predictions, the DEGs belonged to similar GO terms categories in all genotypes (except in *pif457* and *hy5 pif457* after of 1 h of W+FR because of the massive effect in gene expression) (data not shown). Therefore, no obvious and specific process was differentially affected in any genotype. For that reason, we paid attention to the evolution over time of the enrichment of 33 GO terms of biological processes specifically related with shade avoidance, light and growth (13), and five hormone groups (5 of auxins, 4 of gibberellins, 6 of ethylene, 3 of brassinosteroids and 2 of cytokinins) that are able to influence the shade-induced hypocotyl elongation (shown in **Figure Y10**). We observed that most of the GO terms were enriched because of the same pool of DEGs for each genotype (**Supplementary Table SY1**). Then, we checked the p-value of the GO enrichment analyses as an indication of the number of genes found in each genotype that participates in a biological process: the lower the p-value, the higher the significance of the enrichment in a biological process whose expression changes in response to simulated shade. Regarding the functional predictions of

upregulated genes after 1 h of W+FR treatment, we found 12 of the GO terms related to light, growth and shade avoidance, significant in Col-0 seedlings. Most (11) of them were also found in *hy5* with slightly higher p-values (less genes contributing to the GO terms) (**Figure 10A**). In the case of functional predictions related with hormones, after 1 h of shade treatment we found enrichment of 13 of the GO terms involved with auxins, gibberellins, ethylene, brassinosteroids and cytokinins in Col-0. As before, most of them (9) were also found in *hy5* with similar or slightly higher p-values as in wild-type seedlings (**Figure 10A**). Altogether, only 5 GO terms (response to light intensity, auxin transport, auxin polar transport, response to ethylene and response to cytokinins) were found in Col-0 but not in *hy5*. As expected, no GO terms (functional predictions) were found in *pif457* and *hy5 pif457* (that lack shade-induced changes in gene expression, **Figure Y9B**). These results indicate that all these processes (response to light stimulus, response to blue light, hormone related processes…) depend on the presence of PIFs to be activated after 1 h of shade treatment.

In the up-regulated genes after 8 h of W+FR treatment, from the total of GO-terms considered, most were enriched in Col-0 (28), *hy5* (24) and, surprisingly even in the mutant *pif457* (18); a few of them (9) were also enriched in *hy5 pif457* (**Figure 10A**). In comparison to Col-0 and *hy5,* p-values in *pif457* and *hy5 pif457* were higher in several GO-terms (less induced genes contributed to enrich the GO-term), such as response to light stimulus, response to red or far-red light and response to auxin stimulus (**Figure 10A**). These results indicate that at 8 h PIF457s are still playing an important role in regulating several processes. Interestingly, lots of biological processes not found in *pif457* after 1 h of W+FR are detected in the mutant after 8 h and with similar p-values to those of Col-0 and *hy5*, indicating that the PIF457 leading role early after W+FR exposure (1 h) dissipates after longer periods of simulated shade. An exception for this observation was the enrichment in GO terms related with gibberellins, that was absent in *pif457* and *hy5 pif457* after 1 h and 8 h of simulated shade.

Other scenario was found in the case of ethylene-related GO terms after 8 h of W+FR, where ethylene biosynthetic process and ethylene metabolic process were not present in any of the mutants but processes related with ethylene signaling pathway and response to ethylene were enriched in *pif457* and *hy5 pif457* with even slightly lower p-values than in Col-0 (**Figure 10 A**).

Regarding the functional predictions of downregulated DEGs, we found enrichment in a small number of processes related with light and hormones. Despite that, processes enriched after 1 h in Col-0 were also enriched in *hy5* but not in the *pif457* or *hy5 pif457* mutants (**Figure 10 B**). Together, these observations suggested that PIF457 activities are fundamental in the early shade-modulated regulation of these processes, whereas HY5 activity gains importance and PIFs loose it after longer periods of exposure to W+FR.

A

	GO:term	Process	Upregulated genes							
			1h				8h			
			WT	hy5	pif457	mm	WT	hy5	pif457	mm
Shade avoidance, light and growth	GO:0009416	response to light stimulus	1,30E-14	9,60E-09			1,30E-26	1,90E-20	3,20E-07	1,40E-06
	GO:0009642	response to light intensity	2,70E-03					4,10E-04		
	GO:0009637	response to blue light	6,90E-09	2,70E-05			2,20E-12	1,10E-10	1,90E-08	1,60E-04
	GO:0010017	red or far-red light signaling pathway	4,90E-07	4,60E-05			6,20E-11	1,80E-09	7,20E-09	8,20E-07
	GO:0009639	response to red or far red light	2,70E-13	2,20E-09			1,20E-23	5,60E-17	7,60E-09	4,20E-07
	GO:0010114	response to red light					7,70E-10	2,40E-05	1,10E-06	
	GO:0010218	response to far red light	3,60E-06	2,90E-04			1,80E-12	3,10E-07	6,30E-04	
	GO:0040007	growth	5,10E-09	2,20E-04			2,50E-07	7,90E-07	2,00E-04	
	GO:0048589	developmental growth	2,40E-11	4,20E-07			1,90E-07	7,50E-07	2,90E-04	
	GO:0060560	developmental growth involved in morphogenesis	2,20E-09	1,50E-05			1,40E-06	2,30E-05	1,30E-03	
	GO:0016049	cell growth	3,00E-08	5,70E-06			7,50E-07	2,30E-06	1,20E-04	
	GO:0009826	unidimensional cell growth	2,20E-09	1,50E-05			1,40E-06	2,30E-05	1,30E-03	
	GO:0009641	shade avoidance	7,00E-09	2,10E-08			5,30E-07	4,80E-08		
Auxins	GO:0010252	auxin homeostasis	5,4E-06	1,5E-04						
	GO:0060918	auxin transport	4,8E-05				1,1E-05	4,0E-06	1,8E-05	
	GO:0009926	auxin polar transport	4,4E-05				1,0E-05	3,6E-06	1,6E-05	
	GO:0009734	auxin mediated signallyng pathway					2,9E-03			
	GO:0009733	response to auxin stimullus	3,5E-48	1,0E-34			6,2E-33	2,0E-22	3,2E-04	1,1E-03
Gibberelins	GO:0009685	gibberellin metabolic process					3,7E-05	5,3E-05		
	GO:0010476	gibberellin mediated signaling pathway	8,5E-05	3,0E-04			2,4E-03	3,8E-04		
	GO:0009740	gibberellic acid mediated signaling pathway	8,5E-05	3,0E-04			2,4E-03	3,8E-04		
	GO:0009739	response to gibberellin stimulus	2,9E-04	2,3E-03			2,6E-04	1,5E-07		
Ethylene	GO:0009693	ethylene biosynthetic process	1,8E-05	4,8E-04			6,6E-06			
	GO:0009692	ethylene metabolic process	1,8E-05	4,8E-04			6,6E-06			
	GO:0009873	ethylene mediated signaling pathway					1,5E-06	1,8E-05	4,5E-07	6,0E-09
	GO:0010104	regulation of ethylene mediated signaling pathway					2,5E-05	2,4E-06	3,3E-06	1,2E-06
	GO:0010105	negative regulation of ethylene mediated signaling pathway					1,7E-06	1,6E-07	3,1E-07	1,1E-07
	GO:0009723	response to ethylene stimulus	2,7E-04				8,0E-07	4,2E-05	7,0E-05	2,5E-07
Brassisteroids	GO:0016131	brassisteroid metabolic process	3,0E-07	1,8E-04						
	GO:0009742	brassisteroid mediated signaling pathway					2,4E-03			
	GO:0009741	response to brassisteroid stimulus	3,2E-06	1,5E-03			5,3E-05			
Cytokinins	GO:0009736	cytokinin mediated signaling pathway								
	GO:0009735	response to cytokinis stimulus	3,2E-03							

B

	GO:term	Process	Enriched GO terms of downregulated genes (p-value)							
			1h				8h			
			WT	hy5	pif457	hy5 pif457	WT	hy5	pif457	hy5 pif457
Auxins	GO:0010252	auxin homeostasis								
	GO:0060918	auxin transport								
	GO:0009926	auxin polar transport								
	GO:0009734	auxin mediated signallyng pathway								
	GO:0009733	response to auxin stimullus	2,5E-04	2,2E-03						
Cytokinins	GO:0009736	cytokinin mediated signaling pathway					2,4E-04			
	GO:0009735	response to cytokinis stimulus								
Gibberelins	GO:0009685	gibberellin metabolic process								
	GO:0010476	gibberellin mediated signaling pathway								
	GO:0009740	gibberellic acid mediated signaling pathway								
	GO:0009739	response to gibberellin stimulus	9,9E-05	8,5E-04						
Ethylene	GO:0009693	ethylene biosynthetic process								
	GO:0009692	ethylene metabolic process								
	GO:0009873	ethylene mediated signaling pathway								
	GO:0010104	regulation of ethylene mediated signaling pathway								
	GO:0010105	negative regulation of ethylene mediated signaling pathway								
	GO:0009723	response to ethylene stimulus	4,0E-05	4,0E-06			1,9E-04			
Brassisteroids	GO:0016131	brassisteroid metabolic process								
	GO:0009742	brassisteroid mediated signaling pathway								
	GO:0009741	response to brassisteroid stimulus								
Shade avoidance, light and growth	GO:0009416	response to light stimulus	1,60E-03	1,60E-08	1,00E-04					2,90E-06
	GO:0009642	response to light intensity								
	GO:0009637	response to blue light								
	GO:0010017	red or far-red light signaling pathway								
	GO:0009639	response to red or far red light	2,80E-03	3,70E-05						
	GO:0010114	response to red light								
	GO:0010218	response to far red light								
	GO:0040007	growth								
	GO:0048589	developmental growth								
	GO:0060560	developmental growth involved in morphogenesis								
	GO:0016049	cell growth								
	GO:0009826	unidimensional cell growth								
	GO:0009641	shade avoidance								

Figure Y10. Shade-regulated genes of the GO processes related to shade, light, growth and hormones show a main regulatory role of PIF457 at short-term (1 h) and an increasing role of HY5 at later times (8 h). GO enriched categories on the **(A)** upregulated and **(B)** downregulated genes. GO terms enrichments were obtained by using agriGO online analyses tool. We show the predicted GO-terms obtained from Col-0, *hy5*, *pif457* and *hy5 pif457* treated with W+FR for 1 and 8 h. Blue color indicates finding a significative GO term (p-value < 0.05). Magenta color indicates absence of a significant GO term. Numbers in the tables are the p-values for each GO term.

3. DISCUSSION

In the regulation of the SAS in *A. thaliana*, the function of phyB, PIFs, HFR1 and its dependency on auxin biosynthesis via YUCCA-SAV3 to promote the shade-induced hypocotyl elongation has been well established (Ciolfi *et al.*, 2013; Fiorucci *et al.*, 2020; Kohnen *et al.*, 2016; Li *et al.*, 2012; Paulišić *et al.*, 2021; Tao *et al.*, 2008). However, other aspects of the SAS regulatory network, such as the genetic relationship of the negative regulators phyA and HY5 and the temporal and spatial architecture of the network (i.e., when and where its components act), are poorly understood.

Removal of active phyB (PfrB) by exposure to simulated shade de-represses PIFs (particularly PIF7 and, to a lower extent, PIF4 and PIF5), which directly activate the expression of positive (e.g., *YUC* genes) and negative (e.g., *HFR1*) regulators of growth (**Figure Y1**). YUC activity together with SAV3 is required for the IAA biosynthesis that promote shade-induced hypocotyl growth. By contrast, HFR1 negatively regulates PIF457 activities by interacting with them and inhibiting PIF DNA-binding. The observed genetic interactions between *sav3* and *hfr1*, and *pif7/pif457* and *hfr1* (**Figures Y4 A-C**) are consistent with this scenario and points to the existence of a branch or module formed by phyB-PIFs-HFR1-SAV3, which is directly involved in producing the rapid and temporal burst in IAA observed after just 1-4 h of exposure to simulated shade (Bou-Torrent *et al.*, 2014; Kohnen *et al.*, 2016; Li *et al.*, 2012; Tao *et al.*, 2008). Our growth rate studies indicate that the components of this module act in a constant manner during the firsts 2-7 days of seedling development. In addition, HFR1 and phyB gain importance at the end of this period, when *hfr1* and *phyB* seedlings elongated most (**Figure Y6**).

In contrast with the previous genetic analyses, *phyA pif457*, *phyA sav3*, *hy5 pif457* and *hy5 sav3* are still able to elongate in response to shade even in the absence of PIF457 and SAV3 (and presumably without the burst in IAA produced by SAV3 and YUC activity). PhyA is able to interact with PIF1 and PIF3 through their Active Phytochrome A-binding motif (APA, needed for active phyA-specific binding) suppressing their regulatory activity (Al-Sady *et al.*, 2006; Shen *et al.*, 2018). Consequently, in the absence of phyA and PIF457, PIF1 and PIF3 might be able to bind the DNA and promote the auxin biosynthesis related genes what explains the ability to elongate of *phyA pif457*. However, how *phyA sav3*, *hy5 pif457* and *hy5 sav3* are able to elongate remains unclear, unless auxins are generated from another biosynthesis pathway where PIF457 and SAV3 are not required. Other possibility is that these

mutants are elongating without the need of *de novo* synthesis of IAA. Indeed, it has been shown that free and active IAA that is metabolized from IAA-glutamate molecules is able to elicit the shade-induced hypocotyl elongation independently of 3-IPA-mediated IAA biosynthesis in cotyledons (Zheng *et al.*, 2016).

Based on the epistatic effect of phyA over HY5 (**Figure Y3**) and the genetic additivity between phyA and HY5 with the HFR1, PIF457 and SAV3 (**Figures Y3 B, Y4 G-I**), we think that the regulatory activity of phyA and HY5 could form a module somehow separated from that of PIF457-HFR1 and the IAA synthetized by the SAV3-YUC pathway (that we name as the phyB-PIFs-HFR1-SAV3 module). This is reinforced by the observed genetic interaction between phyA and phyB (**Figure Y2**) that have antagonistic activities in the shade conditions used in this work (Martínez-García *et al.*, 2010). The HY5 implication in the phyA-mediated down-regulation of early-induced shade avoidance genes in prolonged low R:FR reinforces this view (Ciolfi *et al.*, 2013; Jang *et al.*, 2013). The possible participation of HY5 and phyA in the same module is supported by the increased resistance to the auxin polar transport inhibitor NPA shared by the *phyA*, *phyA sav3*, *hy5* and *hy5 sav3* mutant lines (**Figure Y5**). Furthermore, our growth rate analyses indicate that phyA and HY5 act early in the seedling development (days 2-5) with a central importance in repressing the shade-induced growth in this period compared to phyB and HFR1 (**Figure Y6**). Together, these results highlight that the two regulatory modules are also distinguished by the moment of the development in which they repress the shade-induced elongation as well as their auxin-dependency.

Perception of the R:FR occurs in the cotyledons, where phyB orchestrates a complex transcriptional cascade through its interaction with PIFs. This signal is transmitted to other cells located in the same (intercellular signaling) or in other organs (interorgan signaling) (Bou-Torrent *et al.*, 2008), i.e., from cotyledons towards hypocotyl, organ where the shade-triggered elongation is observed. It has been pointed the involvement of auxin in the transmission of a shade-related signal originated in the irradiated cotyledons (Tanaka *et al.*, 2002). Based on the pattern of cell length compared to the wild type, the auxin deficient mutant *sav3* and the *phyA sav3* mutant present a limited elongation in the cells situated in the lower part of the hypocotyl indicating that SAV3 and auxins are needed for most of the elongation of this section cells that occurs in Col-0 in W+FR (**Figure Y7 B**). Importantly, among the negative regulator mutants, there is a different impact of the growth along the cells of the hypocotyl axis (**Figure Y7 C-F**) that is translated into a spatial separation of the regulatory activity of the module phyB-PIFs-HFR1-SAV3, acting in the middle and lower half

of the hypocotyl and the module phyA-HY5, mainly repressing cell elongation of the upper half. Moreover, regulatory effect of phyB is weak at the beginning of the development allowing the elongation of the lower-middle part of the hypocotyl at this moment. By contrast, the phyA-HY5 module acts early in the shade-induced development and repress the elongation of the upper part of the hypocotyl. Later, the repression imposed by phyA-HY5 progressively dissipates, and the elongation in that upper part takes place. This temporal and spatial separation of phyB-PIFs-HFR1-SAV3 and phyA-HY5 regulatory activities is consistent with the observed hypocotyl elongation in an acropetal gradient (from de base to the top) that were limited to dark- and W-grown seedlings (Gendreau *et al.*, 1997).

An additional level of regulation refers to when the different SAS components act soon after the beginning of the simulated shade exposure. Our transcriptomic analyses indicate that immediately after shade exposure (within 1 h) PIFs are essential to modulate gene expression compared to later times (8 h), when absence of PIF457 had less impact on the DEGs compared to what was found in Col-0 and *hy5* (**Figure Y9 B-C**). Importantly, almost all the early (1 h, up- and down-regulated) DEGs found in the *hy5* background, required PIF457 to be shade-regulated (**Figure Y9 D-E**), which indicate that PIF457 are epistatic over HY5 at this early time after shade exposure. After 8 h, a substantial part of the DEGs still requires PIF457 activity. However, even in the *pif457* background, an important amount of DEGs were identified (**Figure Y9 B and C**), which suggested that the expression of these DEGs depend either on PIF1 and PIF3, or the effect exerted by unknown regulators that also participate in regulating gene expression under W+FR. In conclusion, after 8 h of shade exposure, the transcriptional response diverges between the various genotypes and it does not ultimately depend only on PIF457 regulation (e.g., 168 genes upregulated and 521 downregulated only in *hy5 pif457*). These results could explain the almost wild-type elongation of *hy5 pif457* hypocotyls and even the residual, but significant elongation detected in shade-grown *pif457* seedlings. (**Supplementary Figure SY4**, **Figure Y9 F-G**).

PIFs are usually presented as positive regulators of the SAS promoting the expression of genes involved in hypocotyl elongation. Our RNA-seq analyses demonstrate that they also have an important function in the repression of gene expression as it has been previously described for some PIFs in shade related processes (Jia *et al.*, 2020; Toledo-Ortiz *et al.*, 2010; Xie *et al.*, 2017) (**Figure Y9C, E, G**). Similarly, HY5 not only participates in the rapid shade-repression of genes, but also is needed to induce gene transcription, roles that in both cases requires PIF457 (**Figure Y9D-G**). The dual function of HY5 as transcriptional repressor

and activator could explain the drop in the upregulated genes observed from 1 h to 8 h of W+FR in *hy5* (**Figure Y9 B**). One possibility to explain this decrease, is that at 1 h, HY5 is mainly acting as a transcriptional repressor whereas at 8 h is acting as a transcriptional activator.

If we focus on the enrichment in GO-terms related with shade avoidance, light, growth and hormones processes after 1 and 8 h of shade treatment, neither PIFs nor HY5 seems to have a critical role in downregulating genes that participate in that kind of biological functions. In contrast, these two types of regulators play a role in promoting the expression of these groups of genes. At 1 h, most of the GO terms predicted in Col-0 are also present in *hy5* but not in *pif457* and *hy5 pif457*, which suggests that PIF457 activities are fundamental for the rapid shade-induction whereas HY5 plays a minor role. By contrast, at 8 h the main role of PIF457 dissipates while HY5 activity starts to increase, i.e., most of GO terms that appear in Col-0 are detected in *pif457* but not in *hy5 pif457.*

Auxin homeostasis processes take place in Col-0 and *hy5*, only at 1 h whereas gibberellin metabolic process (exclusively depending on PIFs) occurs only after 8 h of simulated shade. This is consistent with the increase in auxin levels accompanied by a later increase of the bioactive GA4 (Bou-Torrent *et al*., 2014) that can be the result of the induced expression of genes related to gibberellin biosynthesis. Interestingly, the latter group of genes are also known to be regulated by auxins (Frigerio *et al*., 2006), which suggests that the rapid and transient shade-induced IAA production might cause GA4 accumulation, a possibility that we would like to explore in the future. In the case of ethylene, PIF457 seem to be needed for its biosynthesis and metabolism at 1 and 8 h. This agrees with previous findings that relate PIF activity and ethylene biosynthesis: the expression of *ACC SYNTHASE* (*ACS*) genes (participating in ethylene biosynthesis) is induced by PIF5 (Khanna *et al*. 2007; Paik *et al*., 2017); and ethylene signaling is regulated by PIF3 and EIN3 (Jeong *et al*., 2016; Paik *et al*., 2017; Zhong *et al*., 2014). It has been shown that ethylene indirectly regulates HY5 degradation and activity (Yu *et al*., 2013; Yu & Huang, 2017). Our results also show that this transcription factor could be participating in a feedback regulation affecting ethylene synthesis and metabolism because these processes are not detected in our RNA-seq in *hy5* after 8 h or W+FR.

On the other hand, ethylene signaling processes, that occurs independently of PIF457 and HY5, presented slightly lower p-value in the mutants in comparison to Col-0. This could

be due to similarity in the number of upregulated genes related with ethylene signaling in all the genotypes but a lower number of total upregulated genes in the mutants at 8 h what contributes to an important significance (**Supplementary Table SY1**).

The interdependence observed of HY5 activity on PIF457 in the modulation of gene expression at least at 1 h of W+FR suggests that these two factors might integrate and connect the two mentioned branches. Previously, it has been demonstrated physical interaction between HY5 and PIFs or convergence of their transcriptional activities in non-shade-related processes (Chen *et al.*, 2013; Toledo-Ortiz *et al.*, 2014; Zhang *et al.*, 2017). Thus, PIFs and HY5 could be key players connecting the two regulatory modules in specific moments. However, the crosstalk between PIF457 and HY5 activities might be dynamic and disappear with longer times of shade exposure.

Our findings propose a refined model for the regulation of shade-induced hypocotyl elongation (**Figure Y11**) where the functional importance of the various SAS regulatory elements changes with the moment of the seedling development. These regulatory elements are grouped in two main branches: (1) a well-defined pathway in which participate phyB, PIF457, HFR1 and SAV3, that is highly dependent on auxin biosynthesis, acts along all seedling development (although apparently more strongly at the end of the period analyzed) and targets cells in the lower-middle of the hypocotyl; and (2) an less well-characterized pathway with phyA and HY5 as main components, that is less dependent on auxin biosynthesis and polar transport, acts early in the seedling development and targets upper cells along the hypocotyl axis. A detailed genetic, temporal, spatial and gene expression analyses shows that in these processes, PIF457 regulatory activity is fundamental at 1 h of W+FR and its importance dissipates at 8 h. By contrast, HY5 regulatory role increases at longer times of shade exposure, when its expression is also reported to enhance. Importantly, we found that the two pathways are not totally independent, and several processes are regulated by both HY5 and PIFs such as light, growth and auxin related processes.
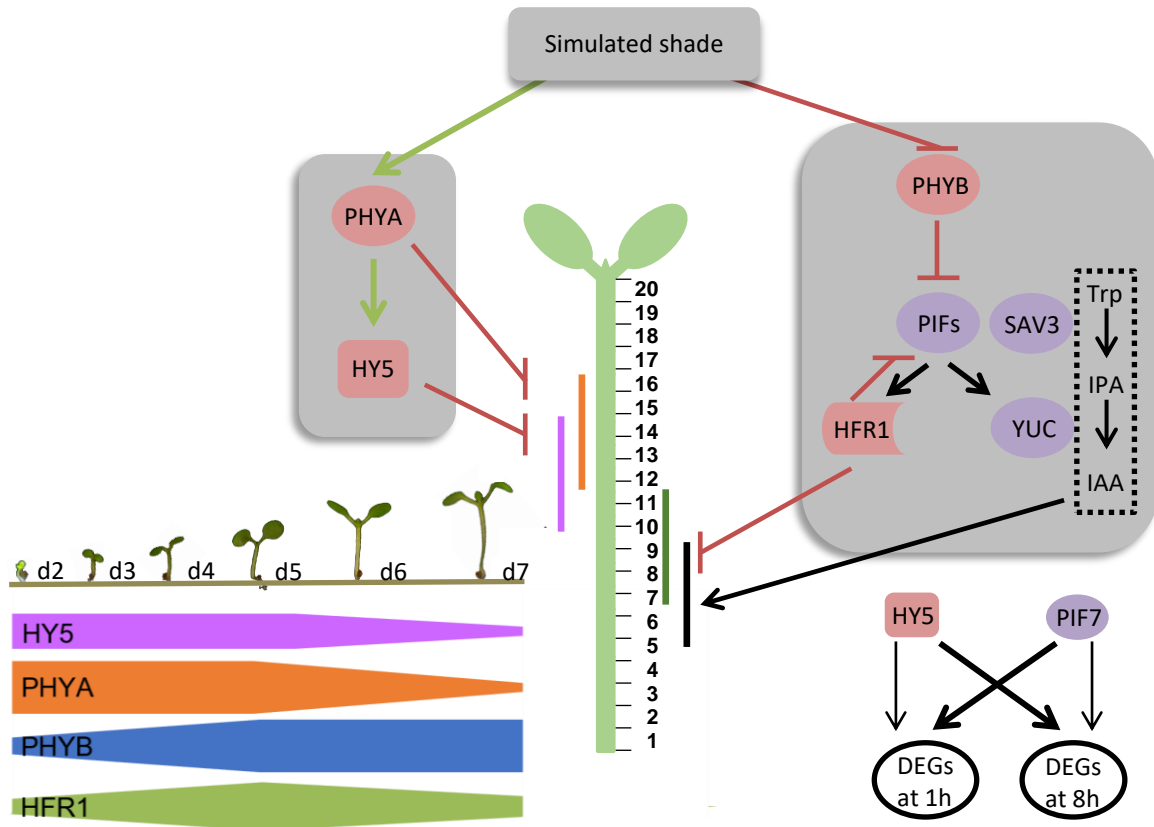
Figure Y11. The SAS regulatory network is divided in two modules: (1) phyB-PIF457-HFR1-SAV3 and (2) phyA-HY5 that act separated in time and target different cells along hypocotyl axis. phyA and HY5 activity represses the elongation of the upper part of the hypocotyl with higher repressive strength at the beginning of development. On the other hand, phyB-PIF457-HFR1-SAV3 activity regulates elongation of the middle-lower part of the hypocotyl and its activity is quite constant during development with presumably higher impact in later stages, when phyA-HY5 activity drops. The two modules are not completely independent one from another and converge through PIF457 and HY5 that participate in the regulation of the expression of common genes. Rapid changes in expression of these genes are highly dependent on PIF457 whereas at longer times PIF457 dependency dissipates and HY5 regulation seems to gain importance.

4. MATERIAL and METHODS

4.1. Plant material and growth conditions.

Arabidopsis thaliana plant material used was in the Columbia-0 (Col-0) background. Single mutants used in this study were described before: *phyA-501* (Martínez-García *et al.*, 2014; SALK_014575), *hy5-2* (Bou-Torrent *et al.*, 2015*;* SALK_056405C*)*, *hfr1-5* (Roig-Villanova *et al.*, 2007; Sessa *et al.*, 2005*;* SALK_049497*)*, *pif7-1* (a mutant allele from the SALK collection -CS68809, www.signal.salk.edu. (Leivar *et al.*, 2008; Li *et al.*, 2012), and *sav3-5* also known as *wei8-4* and *tir2-3* (Stepanova *et al.*, 2008; SALK_022743). The multiple mutants *pif457* (*pif4-101 pif5-3 pif7-1*) (de Wit *et al.*, 2015), *phyA-211 hfr1-101* (Duek & Fankhauser, 2003) and *phyA-211 phyB-*9 (Strasser *et al.*, 2010) used in this study were described elsewhere. To produce seeds of the various *A. thaliana* genotypes, plants were grown in the greenhouse under long day photoperiod (16 h light and 8 h dark).

Fluence rates were measured with a Spectrosense2 meter associated with a 4-channel sensor (SkyeInstruments Ltd., www.skyeinstruments.com), which measures PAR (400 –700 nm) and 10 nm windows in the blue (420 – 480 nm), R (664 – 674 nm) and FR (725 – 735 nm) regions.

4.2. Genetic crosses and genotyping

Some of the mentioned mutants were crossed to generate the following multiple mutants: *phyA hy5* (*phyA-501 hy5-2*), *phyA pif7* (*phyA-501 pif7-1*), *phyA hfr1* (*phyA-501 hfr1-5*), *phyA sav3 (phyA-501 sav3-5)*, *hy5 pif7* (*hy5-2 pif7-1*), *hy5 hfr1* (*hy5-2 hfr1-5*), *hy5 sav3* (*hy5-2 sav3-5*), *hfr1 pif7* (*hfr1-5 pif7-1)*, *hfr1 pif457* (*hfr1-5 pif457*), *hy5 pif457* (*hy5-2 pif457*) and *phyA pif457* (*phyA-501 pif457*). Flowering plants where cross-pollinated. After 17-19 days the seeds from the cross were harvested to carry out a segregation looking for the searched genotype. Crosses were phenotypically selected in F1 and F2 and genotypic analyses were carried out in F2 or F3 to select homozygous plants.

The genotyping was carried out by using homemade Taq polymerase enzyme with 35 cycles amplification (annealing temperature of 50ºC and extension depending on the fragment length) using the primers listed in **Supplementary Table SY2.**

4.3. Measurements of hypocotyl length

For hypocotyl growth assays, seeds were sterilized and sown in solid agar plates without sucrose (GM–; 0.215% (w/v) MS salts plus vitamins, 0.025% (w/v) MES pH 5.80) (Roig-Villanova *et al.*, 2006). After 3-6 days of stratification, plates were incubated in growth chambers at 22°C under continuous white light (W) provided by 4 cool-white vertical fluorescence tubes for 2 days (PAR of 20–25 umol·m^{-2}·s^{-1}, R:FR of about 1.58). After that time, plates were either maintained in W or transferred to simulated shade (W+FR) for 5 days. Simulated shade was generated by enriching W with supplementary FR provided by 4 horizontal LED lamps (PAR of 20–25 umol·m^{-2}·s^{-1}, R:FR of about 0.02). At day 7, seedlings were lied down on the petri dishes and pictures of them were taken. Each biological replicate corresponded to ~25 seedlings per treatment and genotype. Experiments were done with 3 biological replicates.

Hypocotyl measurements were carried out by using the National Institutes of Health (NHS) ImageJ software (Bethesda, MD, USA; http://rsb.info.nih.gov/). Hypocotyl measurements from the different biological replicates were averaged.

4.4. Hypocotyl measurements for the temporal analyses:

Seedlings were grown for up to 7 days either in W or W+FR, as described in the previous section. In these experiments, hypocotyl length measurements were made daily from pictures taken from plants of different ages, from day 2 until day 7 after germination (6 time points). By subtracting hypocotyl length of two consecutive days, the growth rate (mm·day^{-1}) from day 2 to day 7was calculated for each genotype and light treatment (W and W+FR). Each biological replicate corresponded to ~25 seedlings per treatment, genotype and time point. Experiments were done with 3 biological replicates. Hypocotyl measurements from the different biological replicates were averaged. These averaged data were used to calculate the growth rate.

4.5. Cell length measurements along the hypocotyl axis for spatial analysis.

For the cell length measurements, about 100 seedlings of Col-0 seedlings were grown in W and W+FR for 7 days. After the hypocotyl length in each condition was averaged, 15-16 individuals with a hypocotyl length of the estimated averaged value ± 5 % were selected. These seedlings were de-bladed and de-rooted, and the remaining hypocotyls fixed and stained with calcofluor white to visualize cell walls. These samples were observed using

confocal microscopy and cell elongation of several files of epidermal cells of the hypocotyl longitudinal axis per treatment were measured. These values were averaged for each of the 20 cells that make up a cell file, from bottom to top (**Figure Y7A**). The differences in cell length means in W+FR and W were represented for each of the 20 cells that make up a cell file along the hypocotyl longitudinal axis. The staining was carried out as follows: hypocotyls were submerged in a 1x PBS solution (NaCl (137 mM), KCl (2.7 mM), Na_2HPO_4 (10 mM, KH_2HPO_4 (1.8 mM)) with 4% (w/v) paraformaldehyde (PFA) during 60 min at room temperature. Then, hypocotyls were washed twice for 1 min in 1x PBS and cleared after transferring them to ClearSee solution (Xylitol [10% (w/v)] (Sigma), Sodium deoxycholate [final 15% (w/v)] (Sigma), Urea [final 25% (w/v)] (Sigma)). The clearing was carried out for at least 1 week at room temperature. Before imaging taking, hypocotyls were stained with 100 µg·ml^{-1} Calcofluor White (Sigma-Aldrich) in ClearSee solution during 120 min and washed twice with ClearSee solution during 2 days (Kurihara *et al.*, 2015).

Pictures of fixed and stained plant material were taken by using confocal microscopy (Zeiss LSM 780). Calcofluor White stained samples were imaged with 405 nm excitation and detected at 425-475 nm (Kamiya *et al.*, 2015). Cell growth measurements were carried out by using the NHS ImageJ software on the obtained pictures. At least 15 cells of 2 cell files per hypocotyl from 7 plants were measured for each genotype and growth condition.

4.6. RNA extraction and gene expression analyses

Seven-day old seedlings grown in W or W+FR were harvested (about x mg per sample) and frozen in liquid nitrogen. RNA was extracted using commercial kits (Maxwell® RSC Plant RNA kits; www.promega.com) and quantified using *NanoDrop^{TM} 8000 spectophotometer* (ThermoFischer Scientific^{TM}). 2 µg of total RNA were retrotranscribed to cDNA in a final volume of 20 µL by using the Transcriptor First Strand cDNA synthesis KIT (Roche, www.roche.com) and NZY First-Strand cDNA Synthesis Kit, separate oligos (NZYtech). Subsequently cDNA was diluted ten-fold and stored at -20ºC for further analysis.

Relative mRNA abundance was determined via Real-Time Quantitative Polymerase Chain Reaction (RT-qPCR) in a final volume of 10 µL made up of 0.3 µM of both, forward and reverse primers, 5 µL of the LightCycler 480 SYBR Green I Master Mix (Roche) and 2 µL of ten-fold diluted cDNA (Molina-Contreras et al., 2019). The RT-qPCR was carried out in *LightCycler 480 Real-Time PCR system* (Roche). One biological replicate was composed by ~30 seedlings. The analysis was performed with three independent biological replicates for

each condition and three technical replicates for each biological replicate. *ELONGATION FACTOR 1α* (*EF1α*) was used as endogenous reference gene to normalize the expression of the genes of interest. Primers used for the RT-qPCR analyses are provided in supplementary information (**Supplementary Table SY3**).

4.7. RNA-sequencing

Total RNA for sequencing was obtained as in the expression analysis by RT-qPCR. Library preparation was performed from three biological replicates and sequenced at the Centre Nacional de Anàlisi Genòmica (CNAG - CRG) on an Illumina NovaSeq6000 in paired-end 50 bp read length. Mapping to TAIR10 genome and Limma comparisons were performed to obtain the False Discovery Rate (FDR) and the Fold Change (FC) for each gene. Differentially expressed genes (DEGs) were considered when FDR P-value was <0.05 and FC >|1.5|.

4.8. Statistical analyses

The statistical analyses were carried out using the Real Statistics Resource Pack, an Excel add-in that extends Excel's standard statistics capabilities. For the statistics analyses, we compared three values corresponding to three replicates in the case of relative expression and hypocotyl length.

5. SUPPLEMENTARY INFORMATION

5.1. Supplementary Figures

Figure SY1. Combinatory effect of pairs of negative regulators over the hypocotyl length. The graphs represent the hypocotyl length in white light (W) and simulated shade (W+FR) of **(A)** Col-0, *phyA-211*, *hfr1-5* and *phyA-211 hy5-101*. **(B)** Col-0, *hy5-2*, *hfr1-5* and *hy5-2 hfr1-1*. **(C)** Col-0, *phyA-501, hy5-2* and *phyA-501 hy5-2*. All the genotypes were germinated in W for 2 days and then they were either maintained in W or transferred to W+FR for 5 more days. Values are means ± SE of three independent biological replicas. Tukey test was performed and different characters above the data indicate significant differences between genotypes (p-value <0.05).
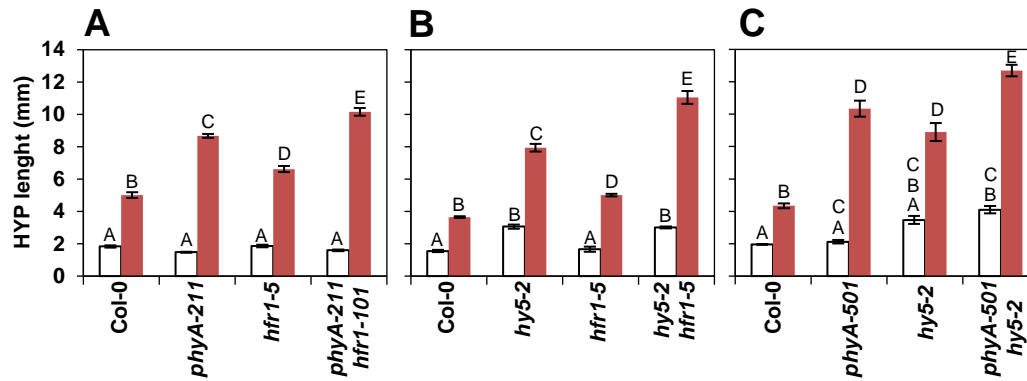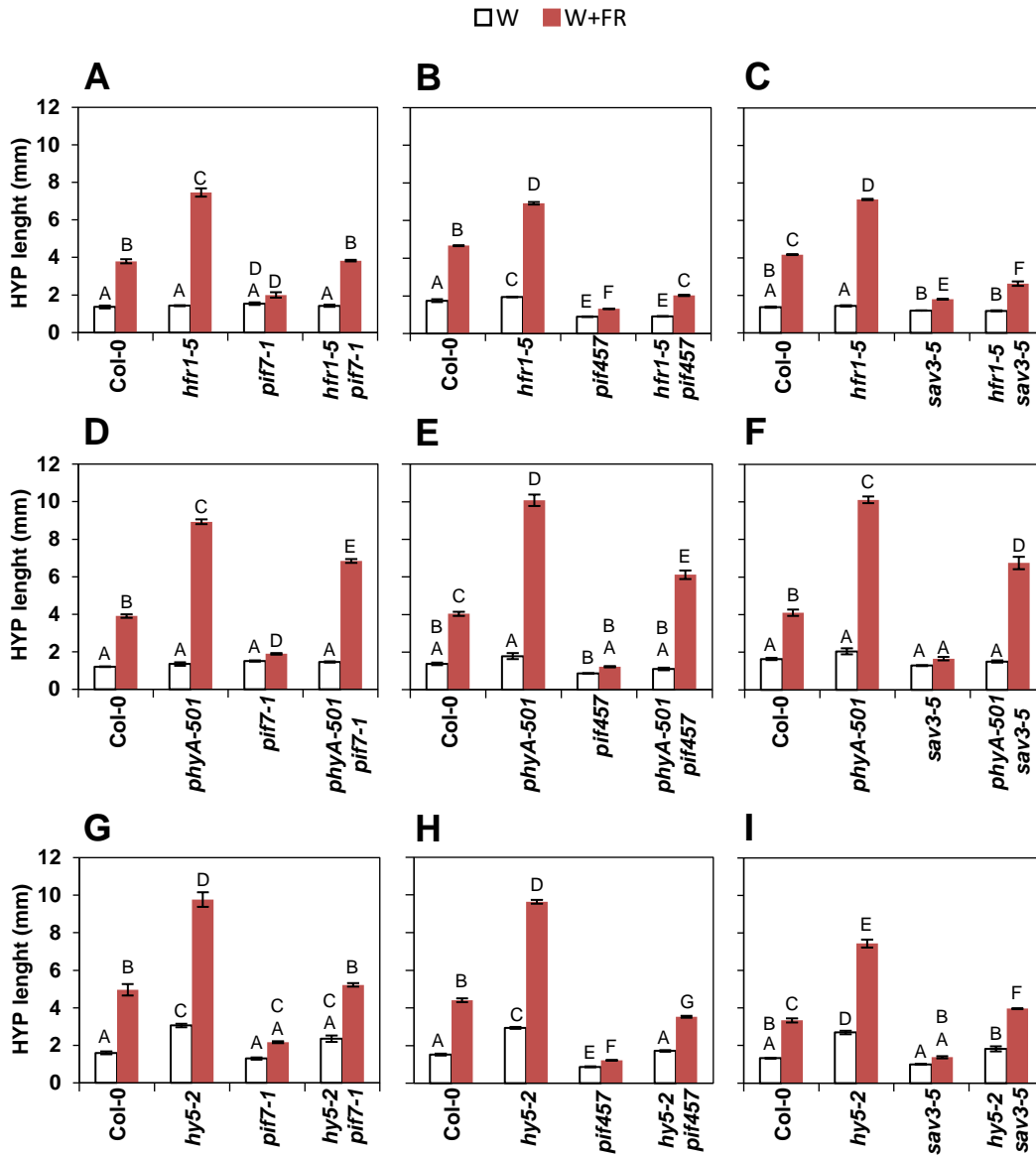
Figure SY2. Combinatory effect of negative and positive regulators over the hypocotyl length. The graphs represent the hypocotyl length in white light (W) and simulated shade (W+FR) of **(A)** Col-0, hfr1-5, pif7-1, hfr1-5 pif7-1. **(B)** Col-0, hfr1-5, pif457, hfr1-5 pif457. **(C)** Col-0, hfr1-5, sav3-5, hfr1-5 sav3-5. **(D)** Col-0, phyA-501, pif7-1, phyA-501 pif7-1. **(E)** Col-0, phyA-501, pif457, phyA-501 pif457. **(F)** Col-0, phyA-501, sav3-5, phyA-501 sav3-5. **(G)** Col-0, hy5-2, pif7-1, hy5-2 pif7-1. **(H)** Col-0, hy5-2, pif457, hy5-2 pif457. **(I)** Col-0, hy5-2, sav3-5, hy5-2 sav3-5. All the genotypes were germinated in W for 2 days and then they were either maintained in W or transferred to W+FR for 5 more days. Values are means ± SE of three independent biological replicas. Tukey test was performed and different characters above the data indicate significant differences between genotypes (p-value <0.05).

5.2. Supplementary Tables

Table SY1. Pool of DEGs contributing to each GO term predicted in each genotype.
Green color beneath GO terms indicates that the gene situated in the left column contributes to the GO term. Fold change in each genotype is indicated with colored bars. Different colors of the bars indicate different scale of the fold change value. Table SY1 is available at https://bit.ly/3kdmPR7.

Table SY2. Primers used for genotyping.

Gene	Primer name	Sequence (5`- 3`)
phyAwt	MSO31	TAG AGC ACC GCA CAG CTG CC
	MSO32	GAA GCT ATC TCC TGC AGG TGG
phya-501	MSO31	TAG AGC ACC GCA CAG CTG CC
	LBb1	GCGTGGACCGCTTGCTGCAACT
HY5wt	hy5-F	GGTAGAGAATCTGGATCGGC
	hy5-R	GCTGAGCTGAAACTCTGTTC
hy5-2	LBb1	GCGTGGACCGCTTGCTGCAACT
	hy5-R	GCTGAGCTGAAACTCTGTTC
PIF4wt	JO138	GCGGAATTCAACAAGTCGAACCAACGATCAGGA
	BO73	CTAGTGGTCCAAACGAGAACCGTCG
pif4-101	LB3	TAGCATCTGAATTTCATAACCAATCTCGATACAC
	BO73	CTAGTGGTCCAAACGAGAACCGTCG
PIF5wt	BO50	CCAACCGAGTTGGTGGGTCTC
	BO51	ATCTCTCCACAATAGCTCCAC
pif5-3	BO50	CCAACCGAGTTGGTGGGTCTC
	LBb1	GCGTGGACCGCTTGCTGCAACT
PIF7	NCO111	CCGTTCATGGTCTAGGCG
	NCO110	CATCCTCTGGTTTATCCTATCACGCCG
pif-1	NCO109	TGATAGTGACCTTAGGCGACTTTTGAACGC
	NCO110	CATCCTCTGGTTTATCCTATCACGCCG
HFR1wt	JO367	CCCTGCAGAATTTACCAATTGGGAGATCG
	JO368	GCGGATCCACCATGTTAGTTAAAGAGATATCGG
hfr1-5	LBb1	GCGTGGACCGCTTGCTGCAACT
	JO368	GCGGATCCACCATGTTAGTTAAAGAGATATCGG
SAV3	RO68	GTGGTGAACCGTCCAGACGAC
	JO401	CAG GGT AAG ATT CGA GTG
sav3-5	RO68	GTGGTGAACCGTCCAGACGAC
	LBb1	GCGTGGACCGCTTGCTGCAACT

Table SY3. Primers used for gene expression analyses.

Gene	Primer name	Sequence (5`- 3`)
ACS8	JRO46	GCAGCCAATTTCCAAAGAGA
	JRO47	CGACATGAAATCCGCCATAG
EF1α	BO95	TGGTGTCAAGCAGATGATTTGC
	BO96	ATGAAGACACCTCCTTGATGATTTC
PAR1	BO109	CACCGTCATGCTCAGCCA
	BO110	TCGGTCTTCACGTACGCTTG

6. REFERENCES

Bou-Torrent, J., Galstyan, A., Gallemí, M., Cifuentes-Esquivel, N., Molina-Contreras, M. J., Salla-Martret, M., Jikumaru, Y., Yamaguchi, S., Kamiya, Y., & Martínez-García, J. F. (2014). Plant proximity perception dynamically modulates hormone levels and sensitivity in Arabidopsis. *Journal of Experimental Botany*, *65*(11), 2937–2947. https://doi.org/10.1093/jxb/eru083

Bou-Torrent, J., Roig-Villanova, I., & Martínez-García, J. F. (2008). Light signaling: back to space. *Trends in Plant Science*, *13*(3), 108–114. https://doi.org/10.1016/j.tplants.2007.12.003

Bou-Torrent, J., Toledo-Ortiz, G., Ortiz-Alcaide, M., Cifuentes-Esquivel, N., Halliday, K. J., Martinez-García, J. F., & Rodriguez-Concepcion, M. (2015). Regulation of carotenoid biosynthesis by shade relies on specific subsets of antagonistic transcription factors and cofactors. *Plant Physiology*, *169*(3), 1584–1594. https://doi.org/10.1104/pp.15.00552

Chen, D., Xu, G., Tang, W., Jing, Y., Ji, Q., Fei, Z., & Lin, R. (2013). Antagonistic basic helix-loop-Helix/bZIP transcription factors form transcriptional modules that integrate light and reactive oxygen species signaling in Arabidopsis. *Plant Cell*, *25*(5), 1657–1673. https://doi.org/10.1105/tpc.112.104869

Cifuentes-Esquivel, N., Bou-Torrent, J., Galstyan, A., Gallemí, M., Sessa, G., Salla Martret, M., Roig-Villanova, I., Ruberti, I., & Martínez-García, J. F. (2013). The bHLH proteins BEE and BIM positively modulate the shade avoidance syndrome in Arabidopsis seedlings. *Plant Journal*, *75*(6), 989–1002. https://doi.org/10.1111/tpj.12264

Ciolfi, A., Sessa, G., Sassi, M., Possenti, M., Salvucci, S., Carabelli, M., Morelli, G., & Ruberti, I. (2013). Dynamics of the shade-avoidance response in Arabidopsis. *Plant Physiology*, *163*(1), 331–353. https://doi.org/10.1104/pp.113.221549

de Wit, M., Keuskamp, D. H., Bongers, F. J., Hornitschek, P., Gommers, C. M. M., Reinen, E., Martínez-Cerón, C., Fankhauser, C., & Pierik, R. (2016). Integration of Phytochrome and Cryptochrome Signals Determines Plant Growth during Competition for Light. *Current Biology*, *26*(24), 3320–3326. https://doi.org/10.1016/j.cub.2016.10.031

de Wit, M., Ljung, K., & Fankhauser, C. (2015). Contrasting growth responses in lamina and petiole during neighbor detection depend on differential auxin responsiveness rather than different auxin levels. *New Phytologist*, *208*(1), 198–209. https://doi.org/10.1111/nph.13449

Devlin, Paul F., Patel, S. R., & Whitelam, G. C. (1998). Phytochrome E influences internode

elongation and flowering time in arabidopsis. *Plant Cell*, *10*(9), 1479–1487. https://doi.org/10.1105/tpc.10.9.1479

Devlin, Paul F., Robson, P. R. H., Patel, S. R., Goosey, L., Sharrock, R. A., & Whitelam, G. C. (1999). Phytochrome D acts in the shade-avoidance syndrome in Arabidopsis by controlling elongation growth and flowering time. *Plant Physiology*, *119*(3), 909–915. https://doi.org/10.1104/pp.119.3.909

Devlin, Paul F., Yanovsky, M. J., & Kay, S. A. (2003). A Genomic Analysis of the Shade Avoidance Response in Arabidopsis. *Plant Physiology*, *133*(4), 1617–1629. https://doi.org/10.1104/pp.103.034397

Duek, P. D., & Fankhauser, C. (2003). HFR1, a putative bHLH transcription factor, mediates both phytochrome A and cryptochrome signalling. *Plant Journal*, *34*(6), 827–836. https://doi.org/10.1046/j.1365-313X.2003.01770.x

Dünser, K., & Kleine-Vehn, J. (2015). Differential growth regulation in plants-the acid growth balloon theory. *Current Opinion in Plant Biology*, *28*, 55–59. https://doi.org/10.1016/j.pbi.2015.08.009

Fiorucci, A. S., Galvão, V. C., Ince, Y. Ç., Boccaccini, A., Goyal, A., Allenbach Petrolati, L., Trevisan, M., & Fankhauser, C. (2020). PHYTOCHROME INTERACTING FACTOR 7 is important for early responses to elevated temperature in Arabidopsis seedlings. *New Phytologist*, *226*(1), 50–58. https://doi.org/10.1111/nph.16316

Franklin, K. A. (2008). Shade avoidance. *New Phytologist*, *179*(4), 930–944. https://doi.org/10.1111/j.1469-8137.2008.02507.x

Frigerio, M., Alabadí, D., Pérez-Gómez, J., García-Cárcel, L., Phillips, A. L., Hedden, P., & Blázquez, M. A. (2006). Transcriptional regulation of gibberellin metabolism genes by auxin signaling in Arabidopsis. *Plant Physiology*, *142*(2), 553–563. https://doi.org/10.1104/pp.106.084871

Gallego-Bartolomé, J., Alabadí, D., & Blázquez, M. A. (2011). DELLA-induced early transcriptional changes during etiolated development in arabidopsis thaliana. *PLoS ONE*, *6*(8). https://doi.org/10.1371/journal.pone.0023918

Galstyan, A., Cifuentes-Esquivel, N., Bou-Torrent, J., & Martinez-Garcia, J. F. (2011). The shade avoidance syndrome in Arabidopsis: A fundamental role for atypical basic helix-loop-helix proteins as transcriptional cofactors. *Plant Journal*, *66*(2), 258–267. https://doi.org/10.1111/j.1365-313X.2011.04485.x

Gangappa, S. N., & Botto, J. F. (2016). The Multifaceted Roles of HY5 in Plant Growth and Development. *Molecular Plant*, *9*(10), 1353–1365.

https://doi.org/10.1016/j.molp.2016.07.002

Gangappa, S. N., Crocco, C. D., Johansson, H., Datta, S., Hettiarachchi, C., Holm, M., & Botto, J. F. (2013). The Arabidopsis B-BOX protein BBX25 interacts with HY5, negatively regulating BBX22 expression to suppress seedling photomorphogenesis. *Plant Cell*, *25*(4), 1243–1257. https://doi.org/10.1105/tpc.113.109751

Gendreau, E., Traas, J., Desnos, T., Grandjean, O., Caboche, M., & Hofte, H. (1997). Cellular basis of hypocotyl growth in Arabidopsis thaliana. *Plant Physiology*, *114*(1), 295–305. https://doi.org/10.1104/pp.114.1.295

Hornitschek, P., Kohnen, M. V., Lorrain, S., Rougemont, J., Ljung, K., López-Vidriero, I., Franco-Zorrilla, J. M., Solano, R., Trevisan, M., Pradervand, S., Xenarios, I., & Fankhauser, C. (2012). Phytochrome interacting factors 4 and 5 control seedling growth in changing light conditions by directly controlling auxin signaling. *Plant Journal*, *71*(5), 699–711. https://doi.org/10.1111/j.1365-313X.2012.05033.x

Hornitschek, P., Lorrain, S., Zoete, V., Michielin, O., & Fankhauser, C. (2009). Inhibition of the shade avoidance response by formation of non-DNA binding bHLH heterodimers. *EMBO Journal*, *28*(24), 3893–3902. https://doi.org/10.1038/emboj.2009.306

Jang, I. C., Henriques, R., & Chua, N. H. (2013). Three transcription factors, HFR1, LAF1 and HY5, regulate largely independent signaling pathways downstream of phytochrome a. *Plant and Cell Physiology*, *54*(6), 907–916. https://doi.org/10.1093/pcp/pct042

Jeong, J., Kim, K., Kim, M. E., Kim, H. G., Heo, G. S., Park, O. K., Park, Y. Il, Choi, G., & Oh, E. (2016). Phytochrome and ethylene signaling integration in Arabidopsis occurs via the transcriptional regulation of genes co-targeted by PIFs and EIN3. *Frontiers in Plant Science*, *7*(2016JULY), 1–14. https://doi.org/10.3389/fpls.2016.01055

Jia, Y., Kong, X., Hu, K., Cao, M., Liu, J., Ma, C., Guo, S., Yuan, X., Zhao, S., Robert, H. S., Li, C., Tian, H., & Ding, Z. (2020). PIFs coordinate shade avoidance by inhibiting auxin repressor ARF18 and metabolic regulator QQS. *New Phytologist*, *228*(2), 609–621. https://doi.org/10.1111/nph.16732

Kamiya, T., Borghi, M., Wang, P., Danku, J. M. C., Kalmbach, L., Hosmani, P. S., Naseer, S., Fujiwara, T., Geldner, N., & Salt, D. E. (2015). The MYB36 transcription factor orchestrates Casparian strip formation. *Proceedings of the National Academy of Sciences of the United States of America*, *112*(33), 10533–10538. https://doi.org/10.1073/pnas.1507691112

Khanna, R., Shen, Y., Marion, C. M., Tsuchisaka, A., Theologis, A., Schäfer, E., & Quail, P. H. (2007). The basic helix-loop-helix transcription factor PIF5 acts on ethylene

biosynthesis and phytochrome signaling by distinct mechanisms. *Plant Cell*, *19*(12), 3915–3929. https://doi.org/10.1105/tpc.107.051508

Kohnen, M. V., Schmid-Siegert, E., Trevisan, M., Petrolati, L. A., Sénéchal, F., Müller-Moulé, P., Maloof, J., Xenarios, I., & Fankhauser, C. (2016). Neighbor detection induces organ-specific transcriptomes, revealing patterns underlying hypocotyl-specific growth. *Plant Cell*, *28*(12), 2889–2904. https://doi.org/10.1105/tpc.16.00463

Kurihara, D., Mizuta, Y., Sato, Y., & Higashiyama, T. (2015). ClearSee: A rapid optical clearing reagent for whole-plant fluorescence imaging. *Development (Cambridge)*, *142*(23), 4168–4179. https://doi.org/10.1242/dev.127613

Lee, J., He, K., Stolc, V., Lee, H., Figueroa, P., Gao, Y., Tongprasit, W., Zhao, H., Lee, I., & Xing, W. D. (2007). Analysis of transcription factor HY5 genomic binding sites revealed its hierarchical role in light regulation of development. *Plant Cell*, *19*(3), 731–749. https://doi.org/10.1105/tpc.106.047688

Leivar, P., Monte, E., Al-Sady, B., Carle, C., Storer, A., Alonso, J. M., Ecker, J. R., & Quaila, P. H. (2008). The Arabidopsis phytochrome-interacting factor PIF7, together with PIF3 and PIF4, regulates responses to prolonged red light by modulating phyB levels. *Plant Cell*, *20*(2), 337–352. https://doi.org/10.1105/tpc.107.052142

Leivar, P., Tepperman, J. M., Cohn, M. M., Monte, E., Al-Sady, B., Erickson, E., & Quail, P. H. (2012). Dynamic antagonism between phytochromes and PIF family basic helix-loop-helix factors induces selective reciprocal responses to light and shade in a rapidly responsive transcriptional network in Arabidopsis. *Plant Cell*, *24*(4), 1398–1419. https://doi.org/10.1105/tpc.112.095711

Li, L., Ljung, K., Breton, G., Schmitz, R. J., Pruneda-Paz, J., Cowing-Zitron, C., Cole, B. J., Ivans, L. J., Pedmale, U. V., Jung, H. S., Ecker, J. R., Kay, S. A., & Chory, J. (2012). Linking photoreceptor excitation to changes in plant architecture. *Genes and Development*, *26*(8), 785–790. https://doi.org/10.1101/gad.187849.112

Lorrain, S., Allen, T., Duek, P. D., Whitelam, G. C., & Fankhauser, C. (2008). Phytochrome-mediated inhibition of shade avoidance involves degradation of growth-promoting bHLH transcription factors. *Plant Journal*, *53*(2), 312–323. https://doi.org/10.1111/j.1365-313X.2007.03341.x

Martínez-García, J. F., Gallemí, M., Molina-Contreras, M. J., Llorente, B., Bevilaqua, M. R. R., & Quail, P. H. (2014). The shade avoidance syndrome in Arabidopsis: The antagonistic role of phytochrome A and B differentiates vegetation proximity and canopy shade. *PLoS ONE*, *9*(10). https://doi.org/10.1371/journal.pone.0109275

Martínez-García, J. F., Galstyan, A., Salla-Martret, M., Cifuentes-Esquivel, N., Gallemí, M., & Bou-Torrent, J. (2010). Regulatory Components of Shade Avoidance Syndrome. In J.-C. Kader & M. Delseny (Eds.), *Advances in Botanical Research* (Vol. 53, pp. 65–116). Academic Press. https://doi.org/https://doi.org/10.1016/S0065-2296(10)53003-9

Morelli, L., Paulišić, S., Qin, W., Iglesias-Sanchez, A., Roig-Villanova, I., Florez-Sarasa, I., Rodriguez-Concepcion, M., & Martinez-Garcia, J. F. (2021). Light signals generated by vegetation shade facilitate acclimation to low light in shade-avoider plants. *Plant Physiology*, *186*(4), 2137–2151. https://doi.org/10.1093/plphys/kiab206

Nagatani, A., Chory, J., & Furuya, M. (1991). Phytochrome B Is Not Detectable in the hy3 Mutant of Arabidopsis, Which Is Deficient in Responding to End-of-Day Far-Red Light Treatments. *Plant and Cell Physiology*, *32*(7), 1119–1122. https://doi.org/10.1093/oxfordjournals.pcp.a078177

Paik, I., Kathare, P. K., Kim, J. II, & Huq, E. (2017). Expanding Roles of PIFs in Signal Integration from Multiple Processes. *Molecular Plant*, *10*(8), 1035–1046. https://doi.org/10.1016/j.molp.2017.07.002

Paulišić, S., Qin, W., Arora Verasztó, H., Then, C., Alary, B., Nogue, F., Tsiantis, M., Hothorn, M., & Martínez-García, J. F. (2021). Adjustment of the PIF7-HFR1 transcriptional module activity controls plant shade adaptation. *The EMBO Journal*, *40*(1), 1–16. https://doi.org/10.15252/embj.2019104273

Procko, C., Crenshaw, C. M., Ljung, K., Noel, J. P., & Chory, J. (2014). Cotyledon-generated auxin is required for shade-induced hypocotyl growth in brassica rapa. *Plant Physiology*, *165*(3), 1285–1301. https://doi.org/10.1104/pp.114.241844

Roig-Villanova, I., Bou-Torrent, J., Galstyan, A., Carretero-Paulet, L., Portolés, S., Rodríguez-Concepción, M., & Martínez-García, J. F. (2007). Interaction of shade avoidance and auxin responses: A role for two novel atypical bHLH proteins. *EMBO Journal*, *26*(22), 4756–4767. https://doi.org/10.1038/sj.emboj.7601890

Roig-Villanova, I., Bou, J., Sorin, C., Devlin, P. F., & Martínez-García, J. F. (2006). Identification of Primary Target Genes of Phytochrome Signaling. Early Transcriptional Control during Shade Avoidance Responses in Arabidopsis. *Plant Physiology*, *141*(1), 85–96. https://doi.org/10.1104/pp.105.076331

Roig-Villanova, I., & Martínez-García, J. F. (2016). Plant responses to vegetation proximity: A whole life avoiding shade. *Frontiers in Plant Science*, *7*(FEB2016), 1–10. https://doi.org/10.3389/fpls.2016.00236

Sessa, G., Carabelli, M., Sassi, M., Ciolfi, A., Possenti, M., Mittempergher, F., Becker, J.,

Morelli, G., & Ruberti, I. (2005). A dynamic balance between gene activation and repression regulates the shade avoidance response in Arabidopsis. *Genes and Development*, *19*(23), 2811–2815. https://doi.org/10.1101/gad.364005

Shi, H., Zhong, S., Mo, X., Liu, N., Nezames, C. D., & Deng, X. W. (2013). HFR1 sequesters PIF1 to govern the transcriptional network underlying light-initiated seed germination in Arabidopsis. *Plant Cell*, *25*(10), 3770–3784. https://doi.org/10.1105/tpc.113.117424

Smith, H. (1982). *STRATEGY*. 481–518.

Somers, D. E., Sharrock, R. A., Tepperman, J. M., & Quail, P. H. (1991). The hy3 long hypocotyl mutant of arabidopsis is deficient in phytochrome B. *Plant Cell*, *3*(12), 1263–1274. https://doi.org/10.2307/3869307

Sorin, C., Salla-Martret, M., Bou-Torrent, J., Roig-Villanova, I., & Martínez-García, J. F. (2009). ATHB4, a regulator of shade avoidance, modulates hormone response in Arabidopsis seedlings. *Plant Journal*, *59*(2), 266–277. https://doi.org/10.1111/j.1365-313X.2009.03866.x

Stepanova, A. N., Robertson-Hoyt, J., Yun, J., Benavente, L. M., Xie, D. Y., Doležal, K., Schlereth, A., Jürgens, G., & Alonso, J. M. (2008). TAA1-Mediated Auxin Biosynthesis Is Essential for Hormone Crosstalk and Plant Development. *Cell*, *133*(1), 177–191. https://doi.org/10.1016/j.cell.2008.01.047

Strasser, B., Sánchez-Lamas, M., Yanovsky, M. J., Casal, J. J., & Cerdán, P. D. (2010). Arabidopsis thaliana life without phytochromes. *Proceedings of the National Academy of Sciences of the United States of America*, *107*(10), 4776–4781. https://doi.org/10.1073/pnas.0910446107

Tanaka, S. I., Nakamura, S., Mochizuki, N., & Nagatani, A. (2002). Phytochrome in cotyledons regulates the expression of genes in the hypocotyl through auxin-dependent and -independent pathways. *Plant and Cell Physiology*, *43*(10), 1171–1181. https://doi.org/10.1093/pcp/pcf133

Tao, Y., Ferrer, J. L., Ljung, K., Pojer, F., Hong, F., Long, J. A., Li, L., Moreno, J. E., Bowman, M. E., Ivans, L. J., Cheng, Y., Lim, J., Zhao, Y., Ballaré, C. L., Sandberg, G., Noel, J. P., & Chory, J. (2008). Rapid Synthesis of Auxin via a New Tryptophan-Dependent Pathway Is Required for Shade Avoidance in Plants. *Cell*, *133*(1), 164–176. https://doi.org/10.1016/j.cell.2008.01.049

Toledo-Ortiz, G., Huq, E., & Rodríguez-Concepción, M. (2010). Direct regulation of phytoene synthase gene expression and carotenoid biosynthesis by phytochrome-interacting factors. *Proceedings of the National Academy of Sciences of the United States of*

America, *107*(25), 11626–11631. https://doi.org/10.1073/pnas.0914428107

Toledo-Ortiz, G., Johansson, H., Lee, K. P., Bou-Torrent, J., Stewart, K., Steel, G., Rodríguez-Concepción, M., & Halliday, K. J. (2014). The HY5-PIF Regulatory Module Coordinates Light and Temperature Control of Photosynthetic Gene Transcription. *PLoS Genetics*, *10*(6). https://doi.org/10.1371/journal.pgen.1004416

Xie, Y., Liu, Y., Wang, H., Ma, X., Wang, B., Wu, G., & Wang, H. (2017). Phytochrome-interacting factors directly suppress MIR156 expression to enhance shade-avoidance syndrome in Arabidopsis. *Nature Communications*, *8*(1). https://doi.org/10.1038/s41467-017-00404-y

Yang, C., Huang, S., Zeng, Y., Liu, C., Ma, Q., Pruneda-Paz, J., Kay, S. A., & Li, L. (2021). Two bHLH transcription factors, bHLH48 and bHLH60, associate with phytochrome interacting factor 7 to regulate hypocotyl elongation in Arabidopsis. *Cell Reports*, *35*(5), 109054. https://doi.org/10.1016/j.celrep.2021.109054

Yang, C., Xie, F., Jiang, Y., Li, Z., Huang, X., & Li, L. (2018). Phytochrome A Negatively Regulates the Shade Avoidance Response by Increasing Auxin/Indole Acidic Acid Protein Stability. *Developmental Cell*, *44*(1), 29-41.e4. https://doi.org/10.1016/j.devcel.2017.11.017

Yu, Y., & Huang, R. (2017). Integration of ethylene and light signaling affects hypocotyl growth in Arabidopsis. *Frontiers in Plant Science*, *8*(January), 2012–2017. https://doi.org/10.3389/fpls.2017.00057

Yu, Y., Wang, J., Zhang, Z., Quan, R., Zhang, H., Deng, X. W., Ma, L., & Huang, R. (2013). Ethylene Promotes Hypocotyl Growth and HY5 Degradation by Enhancing the Movement of COP1 to the Nucleus in the Light. *PLoS Genetics*, *9*(12). https://doi.org/10.1371/journal.pgen.1004025

Zhang, X., Huai, J., Shang, F., Xu, G., Tang, W., Jing, Y., & Lin, R. (2017). A PIF1/PIF3-HY5-BBX23 transcription factor cascade affects photomorphogenesis. *Plant Physiology*, *174*(4), 2487–2500. https://doi.org/10.1104/pp.17.00418

Zhao, Y. (2012). Auxin biosynthesis: A simple two-step pathway converts tryptophan to indole-3-Acetic acid in plants. *Molecular Plant*, *5*(2), 334–338. https://doi.org/10.1093/mp/ssr104

Zheng, Z., Guo, Y., Novák, O., Chen, W., Ljung, K., Noel, J. P., & Chory, J. (2016). Local auxin metabolism regulates environmentinduced hypocotyl elongation. *Nature Plants*, *2*(4), 1–9. https://doi.org/10.1038/NPLANTS.2016.25

Zhong, S., Shi, H., Xue, C., Wei, N., Guo, H., & Deng, X. W. (2014). Ethylene-orchestrated

circuitry coordinates a seedling's response to soil cover and etiolated growth. *Proceedings of the National Academy of Sciences of the United States of America*, *111*(11), 3913–3920. https://doi.org/10.1073/pnas.1402491111

GENERAL DISCUSSION

GENERAL DISCUSSION

GENERAL DISCUSSION

One of the main challenges for humanity in the near future is to guarantee a sufficient amount of resources and food for the increasing human world population whose number is expected to arrive to 9,1 million people by 2050 (FAO - News Article: 2050: A third more mouths to feed). This has to be achieved while preserving sufficient land for wildlife and keeping biodiversity. Indeed, as the surface of arable land is limited, a solution to enhance the production of plant supplies is to grow more plants per surface unit (that is, to increase planting density). However, as many crops are shade-avoider or sun-loving plants, growing in these conditions initiate the SAS responses, which in adult plants results in a reduction in the number of seeds, leaves and/or fruits and therefore in plant yield and productivity (Roig-Villanova & Martínez-García, 2016). Importantly, some of the SAS responses take place even when the amount of sunlight that plants receive is enough to fuel the photosynthesis, i.e., when the plants are growing close to neighboring vegetation but not under their canopy. Thus, it is of vital importance to know the SAS molecular mechanisms in detail to target these mechanisms for plant breeding and generate crops that can grow in high density without activating SAS and hence diminishing their productivity.

Arabidopsis thaliana is the model plant that has allowed to obtain a better knowledge about SAS mechanisms. Due to its versatility, most of the studies about SAS in Arabidopsis has been performed at the seedling stage. This experimental approach has allowed to find several components involved in the SAS processes that are being described also as important players at adult stages and on other species. For example, manipulation of the expression of well-described SAS regulators in Arabidopsis seedlings, leads to suppress shade avoidance responses and increase yield in species such as rice, potato and tomato (Boccalandro *et al.*, 2003; Garg *et al.*, 2006; Iannacone *et al.*, 2008; Kong *et al.*, 2004).

As mentioned, one of the best studied SAS responses in Arabidopsis is the shade-induced hypocotyl elongation at the seedling stage. Hypocotyl growth is a clear, easily detectable and measurable phenotypic change that can be used as an output that reflects the performance of shade signaling. That way, a large number of regulators has been found to participate in the modulation of shade-triggered hypocotyl elongation, whose action is decisive in the initiation of SAS. At the top of this regulatory network are the phytochromes, responsible for perceiving the changes in the R:FR signal (Franklin & Quail, 2010; J. Li *et al.*, 2011). PhyB is the phytochrome with a major role in regulating this response and,

immediately downstream a group of transcription factors called PIFs receive the light signals perceived by phyB and transform them into shade-induced changes in the expression of hundreds of genes that orchestrate the SAS implementation (Leivar, Monte, Al-Sady, *et al.*, 2008; Leivar & Monte, 2014; Roig-Villanova & Martínez-García, 2016). Among the different PIFs described in Arabidopsis, the photostable PIF7 has a prominent role (L. Li *et al.*, 2012). However, the precise molecular mechanism by which this PIF binds to gene promoters to regulate its expression in a shade-dependent manner is not fully understood, i.e., whether its DNA binding activity can be separated from its ability to interact with phyB motif as it has been demonstrated in the case of PIF3 in the regulation of de-etiolation under R *(Al-Sady et al.*, 2008). The structure-function analyses of PIF7 presented in this work showed that binding to DNA through the bHLH domain and to phyB through the APB motif are both necessary for the regulation of shade-induced changes in gene expression and the promotion of hypocotyl elongation. This result contrasts with that found for PIF3 (Al-Sady *et al.*, 2008).

Although an entire chapter of this manuscript is dedicated to the SAS positive regulator PIF7, there are many other regulators that conform the regulatory network that modulates hypocotyl elongation in shade. In the present work (chapter 2), the architecture of this network has been refined by taking a series of complementary approaches, pointing out that the analyzed SAS components can be organized into two main regulatory modules (phyB-PIF457-HFR1 and phyA-HY5) that furthermore act separately not only working at different timepoints but also impacting at different cells along the hypocotyl axis. With this information, we proposed a model where we integrate the genetic relationship between positive and negative SAS regulators and its temporal and/or spatial role (**Figure Y11**). One interesting point of this signaling system is the role of auxin homeostasis and its relation to the different regulatory modules. Interestingly, we have seen that in the absence of de novo auxin biosynthesis (using the *sav3* mutant background) and analyzing the resistance of the *hy5* and *phyA* mutants to NPA application, part of the elongation in shade can be independent of synthesis and polar transport of auxins, a hormone known to be necessary for the shade-induced hypocotyl growth. How the phyA-HY5 module is able to elongate independently of these auxin aspects is something that should be further investigated, as well as differences in the expression or activity of genes involved in SAV3 alternative routes of auxin synthesis in *phyA* and *hy5* mutants.

Importantly, the activity of the two SAS regulatory modules eventually converges at some point to modulate hypocotyl cell elongation, as experiments presented in this work have

suggested. This converge can take place at different levels such as the action of some of these signaling components or much more downstream at the cell level. HY5 and PIF457 are good candidates for this convergence because they regulate the expression of common target genes, many of them involved in processes related to the perception of light, growth, shade and hormones with a role in SAS (**Figure Y9-10**). Based on our genetic analyses, PIF457 and HY5 had an additive role in the shade-induced hypocotyl growth, which points that their activities might not converge (**Figure Y4**). However, this was the result of the analysis of a long-term process, as hypocotyl was measured after 5 days of shade treatment. In great contrast, at short term, transcriptomic analyses showed that PIF457 are epistatic over HY5 in regulating rapid changes in gene expression in response to shade (1 h of treatment) and surprisingly, this epistatic effect dissipates after 8 h of simulated shade (**Figure Y9**) which is consistent with the genetic additivity observed genetically at day 7 (**Figure Y4**). Altogether, these results suggest that the crosstalk between PIF457 and HY5 activities might be dynamic and disappear with longer times of shade exposure.

Mechanistically, the crosstalk to modulate the expression of common targets could be explained by a possible heterodimerization between PIF457 and HY5. In fact, physical interaction between HY5 and other PIFs has been demonstrated in non-shade related processes (D. Chen *et al.*, 2013; Toledo-Ortiz *et al.*, 2014; X. Zhang *et al.*, 2017). Thus, a possible protein-protein interaction between HY5 and PIF457 should be investigated. To be consistent with our transcriptomic data, this interaction would have to be transient and dynamic. Another possibility is that PIF457 and HY5 separately modulate shade-regulated gene expression without direct interaction between both regulators, but by competing for binding to shared target elements in the promoters of its downstream regulated genes. Indeed, HY5 interacts with ACGT elements (NACGTN), such as ACGTG motifs or the well-defined PIFs binding motif G-box (CACGTG) (Burko *et al.*, 2020; J. Lee *et al.*, 2007; H. Zhang *et al.*, 2011). Hence, a more in-depth study on the genes shared between PIF457 and HY5 would be useful to clarify the connection between the two regulatory modules.

For better understanding how shade can impact on the transcription factor binding to its target regions, in the first chapter we address the PIF7 binding sites, using the constitutively active PIF7 derivative (PIF7APBm). We found that PIF7 binding activity is not regulated by shade conditions as it binds PBE-boxes and G-boxes with equal strength in light and shade. This explains the activation of hypocotyl growth in this PIF7 derivative line regardless of light/shade conditions. The fact that the accessibility of PIF7 to the DNA binding sites does

not greatly change when seedlings grow in W or W+FR, suggests that chromatin accessibility to PIF7 is not rapidly affected (at least within 1 h of shade treatment). Indeed, a poorly understood aspect of SAS implementation is its epigenetic regulation. It has been shown that, after DNA binding, PIF7 can attract regulatory complexes that modify chromatin condensation state (Alatwi & Downs, 2015; Brahma *et al.*, 2017; Peng *et al.*, 2018; Willige *et al.*, 2021). However, till date, the chromatin changes driven by PIF7 only have been reported to happen in the gene coding sequence, not in the promoter region. Further investigation must be done to elucidate the connection of remodelers of the chromatin condensation state with PIF7 binding and with other SAS regulators such as HY5 (another potential attractor of chromatin remodelers, (Jing *et al.*, 2013)). Aspects of epigenetic regulation, such as chromatin accessibility and PIF7 ability to bind DNA, should be also investigated after longer exposures to simulated shade. It is known that some epigenetic regulator mutants (e.g., *lhp1*, *mrg1 mrg2*) involved in the state of chromatin condensation have phenotypes that are defective in shade conditions (their hypocotyls do not elongate under shade as much as to wild-type hypocotyls) (Peng *et al.*, 2018; Valdés *et al.*, 2012). Whether PIF7 binding is affected in these mutants remains to be elucidated. In that context, transgenic lines expressing PIF7APBm and PIF7Bm mutated variants will be useful tools to study these processes since, presumably, PIF7APBm would bind constitutively to the target promoters maintaining the gene body in a more relaxed condensation state (accessible for gene transcription) whereas PIF7Bm could not do so as it does not bind to DNA.

The main objective of the present work has been to provide more information on the regulation of the SAS in Arabidopsis, a shade-avoider species. By modifying the shade regulatory signaling network, we expect to be able to generate shade-tolerant species. In fact, by studying a close relative of Arabidopsis, the shade-resistant plant *Cardamine hirsuta*, it has been demonstrated that shade tolerance in *Cardamine* is due to higher biological activity of the SAS negative regulators phyA and HFR1 and an attenuated activity of phyB and the positive regulators PIFs (Molina-Contreras *et al.*, 2019; Paulišić *et al.*, 2021). Understanding how the various SAS orthologous genes have differentially evolved to modulate responses to shade conditions leading to either avoid or tolerate shade, could arise important knowledge to be able to convert a shade-avoider into a shade-tolerant species and specifically apply these strategies to obtain shade-tolerant crops with higher productivity when growing in dense vegetation densities.

CONCLUSIONS

CONCLUSIONS

CONCLUSIONS

1. By means of directed mutagenesis of two known functional domains of PIF7 we were able to uncouple its capacity to bind DNA and to the active phyB.

2. DNA-binding activity is fundamental to rapidly induce the expression of PIF7 targets that promote, among other responses, the hypocotyl growth in shade.

3. By contrast, PIF7 binding to the active phyB photoreceptor is not needed to induce the expression of PIF7 targets and promote hypocotyl growth. However, phyB binding is required to modulate expression in a shade-dependent manner. Therefore, the PIF7 mutant unable to be regulated by phyB becomes a constitutively active form.

4. Interaction of phyB with PIF7 affects its protein stability and binding capacity to DNA. Moreover, using the PIF7 constitutively active form we found that shade does not affect the strength of PIF7 binding to its DNA-binding sites.

5. The SAS regulatory components analyzed seem to be organized in two regulatory modules, whose temporal and spatial activities differ but overlap.

6. The auxin/SAV3-dependent phyB-PIF457-HFR1 module has a constant activity during seedling development with a slightly increase at the end of the analyzed period (day 7). This module affects mainly the elongation of cells situated in the middle-lower part of the hypocotyl axis.

7. The phyA-HY5 module is partially auxin/SAV3-independent and it works mostly at the beginning of seedling development (from day 2 to 5). It preferentially controls the elongation of cells situated in the upper part of the hypocotyl axis.

8. The two regulatory modules are not completely independent, and their activities converge at least through PIF457 and HY5 transcription factors, in charge of regulating changes in gene expression of common targets. Importantly, convergence of transcriptional activities of these transcription factors is dynamic, being PIF dominant after just 1 h of shade exposure and additive to HY5 activity at longer exposure times (8 h).

CONCLUSIONS

GENERAL REFERENCES

GENERAL REFERENCES

Al-Sady, B., Kikis, E. A., Monte, E., & Quail, P. H. (2008). Mechanistic duality of transcription factor function in phytochrome signaling. *Proceedings of the National Academy of Sciences of the United States of America*, *105*(6), 2232–2237. https://doi.org/10.1073/pnas.0711675105

Al-Sady, B., Ni, W., Kircher, S., Schäfer, E., & Quail, P. H. (2006). Photoactivated Phytochrome Induces Rapid PIF3 Phosphorylation Prior to Proteasome-Mediated Degradation. *Molecular Cell*, *23*(3), 439–446. https://doi.org/10.1016/j.molcel.2006.06.011

Alatwi, H. E., & Downs, J. A. (2015). Removal of H2A.Z by INO 80 promotes homologous recombination . *EMBO Reports*, *16*(8), 986–994. https://doi.org/10.15252/embr.201540330

Arsovski, A. A., Galstyan, A., Guseman, J. M., & Nemhauser, J. L. (2012). Photomorphogenesis. *The Arabidopsis Book*, *10*, e0147–e0147. https://doi.org/10.1199/tab.0147

Bae, G., & Choi, G. (2008). Decoding of Light Signals by Plant Phytochromes and Their Interacting Proteins. *Annual Review of Plant Biology*, *59*(1), 281–311. https://doi.org/10.1146/annurev.arplant.59.032607.092859

Bai, M. Y., Shang, J. X., Oh, E., Fan, M., Bai, Y., Zentella, R., Sun, T. P., & Wang, Z. Y. (2012). Brassinosteroid, gibberellin and phytochrome impinge on a common transcription module in Arabidopsis. *Nature Cell Biology*, *14*(8), 810–817. https://doi.org/10.1038/ncb2546

Boccalandro, H. E., Ploschuk, E. L., Yanovsky, M. J., Sánchez, R. A., Gatz, C., & Casal, J. J. (2003). Increased Phytochrome B Alleviates Density Effects on Tuber Yield of Field Potato Crops. *Plant Physiology*, *133*(4), 1539–1546. https://doi.org/10.1104/pp.103.029579

Bou-Torrent, J., Galstyan, A., Gallemí, M., Cifuentes-Esquivel, N., Molina-Contreras, M. J., Salla-Martret, M., Jikumaru, Y., Yamaguchi, S., Kamiya, Y., & Martínez-García, J. F. (2014). Plant proximity perception dynamically modulates hormone levels and sensitivity in Arabidopsis. *Journal of Experimental Botany*, *65*(11), 2937–2947.

https://doi.org/10.1093/jxb/eru083

Bou-Torrent, J., Roig-Villanova, I., & Martínez-García, J. F. (2008). Light signaling: back to space. *Trends in Plant Science*, *13*(3), 108–114. https://doi.org/10.1016/j.tplants.2007.12.003

Brahma, S., Udugama, M. I., Kim, J., Hada, A., Bhardwaj, S. K., Hailu, S. G., Lee, T. H., & Bartholomew, B. (2017). INO80 exchanges H2A.Z for H2A by translocating on DNA proximal to histone dimers. *Nature Communications*, *8*. https://doi.org/10.1038/ncomms15616

Burko, Y., Seluzicki, A., Zander, M., Pedmale, U. V, Ecker, J. R., & Chory, J. (2020). Chimeric Activators and Repressors Define HY5 Activity and Reveal a Light-Regulated Feedback Mechanism[OPEN]. *The Plant Cell*, *32*(4), 967–983. https://doi.org/10.1105/tpc.19.00772

Casal, J. J. (2012). Shade Avoidance. *The Arabidopsis Book*, *10*, e0157. https://doi.org/10.1199/tab.0157

Casal, J. J. (2013). Photoreceptor signaling networks in plant responses to shade. *Annual Review of Plant Biology*, *64*, 403–427. https://doi.org/10.1146/annurev-arplant-050312-120221

Chen, D., Xu, G., Tang, W., Jing, Y., Ji, Q., Fei, Z., & Lin, R. (2013). Antagonistic basic helix-loop-Helix/bZIP transcription factors form transcriptional modules that integrate light and reactive oxygen species signaling in Arabidopsis. *Plant Cell*, *25*(5), 1657–1673. https://doi.org/10.1105/tpc.112.104869

Chen, E., Swartz, T. E., Bogomolni, R. A., & Kliger, D. S. (2007). A LOV story: The signaling state of the phot1 LOV2 photocycle involves chromophore-triggered protein structure relaxation, as probed by far-UV time-resolved optical rotatory dispersion spectroscopy. *Biochemistry*, *46*(15), 4619–4624. https://doi.org/10.1021/bi602544n

Chen, M., Chory, J., & Fankhauser, C. (2004). Light signal transduction in higher plants. *Annual Review of Genetics*, *38*, 87–117. https://doi.org/10.1146/annurev.genet.38.072902.092259

Christie, J. M., Arvai, A. S., Baxter, K. J., Heilmann, M., Pratt, A. J., O'Hara, A., Kelly, S. M., Hothorn, M., Smith, B. O., Hitomi, K., Jenkins, G. I., & Getzoff, E. D. (2012). Plant UVR8

photoreceptor senses UV-B by tryptophan-mediated disruption of cross-dimer salt bridges. *Science*, *335*(6075), 1492–1496. https://doi.org/10.1126/science.1218091

Christie, J. M., Blackwood, L., Petersen, J., & Sullivan, S. (2015). Plant flavoprotein photoreceptors. *Plant and Cell Physiology*, *56*(3), 401–413. https://doi.org/10.1093/pcp/pcu196

Cifuentes-Esquivel, N., Bou-Torrent, J., Galstyan, A., Gallemí, M., Sessa, G., Salla Martret, M., Roig-Villanova, I., Ruberti, I., & Martínez-García, J. F. (2013). The bHLH proteins BEE and BIM positively modulate the shade avoidance syndrome in Arabidopsis seedlings. *Plant Journal*, *75*(6), 989–1002. https://doi.org/10.1111/tpj.12264

Ciolfi, A., Sessa, G., Sassi, M., Possenti, M., Salvucci, S., Carabelli, M., Morelli, G., & Ruberti, I. (2013). Dynamics of the shade-avoidance response in Arabidopsis. *Plant Physiology*, *163*(1), 331–353. https://doi.org/10.1104/pp.113.221549

Clough, R. C., & Vierstra, R. D. (1997). Phytochrome degradation. *Plant, Cell and Environment*, *20*(6), 713–721. https://doi.org/10.1046/j.1365-3040.1997.d01-107.x

De Lucas, M., Davière, J. M., Rodríguez-Falcón, M., Pontin, M., Iglesias-Pedraz, J. M., Lorrain, S., Fankhauser, C., Blázquez, M. A., Titarenko, E., & Prat, S. (2008). A molecular framework for light and gibberellin control of cell elongation. *Nature*, *451*(7177), 480–484. https://doi.org/10.1038/nature06520

de Wit, M., Ljung, K., & Fankhauser, C. (2015). Contrasting growth responses in lamina and petiole during neighbor detection depend on differential auxin responsiveness rather than different auxin levels. *New Phytologist*, *208*(1), 198–209. https://doi.org/10.1111/nph.13449

Dehesh, K., Franci, C., Parks, B. M., Seeley, K. A., Short, T. W., Tepperman, J. M., & Quail, P. H. (1993). Arabidopsis HY8 locus encodes phytochrome A. *The Plant Cell*, *5*(9), 1081–1088. https://doi.org/10.1105/tpc.5.9.1081

Devlin, P. F., Patel, S. R., & Whitelam, G. C. (1998). Phytochrome E influences internode elongation and flowering time in arabidopsis. *Plant Cell*, *10*(9), 1479–1487. https://doi.org/10.1105/tpc.10.9.1479

Devlin, P. F., Robson, P. R. H., Patel, S. R., Goosey, L., Sharrock, R. A., & Whitelam, G. C. (1999). Phytochrome D acts in the shade-avoidance syndrome in Arabidopsis by

controlling elongation growth and flowering time. *Plant Physiology*, *119*(3), 909–915. https://doi.org/10.1104/pp.119.3.909

Eichenberg, K., Bäurle, I., Paulo, N., Sharrock, R. A., Rüdiger, W., & Schäfer, E. (2000). Arabidopsis phytochromes C and E have different spectral characteristics from those of phytochromes A and B. *FEBS Letters*, *470*(2), 107–112. https://doi.org/10.1016/S0014-5793(00)01301-6

Fierro, A. C., Leroux, O., De Coninck, B., Cammue, B. P. A., Marchal, K., Prinsen, E., Van Der Straeten, D., & Vandenbussche, F. (2015). Ultraviolet-B radiation stimulates downward leaf curling in Arabidopsis thaliana. *Plant Physiology and Biochemistry*, *93*(2015), 9–17. https://doi.org/10.1016/j.plaphy.2014.12.012

Fiorucci, A. S., & Fankhauser, C. (2017). Plant Strategies for Enhancing Access to Sunlight. *Current Biology*, *27*(17), R931–R940. https://doi.org/10.1016/j.cub.2017.05.085

Folta, K. M., Lieg, E. J., Durham, T., & Spalding, E. P. (2003). Primary Inhibition of Hypocotyl Growth and Phototropism Depend Differently on Phototropin-Mediated Increases in Cytoplasmic Calcium Induced by Blue Light. *Plant Physiology*, *133*(4), 1464–1470. https://doi.org/10.1104/pp.103.024372

Franklin, K. A. (2008). Shade avoidance. *New Phytologist*, *179*(4), 930–944. https://doi.org/10.1111/j.1469-8137.2008.02507.x

Franklin, K. A., Davis, S. J., Stoddart, W. M., Vierstra, R. D., & Whitelam, G. C. (2003). Mutant analyses define multiple roles for phytochrome C in Arabidopsis photomorphogenesis. *Plant Cell*, *15*(9), 1981–1989. https://doi.org/10.1105/tpc.015164

Franklin, K. A., & Quail, P. H. (2010). Phytochrome functions in Arabidopsis development. *Journal of Experimental Botany*, *61*(1), 11–24. https://doi.org/10.1093/jxb/erp304

Freddolino, P. L., Gardner, K. H., & Schulten, K. (2013). Signaling mechanisms of LOV domains: New insights from molecular dynamics studies. *Photochemical and Photobiological Sciences*, *12*(7), 1158–1170. https://doi.org/10.1039/c3pp25400c

Gallego-Bartolomé, J., Minguet, E. G., Grau-Enguix, F., Abbas, M., Locascio, A., Thomas, S. G., Alabadí, D., & Blázquez, M. A. (2012). Molecular mechanism for the interaction between gibberellin and brassinosteroid signaling pathways in Arabidopsis. *Proceedings of the National Academy of Sciences of the United States of America*, *109*(33), 13446–

13451. https://doi.org/10.1073/pnas.1119992109

Galstyan, A., Cifuentes-Esquivel, N., Bou-Torrent, J., & Martinez-Garcia, J. F. (2011). The shade avoidance syndrome in Arabidopsis: A fundamental role for atypical basic helix-loop-helix proteins as transcriptional cofactors. *Plant Journal*, *66*(2), 258–267. https://doi.org/10.1111/j.1365-313X.2011.04485.x

Galvão, V. C., & Fankhauser, C. (2015). Sensing the light environment in plants: Photoreceptors and early signaling steps. *Current Opinion in Neurobiology*, *34*(Figure 1), 46–53. https://doi.org/10.1016/j.conb.2015.01.013

Gangappa, S. N., Crocco, C. D., Johansson, H., Datta, S., Hettiarachchi, C., Holm, M., & Botto, J. F. (2013). The Arabidopsis B-BOX protein BBX25 interacts with HY5, negatively regulating BBX22 expression to suppress seedling photomorphogenesis. *Plant Cell*, *25*(4), 1243–1257. https://doi.org/10.1105/tpc.113.109751

Garg, A. K., Sawers, R. J. H., Wang, H., Kim, J.-K., Walker, J. M., Brutnell, T. P., Parthasarathy, M. V, Vierstra, R. D., & Wu, R. J. (2006). Light-regulated overexpression of an Arabidopsis phytochrome A gene in rice alters plant architecture and increases grain yield. *Planta*, *223*(4), 627–636. https://doi.org/10.1007/s00425-005-0101-3

Givnish, T. J. (1988). Adaptation to sun and shade: a whole-plant perspective. *Functional Plant Biology*, *15*(2), 63–92.

González-Grandío, E., Poza-Carrión, C., Sorzano, C. O. S., & Cubas, P. (2013). Branched1 promotes axillary bud dormancy in response to shade in Arabidopsis. *Plant Cell*, *25*(3), 834–850. https://doi.org/10.1105/tpc.112.108480

Halliday, K. J., Koornneef, M., & Whitelam, G. C. (1994). Phytochrome B and at least one other phytochrome mediate the accelerated flowering response of Arabidopsis thaliana L. to low red/far-red ratio. *Plant Physiology*, *104*(4), 1311–1315. https://doi.org/10.1104/pp.104.4.1311

Han, Y. J., Song, P. S., & Kim, J. Il. (2007). Phytochrome-mediated photomorphogenesis in plants. *Journal of Plant Biology*, *50*(3), 230–240. https://doi.org/10.1007/BF03030650

Hay, A. S., Pieper, B., Cooke, E., Mandáková, T., Cartolano, M., Tattersall, A. D., Ioio, R. D., McGowan, S. J., Barkoulas, M., Galinha, C., Rast, M. I., Hofhuis, H., Then, C., Plieske, J., Ganal, M., Mott, R., Martinez-Garcia, J. F., Carine, M. A., Scotland, R. W., … Tsiantis,

M. (2014). Cardamine hirsuta: A versatile genetic system for comparative studies. *Plant Journal*, *78*(1), 1–15. https://doi.org/10.1111/tpj.12447

Hayes, S., Velanis, C. N., Jenkins, G. I., & Franklin, K. A. (2014). UV-B detected by the UVR8 photoreceptor antagonizes auxin signaling and plant shade avoidance. *Proceedings of the National Academy of Sciences of the United States of America*, *111*(32), 11894–11899. https://doi.org/10.1073/pnas.1403052111

Heijde, M., & Ulm, R. (2012). UV-B photoreceptor-mediated signalling in plants. *Trends in Plant Science*, *17*(4), 230–237. https://doi.org/10.1016/j.tplants.2012.01.007

Hohm, T., Preuten, T., & Fankhauser, C. (2013). Phototropism: Translating light into directional growth. *American Journal of Botany*, *100*(1), 47–59. https://doi.org/10.3732/ajb.1200299

Hornitschek, P., Kohnen, M. V., Lorrain, S., Rougemont, J., Ljung, K., López-Vidriero, I., Franco-Zorrilla, J. M., Solano, R., Trevisan, M., Pradervand, S., Xenarios, I., & Fankhauser, C. (2012). Phytochrome interacting factors 4 and 5 control seedling growth in changing light conditions by directly controlling auxin signaling. *Plant Journal*, *71*(5), 699–711. https://doi.org/10.1111/j.1365-313X.2012.05033.x

Hornitschek, P., Lorrain, S., Zoete, V., Michielin, O., & Fankhauser, C. (2009). Inhibition of the shade avoidance response by formation of non-DNA binding bHLH heterodimers. *EMBO Journal*, *28*(24), 3893–3902. https://doi.org/10.1038/emboj.2009.306

Hughes, J. E., Morgan, D. C., Lambton, P. A., Black, C. R., & Smith, H. (1984). Photoperiodic time signals during twilight. *Plant, Cell & Environment*, *7*(4), 269–277. https://doi.org/https://doi.org/10.1111/1365-3040.ep11589464

Iannacone, R., Mittempergher, F., Morelli, G., Panio, G., Perito, A., Ruberti, I., Sessa, G., & Cellini, F. (2008). Influence of an Arabidopsis dominant negative athb2 mutant on tomato plant development. *Acta Horticulturae*.

Ito, S., Song, Y. H., & Imaizumi, T. (2012). LOV domain-containing F-box proteins: Light-dependent protein degradation modules in Arabidopsis. *Molecular Plant*, *5*(3), 573–582. https://doi.org/10.1093/mp/sss013

Jenkins, G. I. (2017). Photomorphogenic responses to ultraviolet-B light. *Plant Cell and Environment*, 2544–2557. https://doi.org/10.1111/pce.12934

Jing, Y., Zhang, D., Wang, X., Tang, W., Wang, W., Huai, J., Xu, G., Chen, D., Li, Y., & Lin, R. (2013). Arabidopsis Chromatin Remodeling Factor PICKLE Interacts with Transcription Factor HY5 to Regulate Hypocotyl Cell Elongation . *The Plant Cell*, *25*(1), 242–256. https://doi.org/10.1105/tpc.112.105742

Josse, E. M., & Halliday, K. J. (2008). Skotomorphogenesis: The Dark Side of Light Signalling. *Current Biology*, *18*(24), R1144–R1146. https://doi.org/10.1016/j.cub.2008.10.034

Kami, C., Lorrain, S., Hornitschek, P., & Fankhauser, C. (2010). Chapter Two - Light-Regulated Plant Growth and Development. In M. C. P. B. T.-C. T. in D. B. Timmermans (Ed.), *Plant Development* (Vol. 91, pp. 29–66). Academic Press. https://doi.org/https://doi.org/10.1016/S0070-2153(10)91002-8

Keller, M. M., Jaillais, Y., Pedmale, U. V., Moreno, J. E., Chory, J., & Ballaré, C. L. (2011). Cryptochrome 1 and phytochrome B control shade-avoidance responses in Arabidopsis via partially independent hormonal cascades. *Plant Journal*, *67*(2), 195–207. https://doi.org/10.1111/j.1365-313X.2011.04598.x

Keuskamp, D. H., Sasidharan, R., Vos, I., Peeters, A. J. M., Voesenek, L. A. C. J., & Pierik, R. (2011). Blue-light-mediated shade avoidance requires combined auxin and brassinosteroid action in Arabidopsis seedlings. *Plant Journal*, *67*(2), 208–217. https://doi.org/10.1111/j.1365-313X.2011.04597.x

Kinoshita, T., Doi, M., & Suetsugu, N. (2001). Regulation of Stomatal Opening. *Nature*, *414*(December), 0–4.

Kitajima, K. (1994). Relative importance of photosynthetic traits and allocation patterns as correlates of seedling shade tolerance of 13 tropical trees. *Oecologia*, *98*(3), 419–428. https://doi.org/10.1007/BF00324232

Kleine, T., Lockhart, P., & Batschauer, A. (2003). An Arabidopsis protein closely related to Synechocystis cryptochrome is targeted to organelles. *Plant Journal*, *35*(1), 93–103. https://doi.org/10.1046/j.1365-313X.2003.01787.x

Kohnen, M. V., Schmid-Siegert, E., Trevisan, M., Petrolati, L. A., Sénéchal, F., Müller-Moulé, P., Maloof, J., Xenarios, I., & Fankhauser, C. (2016). Neighbor detection induces organ-specific transcriptomes, revealing patterns underlying hypocotyl-specific growth. *Plant*

Cell, *28*(12), 2889–2904. https://doi.org/10.1105/tpc.16.00463

Kong, S.-G., Lee, D.-S., Kwak, S.-N., Kim, J.-K., Sohn, J.-K., & Kim, I.-S. (2004). Characterization of sunlight-grown transgenic rice plants expressing Arabidopsis phytochrome A. *Molecular Breeding*, *14*(1), 35–46. https://doi.org/10.1023/B:MOLB.0000037993.79486.7b

Kreslavski, V. D., Los, D. A., Schmitt, F. J., Zharmukhamedov, S. K., Kuznetsov, V. V., & Allakhverdiev, S. I. (2018). The impact of the phytochromes on photosynthetic processes. *Biochimica et Biophysica Acta - Bioenergetics*, *1859*(5), 400–408. https://doi.org/10.1016/j.bbabio.2018.03.003

Łabuz, J., Sztatelman, O., Banaś, A. K., & Gabryś, H. (2012). The expression of phototropins in Arabidopsis leaves: developmental and light regulation. *Journal of Experimental Botany*, *63*(4), 1763–1771. https://doi.org/10.1093/jxb/ers061

Lee, J., He, K., Stolc, V., Lee, H., Figueroa, P., Gao, Y., Tongprasit, W., Zhao, H., Lee, I., & Xing, W. D. (2007). Analysis of transcription factor HY5 genomic binding sites revealed its hierarchical role in light regulation of development. *Plant Cell*, *19*(3), 731–749. https://doi.org/10.1105/tpc.106.047688

Lee, N., & Choi, G. (2017). ScienceDirect Phytochrome-interacting factor from Arabidopsis to liverwort. *Current Opinion in Plant Biology*, *35*, 54–60. https://doi.org/10.1016/j.pbi.2016.11.004

Leivar, P., & Monte, E. (2014). PIFs: Systems integrators in plant development. *Plant Cell*, *26*(1), 56–78. https://doi.org/10.1105/tpc.113.120857

Leivar, P., Monte, E., Al-Sady, B., Carle, C., Storer, A., Alonso, J. M., Ecker, J. R., & Quaila, P. H. (2008). The Arabidopsis phytochrome-interacting factor PIF7, together with PIF3 and PIF4, regulates responses to prolonged red light by modulating phyB levels. *Plant Cell*, *20*(2), 337–352. https://doi.org/10.1105/tpc.107.052142

Leivar, P., Monte, E., Oka, Y., Liu, T., Carle, C., Castillon, A., Huq, E., & Quail, P. H. (2008). Multiple Phytochrome-Interacting bHLH Transcription Factors Repress Premature Seedling Photomorphogenesis in Darkness. *Current Biology*, *18*(23), 1815–1823. https://doi.org/10.1016/j.cub.2008.10.058

Leivar, P., & Quail, P. H. (2011). PIFs: Pivotal components in a cellular signaling hub. *Trends*

in Plant Science, *16*(1), 19–28. https://doi.org/10.1016/j.tplants.2010.08.003

Leone, M., Keller, M. M., Cerrudo, I., & Ballaré, C. L. (2014). To grow or defend? Low red: Far-red ratios reduce jasmonate sensitivity in Arabidopsis seedlings by promoting DELLA degradation and increasing JAZ10 stability. *New Phytologist*, *204*(2), 355–367. https://doi.org/10.1111/nph.12971

Li, J., Li, G., Wang, H., & Wang Deng, X. (2011). Phytochrome Signaling Mechanisms. *The Arabidopsis Book*, *9*, e0148. https://doi.org/10.1199/tab.0148

Li, L., Ljung, K., Breton, G., Schmitz, R. J., Pruneda-Paz, J., Cowing-Zitron, C., Cole, B. J., Ivans, L. J., Pedmale, U. V., Jung, H. S., Ecker, J. R., Kay, S. A., & Chory, J. (2012). Linking photoreceptor excitation to changes in plant architecture. *Genes and Development*, *26*(8), 785–790. https://doi.org/10.1101/gad.187849.112

Li, Q.-H., & Yang, H.-Q. (2007). Cryptochrome Signaling in Plants†. *Photochemistry and Photobiology*, *83*(1), 94–101. https://doi.org/10.1562/2006-02-28-ir-826

Liu, H., Liu, B., Zhao, C., Pepper, M., & Lin, C. (2011). The action mechanisms of plant cryptochromes. *Trends in Plant Science*, *16*(12), 684–691. https://doi.org/10.1016/j.tplants.2011.09.002

Liu, Y., Li, X., Li, K., Liu, H., & Lin, C. (2013). Multiple bHLH Proteins form Heterodimers to Mediate CRY2-Dependent Regulation of Flowering-Time in Arabidopsis. *PLoS Genetics*, *9*(10). https://doi.org/10.1371/journal.pgen.1003861

Liu, Y., Li, X., Ma, D., Chen, Z., Wang, J., & Liu, H. (2018). CIB 1 and CO interact to mediate CRY 2-dependent regulation of flowering . *EMBO Reports*, *19*(10), 1–10. https://doi.org/10.15252/embr.201845762

Lorrain, S., Allen, T., Duek, P. D., Whitelam, G. C., & Fankhauser, C. (2008). Phytochrome-mediated inhibition of shade avoidance involves degradation of growth-promoting bHLH transcription factors. *Plant Journal*, *53*(2), 312–323. https://doi.org/10.1111/j.1365-313X.2007.03341.x

Luccioni, L. G., Oliverio, K. A., Yanovsky, M. J., Boccalandro, H. E., & Casal, J. J. (2002). Brassinosteroid Mutants Uncover Fine Tuning of Phytochrome Signaling. *Plant Physiology*, *128*(1), 173–181. https://doi.org/10.1104/pp.010668

Martínez-García, J. F., Gallemí, M., Molina-Contreras, M. J., Llorente, B., Bevilaqua, M. R.

R., & Quail, P. H. (2014). The shade avoidance syndrome in Arabidopsis: The antagonistic role of phytochrome A and B differentiates vegetation proximity and canopy shade. *PLoS ONE*, *9*(10). https://doi.org/10.1371/journal.pone.0109275

Martínez-García, J. F., Galstyan, A., Salla-Martret, M., Cifuentes-Esquivel, N., Gallemí, M., & Bou-Torrent, J. (2010). Regulatory Components of Shade Avoidance Syndrome. In J.-C. Kader & M. Delseny (Eds.), *Advances in Botanical Research* (Vol. 53, pp. 65–116). Academic Press. https://doi.org/https://doi.org/10.1016/S0065-2296(10)53003-9

Mazza, C. A., & Ballaré, C. L. (2015). Photoreceptors UVR8 and phytochrome B cooperate to optimize plant growth and defense in patchy canopies. *New Phytologist*, *207*(1), 4–9. https://doi.org/10.1111/nph.13332

Möglich, A., Yang, X., Ayers, R. A., & Moffat, K. (2010). Structure and function of plant photoreceptors. *Annual Review of Plant Biology*, *61*, 21–47. https://doi.org/10.1146/annurev-arplant-042809-112259

Molina-Contreras, M. J., Paulišić, S., Then, C., Moreno-Romero, J., Pastor-Andreu, P., Morelli, L., Roig-Villanova, I., Jenkins, H., Hallab, A., Gan, X., Gomez-Cadenas, A., Tsiantis, M., Rodríguez-Concepción, M., & Martínez-García, J. F. (2019). Photoreceptor Activity Contributes to Contrasting Responses to Shade in Cardamine and Arabidopsis Seedlings. *The Plant Cell*, *31*(11), 2649–2663. https://doi.org/10.1105/tpc.19.00275

Morales, L. O., Brosché, M., Vainonen, J., Jenkins, G. I., Wargent, J. J., Sipari, N., Strid, Å., Lindfors, A. V., Tegelberg, R., & Aphalo, P. J. (2013). Multiple roles for UV RESISTANCE LOCUS8 in regulating gene expression and metabolite accumulation in arabidopsis under solar ultraviolet radiation. *Plant Physiology*, *161*(2), 744–759. https://doi.org/10.1104/pp.112.211375

Müller-Moulé, P., Nozue, K., Pytlak, M. L., Palmer, C. M., Covington, M. F., Wallace, A. D., Harmer, S. L., & Maloof, J. N. (2016). YUCCA auxin biosynthetic genes are required for Arabidopsis shade avoidance. *PeerJ*, *4*, e2574.

Nagatani, A, Reed, J. W., & Chory, J. (1993). Isolation and Initial Characterization of Arabidopsis Mutants That Are Deficient in Phytochrome A. *Plant Physiology*, *102*(1), 269–277. https://doi.org/10.1104/pp.102.1.269

Nagatani, Akira. (2004). Light-regulated nuclear localization of phytochromes. *Current*

Opinion in Plant Biology, *7*(6), 708–711. https://doi.org/10.1016/j.pbi.2004.09.010

Nagatani, Akira, Chory, J., & Furuya, M. (1991). Phytochrome B Is Not Detectable in the hy3 Mutant of Arabidopsis, Which Is Deficient in Responding to End-of-Day Far-Red Light Treatments. *Plant and Cell Physiology*, *32*(7), 1119–1122. https://doi.org/10.1093/oxfordjournals.pcp.a078177

Nawkar, G. M., Kang, C. H., Maibam, P., Park, J. H., Jung, Y. J., Chae, H. B., Chi, Y. H., Jung, I. J., Kim, W. Y., Yun, D. J., & Lee, S. Y. (2017). HY5, a positive regulator of light signaling, negatively controls the unfolded protein response in Arabidopsis. *Proceedings of the National Academy of Sciences of the United States of America*, *114*(8), 2084–2089. https://doi.org/10.1073/pnas.1609844114

Neff, M. M., Fankhauser, C., & Chory, J. (2000). Eight: An indicator of time and place. *Genes and Development*, *14*(3), 257–271. https://doi.org/10.1101/gad.14.3.257

Niinemets, Ü., & Tenhunen, J. D. (1997). A model separating leaf structural and physiological effects on carbon gain along light gradients for the shade-tolerant species Acer saccharum. *Plant, Cell and Environment*, *20*(7), 845–866. https://doi.org/10.1046/j.1365-3040.1997.d01-133.x

Paik, I., Kathare, P. K., Kim, J. II, & Huq, E. (2017). Expanding Roles of PIFs in Signal Integration from Multiple Processes. *Molecular Plant*, *10*(8), 1035–1046. https://doi.org/10.1016/j.molp.2017.07.002

Parks, B. M., & Quail, P. H. (1993). hy8, a new class of arabidopsis long hypocotyl mutants deficient in functional phytochrome A. *Plant Cell*, *5*(1), 39–48. https://doi.org/10.1105/tpc.5.1.39

Paulišić, S., Qin, W., Arora Verasztó, H., Then, C., Alary, B., Nogue, F., Tsiantis, M., Hothorn, M., & Martínez-García, J. F. (2021). Adjustment of the PIF7-HFR1 transcriptional module activity controls plant shade adaptation. *The EMBO Journal*, *40*(1), 1–16. https://doi.org/10.15252/embj.2019104273

Pedmale, U. V., Huang, S. S. C., Zander, M., Cole, B. J., Hetzel, J., Ljung, K., Reis, P. A. B., Sridevi, P., Nito, K., Nery, J. R., Ecker, J. R., & Chory, J. (2016). Cryptochromes Interact Directly with PIFs to Control Plant Growth in Limiting Blue Light. *Cell*, *164*(1–2), 233–245. https://doi.org/10.1016/j.cell.2015.12.018

Peng, M., Li, Z., Zhou, N., Ma, M., Jiang, Y., Dong, A., Shen, W. H., & Li, L. (2018). Linking phytochrome-interacting factor to histone modification in plant shade avoidance. *Plant Physiology*, *176*(2), 1341–1351. https://doi.org/10.1104/pp.17.01189

Pierik, R., Cuppens, M. L. C., Voesenek, L. A. C. J., & Visser, E. J. W. (2004). Interactions between Ethylene and Gibberellins in Phytochrome-Mediated Shade Avoidance Responses in Tobacco. *Plant Physiology*, *136*(2), 2928–2936. https://doi.org/10.1104/pp.104.045120

Pierik, R., & Testerink, C. (2014). The Art of Being Flexible: How to Escape from Shade, Salt, and Drought. *Plant Physiology*, *166*(1), 5–22. https://doi.org/10.1104/pp.114.239160

Possart, A., Fleck, C., & Hiltbrunner, A. (2014). Shedding (far-red) light on phytochrome mechanisms and responses in land plants. *Plant Science*, *217–218*(316), 36–46. https://doi.org/10.1016/j.plantsci.2013.11.013

Qian-Feng, L., Chunming, W., Lei, J., Shuo, L., M., S. S. S., & Jun-Xian, H. (2012). An Interaction Between BZR1 and DELLAs Mediates Direct Signaling Crosstalk Between Brassinosteroids and Gibberellins in Arabidopsis. *Science Signaling*, *5*(244), ra72–ra72. https://doi.org/10.1126/scisignal.2002908

Quail, P. H. (1997). An emerging molecular map of the phytochromes. *Plant, Cell and Environment*, *20*(6), 657–665. https://doi.org/10.1046/j.1365-3040.1997.d01-108.x

Quail, P. H, Boylan, M. T., Parks, B. M., Short, T. W., Xu, Y., & Wagner, D. (1995). Phytochromes: photosensory perception and signal transduction. *Science*, *268*(5211), 675–680.

Reed, J. W., Nagatani, A., Elich, T. D., Fagan, M., & Chory, J. (1994). Phytochrome A and Phytochrome B Have Overlapping but Distinct Functions in Arabidopsis Development. *Plant Physiology*, *104*(4), 1139–1149. https://doi.org/10.1104/pp.104.4.1139

Rizzini, L., Favory, J. J., Cloix, C., Faggionato, D., O'Hara, A., Kaiserli, E., Baumeister, R., Schäfer, E., Nagy, F., Jenkins, G. I., & Ulm, R. (2011). Perception of UV-B by the arabidopsis UVR8 protein. *Science*, *332*(6025), 103–106. https://doi.org/10.1126/science.1200660

Rockwell, N. C., & Lagarias, J. C. (2006). The structure of phytochrome: A picture is worth a thousand spectra. *Plant Cell*, *18*(1), 4–14. https://doi.org/10.1105/tpc.105.038513

Roig-Villanova, I., Bou-Torrent, J., Galstyan, A., Carretero-Paulet, L., Portolés, S., Rodríguez-Concepción, M., & Martínez-García, J. F. (2007). Interaction of shade avoidance and auxin responses: A role for two novel atypical bHLH proteins. *EMBO Journal*, *26*(22), 4756–4767. https://doi.org/10.1038/sj.emboj.7601890

Roig-Villanova, I., Bou, J., Sorin, C., Devlin, P. F., & Martínez-García, J. F. (2006). Identification of Primary Target Genes of Phytochrome Signaling. Early Transcriptional Control during Shade Avoidance Responses in Arabidopsis. *Plant Physiology*, *141*(1), 85–96. https://doi.org/10.1104/pp.105.076331

Roig-Villanova, I., & Martínez-García, J. F. (2016). Plant responses to vegetation proximity: A whole life avoiding shade. *Frontiers in Plant Science*, *7*(FEB2016), 1–10. https://doi.org/10.3389/fpls.2016.00236

Sakai, T., Kagawa, T., Kasahara, M., Swartz, T. E., Christie, J. M., Briggs, W. R., Wada, M., & Okada, K. (2001). Arabidopsis nph1 and npl1: Blue light receptors that mediate both phototropism and chloroplast relocation. *Proceedings of the National Academy of Sciences of the United States of America*, *98*(12), 6969–6974. https://doi.org/10.1073/pnas.101137598

Salter, M. G., Franklin, K. A., & Whitelam, G. C. (2003). Gating of the rapid shade-avoidance response by the circadian clock in plants. *Nature*, *426*(6967), 680–683.

Schwechheimer, C., & Willige, B. C. (2009). Shedding light on gibberellic acid signalling. *Current Opinion in Plant Biology*, *12*(1), 57–62. https://doi.org/10.1016/j.pbi.2008.09.004

Sellaro, R., Yanovsky, M. J., & Casal, J. J. (2011). Repression of shade-avoidance reactions by sunfleck induction of HY5 expression in Arabidopsis. *Plant Journal*, *68*(5), 919–928. https://doi.org/10.1111/j.1365-313X.2011.04745.x

Sessa, G., Carabelli, M., Sassi, M., Ciolfi, A., Possenti, M., Mittempergher, F., Becker, J., Morelli, G., & Ruberti, I. (2005). A dynamic balance between gene activation and repression regulates the shade avoidance response in Arabidopsis. *Genes and Development*, *19*(23), 2811–2815. https://doi.org/10.1101/gad.364005

Shalitin, D., Yang, H., Mockler, T. C., Maymon, M., Guo, H., Whitelam, G. C., & Lin, C. (2002). Regulation of Arabidopsis cryptochrome 2 by blue-light-dependent phosphorylation. *Nature*, *417*(6890), 763–767. https://doi.org/10.1038/nature00815

Sheerin, D. J., & Hiltbrunner, A. (2017). Molecular mechanisms and ecological function of far-red light signalling. *Plant Cell and Environment*, 2509–2529. https://doi.org/10.1111/pce.12915

Shen, H., Zhu, L., Castillon, A., Majee, M., Downie, B., & Huq, E. (2008). Light-induced phosphorylation and degradation of the negative regulator phytochrome-interacting factor1 from Arabidopsis depend upon its direct physical interactions with photoactivated phytochromes. *Plant Cell*, *20*(6), 1586–1602. https://doi.org/10.1105/tpc.108.060020

Shen, Y., Khanna, R., Carle, C. M., & Quail, P. H. (2007). Phytochrome induces rapid PIF5 phosphorylation and degradation in response to red-light activation. *Plant Physiology*, *145*(3), 1043–1051. https://doi.org/10.1104/pp.107.105601

Shinomura, T., Nagatani, A., Hanzawa, H., Kubota, M., Watanabe, M., & Furuya, M. (1996). Action spectra for phytochrome A- and B-specific photoinduction of seed germination in Arabidopsis thaliana. *Proceedings of the National Academy of Sciences of the United States of America*, *93*(15), 8129–8133. https://doi.org/10.1073/pnas.93.15.8129

Smith, H. (2000). Phytochromes and light signal perception. *Nature*, *407*, 585.

Smith, H., & Whitelam, G. C. (1997). The shade avoidance syndrome: Multiple responses mediated by multiple phytochromes. *Plant, Cell and Environment*, *20*(6), 840–844. https://doi.org/10.1046/j.1365-3040.1997.d01-104.x

Smith, Harry. (1982). *STRATEGY*. 481–518.

Somers, D. E., Sharrock, R. A., Tepperman, J. M., & Quail, P. H. (1991). The hy3 long hypocotyl mutant of arabidopsis is deficient in phytochrome B. *Plant Cell*, *3*(12), 1263–1274. https://doi.org/10.2307/3869307

Song, B., Zhao, H., Dong, K., Wang, M., Wu, S., Li, S., Wang, Y., Chen, P., Jiang, L., & Tao, Y. (2020). Phytochrome A inhibits shade avoidance responses under strong shade through repressing the brassinosteroid pathway in Arabidopsis. *Plant Journal*, *104*(6), 1520–1534. https://doi.org/10.1111/tpj.15018

Song, Y. H., Estrada, D. A., Johnson, R. S., Kim, S. K., Lee, S. Y., MacCoss, M. J., & Imaizumi, T. (2014). Distinct roles of FKF1, GIGANTEA, and ZEITLUPE proteins in the regulation of constans stability in Arabidopsis photoperiodic flowering. *Proceedings of the National Academy of Sciences of the United States of America*, *111*(49), 17672–

17677. https://doi.org/10.1073/pnas.1415375111

Sorin, C., Salla-Martret, M., Bou-Torrent, J., Roig-Villanova, I., & Martínez-García, J. F. (2009). ATHB4, a regulator of shade avoidance, modulates hormone response in Arabidopsis seedlings. *Plant Journal*, *59*(2), 266–277. https://doi.org/10.1111/j.1365-313X.2009.03866.x

Tao, Y., Ferrer, J. L., Ljung, K., Pojer, F., Hong, F., Long, J. A., Li, L., Moreno, J. E., Bowman, M. E., Ivans, L. J., Cheng, Y., Lim, J., Zhao, Y., Ballaré, C. L., Sandberg, G., Noel, J. P., & Chory, J. (2008). Rapid Synthesis of Auxin via a New Tryptophan-Dependent Pathway Is Required for Shade Avoidance in Plants. *Cell*, *133*(1), 164–176. https://doi.org/10.1016/j.cell.2008.01.049

Toledo-Ortiz, G., Johansson, H., Lee, K. P., Bou-Torrent, J., Stewart, K., Steel, G., Rodríguez-Concepción, M., & Halliday, K. J. (2014). The HY5-PIF Regulatory Module Coordinates Light and Temperature Control of Photosynthetic Gene Transcription. *PLoS Genetics*, *10*(6). https://doi.org/10.1371/journal.pgen.1004416

Valdés, A. E., Rizzardi, K., Johannesson, H., Para, A., Sundås-Larsson, A., & Landberg, K. (2012). Arabidopsis thaliana TERMINAL FLOWER2 is involved in light-controlled signalling during seedling photomorphogenesis. *Plant, Cell and Environment*, *35*(6), 1013–1025. https://doi.org/10.1111/j.1365-3040.2011.02468.x

Vandenbussche, F., Pierik, R., Millenaar, F. F., Voesenek, L. A. C. J., & Van Der Straeten, D. (2005). Reaching out of the shade. *Current Opinion in Plant Biology*, *8*(5), 462–468. https://doi.org/10.1016/j.pbi.2005.07.007

Whitelam, G. C., Johnson, E., Peng, J., Carol, P., Anderson, M. L., Cowl, J. S., & Harberd, N. P. (1993). Phytochrome A null mutants of Arabidopsis display a wild-type phenotype in white light. *The Plant Cell*, *5*(7), 757–768. https://doi.org/10.1105/tpc.5.7.757

Willige, B. C., Zander, M., Yoo, C. Y., Phan, A., Garza, R. M., Trigg, S. A., He, Y., Nery, J. R., Chen, H., Chen, M., Ecker, J. R., & Chory, J. (2021). PHYTOCHROME-INTERACTING FACTORs trigger environmentally responsive chromatin dynamics in plants. *Nature Genetics*, *53*(7), 955–961. https://doi.org/10.1038/s41588-021-00882-3

Wu, G., & Spalding, E. P. (2007). Separate functions for nuclear and cytoplasmic cryptochrome 1 during photomorphogenesis of Arabidopsis seedlings. *Proceedings of*

the *National Academy of Sciences of the United States of America*, *104*(47), 18813–18818. https://doi.org/10.1073/pnas.0705082104

Yang, X., Montano, S., & Ren, Z. (2015). How Does Photoreceptor UVR8 Perceive a UV-B Signal. *Photochemistry and Photobiology*, *91*(5), 993–1003. https://doi.org/10.1111/php.12470

Yang, Z., Liu, B., Su, J., Liao, J., Lin, C., & Oka, Y. (2017). Cryptochromes Orchestrate Transcription Regulation of Diverse Blue Light Responses in Plants. *Photochemistry and Photobiology*, *93*(1), 112–127. https://doi.org/10.1111/php.12663

Zhang, H., He, H., Wang, X., Wang, X., Yang, X., Li, L., & Deng, X. W. (2011). Genome-wide mapping of the HY5-mediated genenetworks in Arabidopsis that involve both transcriptional and post-transcriptional regulation. *The Plant Journal*, *65*(3), 346–358. https://doi.org/https://doi.org/10.1111/j.1365-313X.2010.04426.x

Zhang, X., Huai, J., Shang, F., Xu, G., Tang, W., Jing, Y., & Lin, R. (2017). A PIF1/PIF3-HY5-BBX23 transcription factor cascade affects photomorphogenesis. *Plant Physiology*, *174*(4), 2487–2500. https://doi.org/10.1104/pp.17.00418

Zhang, Y., Mayba, O., Pfeiffer, A., Shi, H., Tepperman, J. M., Speed, T. P., & Quail, P. H. (2013). A Quartet of PIF bHLH Factors Provides a Transcriptionally Centered Signaling Hub That Regulates Seedling Morphogenesis through Differential Expression-Patterning of Shared Target Genes in Arabidopsis. *PLoS Genetics*, *9*(1), 11–13. https://doi.org/10.1371/journal.pgen.1003244

Zuo, Z., Liu, H., Liu, B., Liu, X., & Lin, C. (2011). Blue light-dependent interaction of CRY2 with SPA1 regulates COP1 activity and floral initiation in arabidopsis. *Current Biology*, *21*(10), 841–847. https://doi.org/10.1016/j.cub.2011.03.048